Berichte

zur Polar- und Meeresforschung

Reports

on Polar and Marine Research

Long-term evolution of (millennial-scale) climate variability in the North Atlantic over the last four million years

Results from Integrated Ocean Drilling Project Site U1313

Bernhard David Adriaan Naafs

Hinweis

Die Berichte zur Polar- und Meeresforschung werden vom Alfred-Wegener-Institut für Polar- und Meeresforschung in Bremerhaven* in unregelmäßiger Abfolge herausgegeben.

Sie enthalten Beschreibungen und Ergebnisse der vom Institut (AWI) oder mit seiner Unterstützung durchgeführten Forschungsarbeiten in den Polargebieten und in den Meeren.

Es werden veröffentlicht:

— Expeditionsberichte
  (inkl. Stationslisten und Routenkarten)

— Expeditionsergebnisse
  (inkl. Dissertationen)

— wissenschaftliche Ergebnisse der Antarktis-Stationen und anderer Forschungs-Stationen des AWI

— Berichte wissenschaftlicher Tagungen

Die Beiträge geben nicht notwendigerweise die Auffassung des Instituts wieder.

Notice

The Reports on Polar and Marine Research are issued by the Alfred Wegener Institute for Polar and Marine Research in Bremerhaven*, Federal Republic of Germany. They are published in irregular intervals.

They contain descriptions and results of investigations in polar regions and in the seas either conducted by the Institute (AWI) or with its support.

The following items are published:

— expedition reports
  (incl. station lists and route maps)

— expedition results
  (incl. Ph.D. theses)

— scientific results of the Antarctic stations and of other AWI research stations

— reports on scientific meetings

The papers contained in the Reports do not necessarily reflect the opinion of the Institute.

The „Berichte zur Polar- und Meeresforschung"
continue the former „Berichte zur Polarforschung"

Long-term evolution of (millennial-scale) climate variability in the North Atlantic over the last four million years

Results from Integrated Ocean Drilling Project Site U1313

Bernhard David Adriaan Naafs

Bernhard David Adriaan Naafs
Alfred Wegener Institute for Polar and Marine Research
Am Alten Hafen 26
D-27658 Bemerhaven
Germany
david.naafs@awi.de

I almost wish I hadn't gone down that rabbit-hole—and yet—and yet—it's rather curious, you know, this sort of life!

- Alice in Wonderland

Table of Contents

Abstract

During the past 4 million years (Ma) global climate has changed dramatically. From a state in which global average temperatures were several degrees higher than today and continental ice sheets in the Northern Hemisphere were absent or small it gradually developed towards the regular paced glacial/interglacial cycles that characterize the last 700 thousand years (ka) and during which large continental ice sheets episodically covered large parts of Europe and North America. This PhD thesis examines climate-induced changes in ocean surface characteristics, ice-rafting events, and aeolian input to the North Atlantic during the past 4 Ma. For this purpose changes in the organic geochemical and mineralogical composition in marine sediments from Integrated Ocean Drilling Project (IODP) Expedition 306 Site U1313 are investigated. Site U1313, a re-drill of Deep Sea Drilling Project (DSDP) Site 607, is located in the North Atlantic (41 ºN; 32.57 ºW) at one of the most climatologically sensitive positions in the world. The principal aim of this thesis is to reconstruct the long-term evolution of (millennial-scale) climate variability in the North Atlantic in order to gain more understanding in the mechanisms that drove Quaternary climate change, as these are still largely unknown.

In *Chapter 5* surface water characteristics, sea surface temperatures (SSTs) and marine productivity based on the alkenone biomarker, are reconstructed for the period between 3.68 and 2.45 Ma to gain more understanding in the role of ocean circulation in the North Atlantic during the intensification of the Northern Hemisphere glaciation (NHG). The results demonstrate that during the intensification of the NHG the ocean circulation in the North Atlantic changed significantly. This could be concluded from a decrease in SSTs and increase in marine productivity starting at Site U1313 around 3.1 Ma, which indicate a weakened influence of the warm surface waters from the North Atlantic Current (NAC) and increased influence of the high productivity area associated to the arctic front (AF). The diminished northward heat transport associated with the change in position of the NAC would have caused a cooling of the higher latitudes, which may have encouraged the growth of large continental ice sheets in the Northern Hemisphere.

Chapter 6 provides a reconstruction of changes in mass accumulation rates of lipids derived from terrestrial higher plants waxes (long-chain *n*-alkanes and *n*-alkan-1-ols) at IODP Site U1313 for the past 3.4 Ma to reconstruct changes in aeolian input to the North Atlantic. The results show that together with a change in ocean circulation, the intensification of NHG was associated with a drastic increase in the aeolian input of terrestrial material to the mid-latitude

North Atlantic. During every glacial of the Quaternary the aeolian input to the North Atlantic was up to 30 times higher compared to interglacials. This increase is likely related to a strengthening of the North American sources in the late Pliocene due to the appearance of continental ice sheets and associated glacial outwash plains. Evolutional spectral analysis of the *n*-alkane records demonstrates that throughout the early Pleistocene, variance in the obliquity period (41-ka) dominates aeolian input and hence North American ice sheet dynamics. This argues against suggestions of precession-related variations in Northern Hemisphere ice volume during the early Pleistocene. The close correspondence between aeolian input to the North Atlantic and other dust records indicates a globally uniform response of dust sources to Quaternary climate variability.

In *Chapter 7* a high-resolution record of millennial-scale climate variability, SSTs and ice-rafted debris (IRD) characteristics based on organic geochemical and mineralogical proxies, for the period between 960 and 320 ka is used to gain more understanding of abrupt climate change during periods with different boundary conditions. The results show that following the middle Pleistocene transition (MPT), the source of IRD in the eastern North Atlantic changed. During marine isotope stage (MIS) 16 (~ 643 ka) both the organic geochemical and mineralogical characteristics of IRD indicate the first occurrence of Hudson Strait (HS) Heinrich(-like) events. HS Heinrich events, massive ice-rafting events in the North Atlantic originating from the Laurentide ice sheet (LIS), are among the most dramatic examples of millennial-scale climate variability. As SSTs during MIS 16 were higher compared to previous glacials, the occurrence of HS Heinrich events indicates enhanced ice discharge from the LIS at this time, not simply the survivability of icebergs due to cold conditions in the North Atlantic.

Zusammenfassung

Während der letzten 4.000.000 Jahre (Ma) hat sich das globale Klima dramatisch verändert. Von einem Zustand, in dem die durchschnittlichen globalen Temperaturen mehrere Grad höher waren als heute und kontinentale Eisschilde in der nördlichen Hemisphäre abwesend oder klein waren, entwickelte es sich allmählich hin zu regelmäßigen Glazial/Interglazialzyklen, welche die letzten 700.000 Jahre (ka) charakterisieren und in denen große, kontinentale Eisschilde episodisch große Teile Europas und Nordamerikas bedeckten. Diese Dissertation untersucht Klima induzierte Veränderungen der Meeresoberflächeneigenschaften, Eis-Rafting Ereignisse und den äolischen Eintrag organischen Materials in den Nordatlantik während der letzten 4 Ma. Zu diesem Zweck werden Veränderungen in der organischen, geochemischen und mineralogischen Zusammensetzung mariner Sedimente der Integrated Ocean Drilling Project (IODP) Expedition 306 Site U1313 untersucht. Site U1313, eine Nachbohrung der Deep Sea Drilling Project (DSDP) Site 607, liegt im Nordatlantik (41° N; 32,57° W) an einer der klimatisch sensibelsten Positionen der Welt. Das Hauptziel dieser Doktorarbeit besteht in der Rekonstruktion der langfristigen Entwicklung von Klimavariabilitäten im Nordatlantik, um zu einem besseren Verständnis der noch weitgehend unbekannten Mechanismen, die den quartären Klimawandel bestimmten, beizutragen.

In Kapitel 5 werden Oberflächeneigenschaften, Wasseroberflächentemperaturen (WOT) und marine Produktivität basierend auf Alkenon-Biomarkern für die Zeit zwischen 3,68 und 2,45 Ma rekonstruiert, um die Rolle der Ozeanzirkulation im Nordatlantik während der Intensivierung der Nordhemisphären-Vereisung (NHV) besser zu verstehen. Die Ergebnisse zeigen, dass sich die Ozeanzirkulation im Nordatlantik während der Intensivierung der NHV stark veränderte. Dies könnte aus dem Rückgang der WOT und der Erhöhung der marinen Produktivität an Site U1313 ab rund 3,1 Ma geschlossen werden, was auf einen geschwächten Einfluss des warmen Oberflächenwassers aus dem Nordatlantik-Strom (NAS) und einen erhöhten Einfluss der sich durch hohe Produktivität auszeichnenden Arktischen Front (AF) hindeutet. Die durch Änderung der Position des NAS verursachte Abschwächung des nordwärts gerichteten Wärmetransports führte zu einer Abkühlung in höheren Breiten, die wiederum das Wachstum der großen, kontinentalen Eisschilde in der nördlichen Hemisphäre gefördert haben könnte.

Kapitel 6 enthält eine Rekonstruktion der Veränderungen der Massenakkumulationsraten von Lipiden aus Wachsen höherer terrestrischer Pflanzen (langkettige *n*-Alkane und *n*-Alkan-1-

ole) an IODP Site U1313 für die letzten 3,4 Ma, die Veränderungen im äolischen Eintrag in den Nordatlantik zeigen. Die Ergebnisse zeigen, dass eine Änderung der Ozeanzirkulation mit der Intensivierung der NHV und einer drastischen Erhöhung des äolischen Eintrags terrestrischen Materials in mittleren Breiten des Nordatlantik einhergingen. Während jeder Eiszeit des Quartärs war der äolische Eintrag in den Nordatlantik bis zu 30-mal höher als während der Interglaziale. Dieser Anstieg ist wahrscheinlich mit einer Intensivierung der nordamerikanischen Quellen im späten Pliozän verbunden, die auf die Entwicklung der kontinentalen Eisschilde und Gletscher-assoziierten Sanderflächen zurückzuführen ist. Eine auf evolutionärer Zeitskala durchgeführte Spektralanalyse in den *n*-Alkan-Datensätzen zeigt, dass die Varianz der Obliquität (41-ka) (Schiefe der Erdachse) während des frühen Pleistozäns den äolischen Eintrag und damit die Dynamik des nordamerikanischen Eisschilds dominiert. Dies spricht gegen präzessionsassoziierte Schwankungen im Eisvolumen der nördlichen Hemisphäre im frühen Pleistozän. Der enge Zusammenhang zwischen äolischen Einträgen in den Nordatlantik und anderen Staubdatensätzen deutet auf eine weltweit einheitliche Reaktion der Staubquellen auf die quartäre Klimavariabilität hin.

In Kapitel 7 werden ein hoch aufgelöster Datensatz zur Klimavariabilität auf tausendjähriger Zeitskala, WOTen und Eis-Schutt-Charakteristika (IRD) basierend auf organischen, geochemischen und mineralogischen Proxies für den Zeitraum zwischen 960 und 320 ka herangezogen, um zu einem besseren Verständnis abrupter Klimaveränderungen bei unterschiedlichen Rahmenbedingungen zu gelangen. Die Ergebnisse zeigen, dass sich die IRD-Quelle im östlichen Nordatlantik nach dem mittleren Pleistozänübergang (MPT) veränderte. Während des Marinen Isotopenstadiums (MIS) 16 (~ 643 ka) zeigen sowohl die organisch-geochemischen als auch die mineralogischen Merkmale des IRD das erste Auftreten von Hudson-Strait (HS) Heinrich(-like) Events. HS Heinrich Events, massive Eis-Rafting Ereignisse im Nordatlantik aus dem Laurentidischen Eisschild, gehören zu den dramatischsten Beispielen für Klimavariabilität im Bereich tausendjähriger Skalen. Da SOTs während MIS 16 höher waren als in früheren Eiszeiten, deutet das Auftreten von HS Heinrich Events auf verstärktes Kalben des Laurentidischen Eisschildes in dieser Zeit hin, und nicht auf eine lediglich bessere Überlebensfähigkeit von Eisbergen aufgrund kälterer Bedingungen im Nordatlantik.

Samenvatting

Gedurende de laatste 4 miljoen jaar (Ma) heeft het mondiale klimaat grote veranderingen ondergaan. Van een staat waarin oppervlakte temperaturen verschillende graden hoger waren dan huidig en continentale ijskappen op het noordelijke halfrond afwezig of klein waren, veranderderde het geleidelijk naar de regelmatige glaciaal/interglaciaal cycli die de laatste 700 duizend jaar (ka) kenmerken en gedurende welke enorme ijskappen soms grote delen van Noord-Amerika en Europa bedekte. In deze PhD thesis worden klimaat gerelateerde veranderingen in oppervlakte water karakteristieken (temperatuur en productiviteit), het voorkomen van ijsbergen, en eolische input in de Noord Atlantische Oceaan over de laatste 4 Ma bestudeerd. Hiervoor worden veranderingen in de organisch geochemische en mineralogisch samenstelling in het sediment van IODP Expeditie 306 Site U1313 gebruikt. Site U1313 is geboord op dezelfde locatie als DSDP Site 607 en ligt in de Noord Atlantische Oceaan (41 ºN; 32.57 ºW) op een van de meest klimatologisch gevoelige locaties in de wereld. Het hoofddoel van deze thesis is de lange-termijn-reconstructie van (abrupte) klimaatverandering in de Noord Atlantische Oceaan om meer inzicht te krijgen in de mechanismen achter de variabiliteit in klimaat gedurende het Quartair (de laatste 2.6 Ma), welke tot op heden nog grotendeels onbekend zijn.

In *Hoofdstuk 5* worden oppervlaktewater temperaturen en productiviteit, gebaseerd op variaties in the organisch geochemische samenstelling van het sediment, gereconstrueerd om meer inzicht te krijgen in de rol van de oppervlaktecirculatie in the Noord-Atlantische Oceaan gedurende de intensivering van de glaciatie van het noordelijke halfrond. De resultaten laten zien dat gedurende de intensivering van de glaciatie van het noordelijke halfrond de oppervlaktecirculatie in the Noord Atlantische Oceaan veranderde. Dit kan worden geconcludeerd uit de lagere oppervlakte-temperaturen en hogere oppervlakte productiviteit op Site U1313 die rond 3.1 Ma begon en een verminderde invloed van de Noord Atlantische Stroming en toenemende invloed van het Arctische Front impliceren. De afname in noordwaarts warmtetransport, die gepaard ging met de verandering in oppervlakte circulatie, zal tot een afkoeling van de hogere breedtegraden hebben geleid, welke mogelijk heeft bijgedragen tot de groei van grote ijskappen in het noordelijke halfrond.

In *Hoofdstuk 6* worden de veranderingen in the accumulatie van lipiden afkomstig van hogere land planten (lange-keten *n*-alkanen en *n*-alkanolen) in het sediment van Site U1313 gedurende de laatste 3.4 Ma gebruikt om variaties in eolische input te reconstrueren. De resultaten laten zien dat gelijktijdig met de verandering in oceaan circulatie, de intensivering

van de glaciatie van het noordelijke halfrond was gepaard met een dramatische toename in de eolische input in de Noord Atlantische Oceaan. Gedurende elk glaciaal van het Quartair was de eolische input in the Noord Atlantische Oceaan tot maximaal 30 keer hoger dan gedurende interglacialen. Deze toename in eolische input in het laat Plioceen is waarschijnlijk gerelateerd aan de versterking van de stofbronnen in Noord-Amerika door de verschijning van continentale ijskappen en spoelzandwaaiers. Evolutie spectra van de *n*-alkaan records laten zien dat gedurende het vroege Pleistoceen, veranderingen in de Noord-Amerikaanse ijskap werden gedomineerd door veranderingen in planetaire obliquiteit. Dit komt niet overeen met eerdere suggesties die suggereerden dat planetaire precessie het belangrijkst was. Het begin van verhoogde eolische input rond 2.7 Ma valt samen met een gelijke toename op andere plekken in de wereld. Samen met de overeenkomst tussen de eolische input in de Noord Atlantische Oceaan en Antarctica gedurende de laatste 800 ka laat dit zien dat de verschillende stof bronnen uniform reageerden op de klimaatverandering gedurende het Quartair.

In *Hoofdstuk 7* wordt een record met hoge resolutie van oppervlaktewatertemperaturen en ht voorkomen van ijsbergen in de periode van 960 en 320 ka gebruikt om meer inzicht te krijgen in het voorkomen van abrupte klimaatveranderingen gedurende periodes met andere randvoorwaarden. De resultaten laten zien dat na de midden Pleistoceen transitie de bron van ijsbergen in de Noord-Atlantische Oceaan veranderde. Gedurende Mariene isotopen stadium (MIS) 16 (~ 643 ka) veranderde zowel de organisch geochemische als mineralogisch samenstelling van puin afkomstig van ijsbergen, wat er op wijst dat materiaal afkomstig van de Laurentide ijskap voor de eerste keer Site U1313 bereikte. Gedurende deze abrupte gebeurtenissen, Hudson Strait (HS) Heinrich Events genaamd naar de Hudson Strait in Canada waar de meeste ijsbergen vandaan kwamen, was een groot deel van Noord-Atlantische Oceaan bedekt met ijsbergen afkomstig van de Laurentide ijskap. Omdat oppervlaktewatertemperaturen hoger waren tijdens MIS 16 dan voordien, betekent dit dat het eerste HS Heinrich Event gerelateerd was aan een toename in het afbreken van ijsbergen van de Laurentide ijskap en niet simpel door het langere overleven van de ijsbergen in de Noord-Atlantische Oceaan vanwege koudere oppervlaktewatertemperaturen.

1   General Introduction and Outline

Understanding the mechanisms and causes of abrupt climate change is one of the major challenges in global climate change research today [Clark *et al.*, 1999b] and constitutes a vital initiative of the Initial Science Plan of IODP. In this context, determining the long-term evolution of (millennial-scale) climate change may provide clues to the mechanisms responsible for (abrupt) climate change and was the overall objective of the international multidisciplinary research program of IODP Expedition 303/306 [Channell *et al.*, 2004]. In this thesis sediment samples recovered during IODP Expedition 306 at Site U1313, located in the North Atlantic, are used to study the long-term evolution of (millennial-scale) climate variability in the North Atlantic. Using various organic geochemical and mineralogical proxies variations in sea surface temperature (SST), ice sheet dynamics (ice-rafting events), and atmospheric input in the North Atlantic over the last 4 million years (Ma) are reconstructed.

In the following 3 Chapters of this thesis a general introduction to the topic is provided. *Chapter 2* provides a general introduction into ocean circulation in the North Atlantic. *Chapter 3* provides an overview of climate during the past 4 Ma. *Chapter 4* provides an introduction into the material and methods used in this thesis. These three chapters are followed by the three chapters that contain the manuscripts that are published, submitted, or in preparation and present the main results. In these manuscripts the questions state below will be addressed and provide new insights into the mechanisms behind Quaternary climate variability. To conclude, *Chapter 8* contains a summary of the main conclusions and provides future perspectives.

- **Q1**: Did surface circulation in the North Atlantic differ in the geological past and what influence did changes in surface circulation have on climate? In particular, did the surface circulation change during the intensification of Northern Hemisphere glaciation during the late Pliocene?

In *Chapter 5*, a detailed record of alkenone based estimates of SSTs and surface productivity provides new insights in the position of the North Atlantic current (NAC) during the late Pliocene. The results demonstrate that the position of the NAC changed during the intensification of Northern Hemisphere glaciation, which probably led to a reduction in northward heat transport during this period and possible contributed to the onset of widespread glaciation.

• **Q2**: What was the long-term trend in SSTs in the North Atlantic over the past 4 Ma? Does this resemble the increasing trend seen in benthic foraminiferal $\delta^{18}O$ records?

In *Chapter 6*, an orbitally-resolved record of alkenone-based SSTs covering the past 3.5 Ma is provided. The record demonstrates that surface waters in the North Atlantic were cooling during the last 3 Ma, with two major steps occurring between 3.1-2.1 Ma and 1.5-0.3 Ma. Cooling is the most pronounced during glacials between 1.3 and 0.4 Ma, while interglacial SSTs remained constant during the last 1 Ma. These trends are similar as seen in benthic foraminiferal $\delta^{18}O$ records. When compared to the SST record from the more northern located ODP Site 982, the results demonstrate that the long-term latitudinal SST-gradient between 57 and 41 ºN in the North Atlantic did not significantly change during the Pleistocene as the cooling in the North Atlantic was uniform.

• **Q3**: Marine and ice core records from the Southern Hemisphere demonstrated that during glacials the dust sources strengthened, predominantly related to the development of large glacial outwash plains in Patagonia. However, no long-term records from the northern North Atlantic exist that lies downwind from the glacial outwash plains in North America. It therefore remains unknown whether variations in aeolian input on a glacial/interglacial basis, similar as observed in the Southern Hemisphere, took place in the Northern Hemisphere. More over, the use of long sediment records that extend beyond the last 800 ka, which at current is the limited for the Antarctic ice cores, could provide information about the onset of increased aeolian input during glacials.

In *Chapter 6*, an orbitally-resolved record of variations in aeolian input into the North Atlantic is given. Using the accumulation rate of biomarkers specific for higher plant material, it is shown that during the intensification of the Northern Hemisphere glaciation the aeolian input of terrestrial material into the North Atlantic drastically increased. During the last 2.7 Ma the aeolian input was high during glacials, while low during interglacials. The variation in aeolian input is identical as seen in the Southern Hemisphere and is suggested to be linked to the appearance of large glacial outwash plains on the North American continent around 2.7 Ma.

• **Q4**: According to the classical Milankovitchs theory, variations in high-latitude summer solstice insolation were the primary forcing for the glacial/interglacial cycles of the Quaternary. A major problem for the standard orbital hypothesis is that although high-latitude summer insolation is mainly driven by changes in precession, records of early Pleistocene benthic foraminiferal $\delta^{18}O$ (reflecting predominantly variations in continental ice volume) varied mainly at the obliquity period. What was the dominant orbital

parameter in the records of surface water characteristics at Site U1313? Did obliquity also dominate these records during the early Pleistocene?

In *Chapter 6,* evolutionary spectra for the long-term records from Site U1313 are computed and show that both sea surface temperatures and aeolian input at Site U1313 are dominated by obliquity during the early Pleistocene. The absence of strong precession periods (23 and 19 ka) in the records of aeolian input during the early Pleistocene suggest that the North American ice-sheet did not vary significantly according to precession during the early Pleistocene. According to these results it is unlikely that strong precession related changes in ice volume in both Hemispheres did occur but cancel out in globally integrated proxies such as foraminiferal $\delta^{18}O$ as previously suggested. Other mechanisms are therefore needed to explain the strong dominance of the obliquity period during the early Pleistocene.

• **Q5**: Was millennial-scale climate variability a persistent feature of global climate during the Pleistocene? Did SSTs control the occurrence of IRD-events in the North Atlantic during the Pleistocene? Did changes occur in the source of ice-rafting events over time?

In *Chapter 7*, a high-resolution record (0.5 ka resolution) of alkenone-based SSTs together with a record of IRD-characteristics covering the period from 960 to 320 ka; the end of the middle Pleistocene transition (MPT), is provided. The results show that millennial-scale climate variability characterized the entire record, with IRD-events occurring during every glacial. However, the end of the MPT is characterized by a change in IRD-source with material originating from the Laurentide ice sheet appearing in the North Atlantic; Hudson Strait (HS) Heinrich(-like) Events. Our results show that SSTs did not control this onset of HS Heinrich(-like) Events and thus indicate enhanced ice discharge from the Laurentide ice sheet at this time, not simply the survivability of icebergs due to cold conditions in the North Atlantic.

• **Q6**: HS Heinrich Events have a large impact on global climate due to associated feedback mechanisms in the Southern Ocean and have been proposed to initiate the major glacial terminations that characterize the last 450 ka. Did HS Heinrich(-like) Events occur prior to 450 ka, when "luke-warm" conditions dominated interglacials in Antarctica?

The results presented in *Chapter 7*, indicate that HS Heinrich(-like) Events did occur prior to 450 ka and thus suggest that the occurrence of HS Heinrich events alone is not enough to initiate dramatic deglaciations.

2   The North Atlantic Ocean

The oceans play an important role in global climate due to their capacity of redistributing heat across the globe and regulating atmospheric CO_2 levels on glacial/interglacial time scales. The North Atlantic plays a crucial role as it is one of the few regions in the world where deep water formation takes place (Figure 1). At present the North Atlantic is characterized by a continuous flow of warm and salty surface waters from the (sub)tropics towards the higher latitudes by means of the Gulf Stream and North Atlantic Current (NAC). In the higher latitudes of the North Atlantic (e.g., north of 50 °N) the temperature contrast between the warm surface waters and overlying cold atmosphere leads to a cooling of the surface waters as sensible heat is lost from the ocean to the atmosphere, which increases the density of the surface waters as they move northwards. The release of sensible heat has a large influence on climate in the region of the North Atlantic. In the northern North Atlantic the continuous cooling causes surface waters to become denser than the underlying waters and as a result they ultimately sink to the deep ocean to form well-ventilated and nutrient-poor North Atlantic Deep Water (NADW). The northward transport of warm and salty surface waters together with the return flow of cold and dense waters NADW in the deep ocean constitutes the North Atlantic limb of the meridional overturning circulation (MOC).
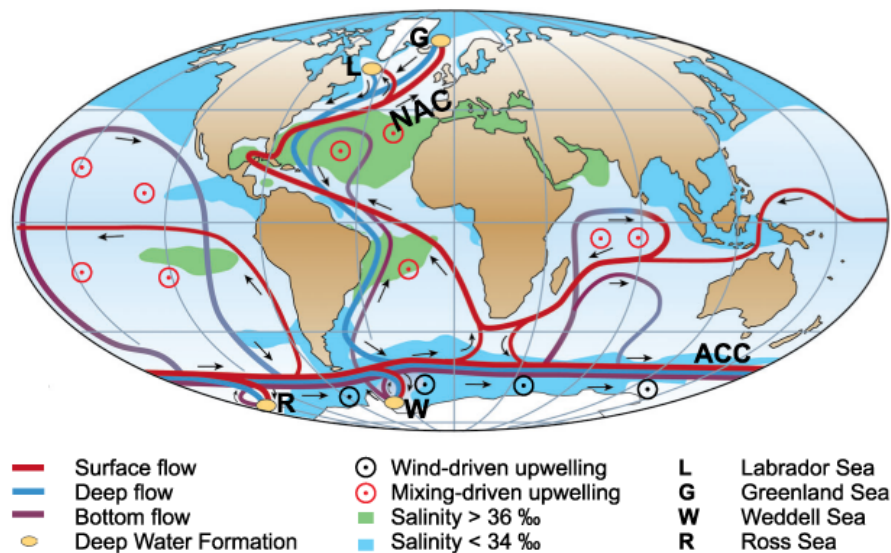
Figure 1; Meridional overturning circulation

Overview of global ocean circulation that shows the northward movement of warm and salty surface waters in the North Atlantic and the return flow to the south of cold waters in the deep ocean [Rahmstorf, 2007]. NAC = North Atlantic current.

As ocean circulation plays such an important role in redistributing heat towards the polar regions and the rate of deep water formation controls atmospheric CO_2 levels, variations in ocean circulation have a significant impact on climate. However, the interaction between ocean circulation and climate is not a simple one-way system as the conditions around the North Atlantic itself can also have an impact on ocean circulation. For example, during the last glacial the episodic input of fresh water to the North Atlantic, due to the melting of the continental ice sheets (cryosphere), negatively influenced the flow of warm surface waters northwards and rate of deep water formation in the higher latitudes (see *Chapter 3*). In addition, the surface currents in the North Atlantic are mainly wind-driven and changes in the atmospheric circulation thus can influence ocean surface currents. The complex interactions between the ocean, atmosphere, and cryosphere make the North Atlantic one of the most climatically sensitive regions in the world that responds quickly to changes in climate as explained in the following chapter.

3   Climate during the past 4 Ma

Over the past 4 Ma, global climate changed significantly with the largest climatically changes taking place in the Northern Hemisphere, predominantly circum the North Atlantic. In the Pliocene global climate was significantly warmer than today with average temperatures 2-3 degrees higher than today [e.g., Haywood *et al.*, 2005]. The ice sheets in the Northern Hemisphere were absent (North American and Eurasian ice sheets) or present as small and local ice sheets (Greenland) [Kleiven *et al.*, 2002; Lunt *et al.*, 2008] and surface water temperatures in the North Atlantic were several degrees higher due to an intense North Atlantic current [Cronin, 1991; Dowsett *et al.*, 1992; Robinson, 2009]. However, for largely unknown reasons, these warm conditions terminated during the late Pliocene (~ 2.7 Ma) as the glaciation of the Northern Hemisphere intensified and extensive continental ice sheets appeared circum the North Atlantic [e.g., Shackleton *et al.*, 1984; Maslin *et al.*, 1998; Kleiven *et al.*, 2002; Balco and Rovey, 2010].

Continental ice sheets have a large influence on global climate as they have the ability to amplify and transmit local variations in climate (e.g., high-latitude insolation) [Clark *et al.*, 1999a]. Most knowledge about the variations in global climate is based on studies using benthic foraminiferal $\delta^{18}O$ that predominantly is used as a measure of global ice volume, although deep ocean temperatures can also influence this proxy. Over the last 35 years the numerous studies showed that after the intensification of the Northern Hemisphere glaciation, during the early Pleistocene benthic foraminiferal $\delta^{18}O$ varied with symmetrical low-

amplitude variations, presumably responding linearly to the 41 thousand years (ka) obliquity frequency [Imbrie *et al.*, 1992] (Figure 2). This changed during the middle Pleistocene transition, between 1.25 and 0.7 Ma [Clark *et al.*, 2006], when glacial conditions intensified and the glacial/interglacial variability changed to a 100 ka variance with high-amplitude asymmetrical variations in δ^{18}O [Maslin and Ridgwell, 2005]. During the last 700 ka global climate is dominated by this regular 100-ka paced "saw-tooth" pattern of glacial/interglacial changes that are the result of a non-linear response of the climate system to orbital forcing [e.g., Hays *et al.*, 1976; Imbrie *et al.*, 1993]. It is important to note that not only the benthic foraminiferal δ^{18}O record demonstrates this pattern of glacial/interglacial changes, but that the variations in (high-latitude) ice volume influenced global climate with changes in dust deposition, sea surface temperatures, ice-rafting events, etc. taking place around the world during glacials.
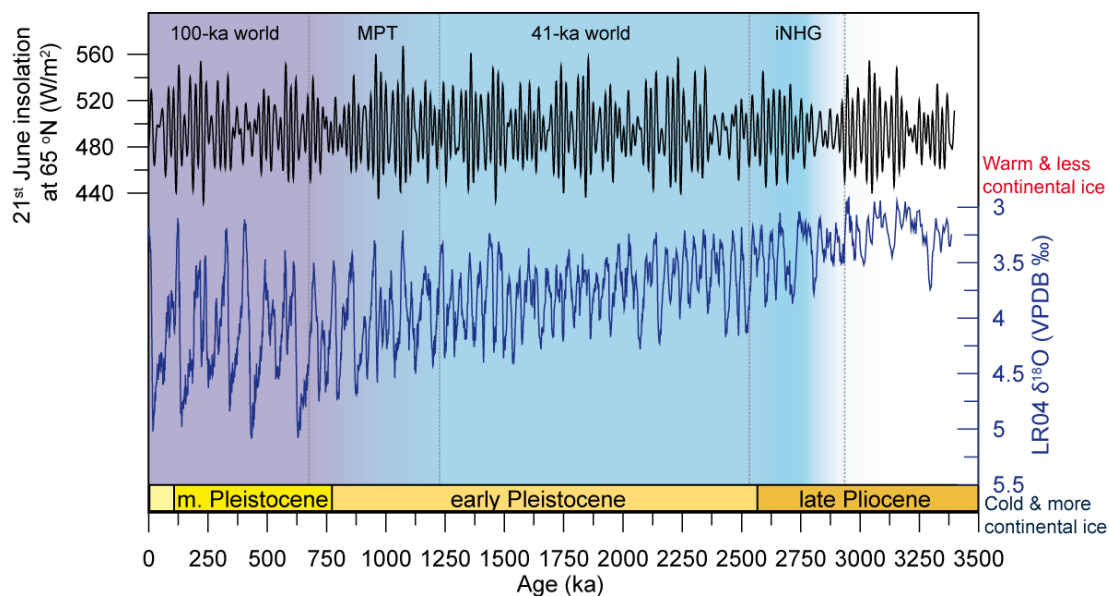
Figure 2; Plio- and Pleistocene climate

Benthic foraminiferal δ^{18}O stack of the last 3.5 Ma [Lisiecki and Raymo, 2005] together with the summer solstice insolation at 65 ºN [Laskar *et al.*, 2004], the classically assumed main control on Northern Hemisphere ice volume [Milankovitch, 1941]. The δ^{18}O stack demonstrates a general cooling trend in global climate together with an increase in global ice volume over the past 3 Ma. The glacial/interglacial variability changed from symmetrical low-amplitude variations during the early Pleistocene (the "41-ka world") to high-amplitude asymmetrical variations during the middle and late Pleistocene (the "100-ka world"). iNHG = intensification of the Northern Hemisphere glaciation, MPT= middle Pleistocene transition.

Superimposed on this regular glacial/interglacial variability, the last glacial cycle is characterized by high-amplitude millennial-scale climate variability as manifested by Dansgaard/Oeschger cycles and, most importantly, Heinrich Events [e.g., Bond and Lotti, 1995; EPICA Community Members, 2006]. Heinrich events are episodes of massive ice rafting in the North Atlantic due to the collapse of the continental ice sheets in the Northern Hemisphere [e.g., Heinrich, 1988; Hemming, 2004]. During Heinrich events the melting of icebergs and associated meltwater pulse led to increased deposition of ice-rafted debris (IRD) [Bond *et al.*, 1992], severe cooling of surface water, and collapse of surface water productivity in the North Atlantic [Villanueva *et al.*, 1997; Bard *et al.*, 2000]. Although Heinrich events were local phenomena with IRD-depostion restricted to the northern North Atlantic (the IRD-belt between 60 and 40 ºN [Ruddiman, 1977]), they had a global impact (Figure 3). This can be explained by the feedback mechanisms associated to these events.
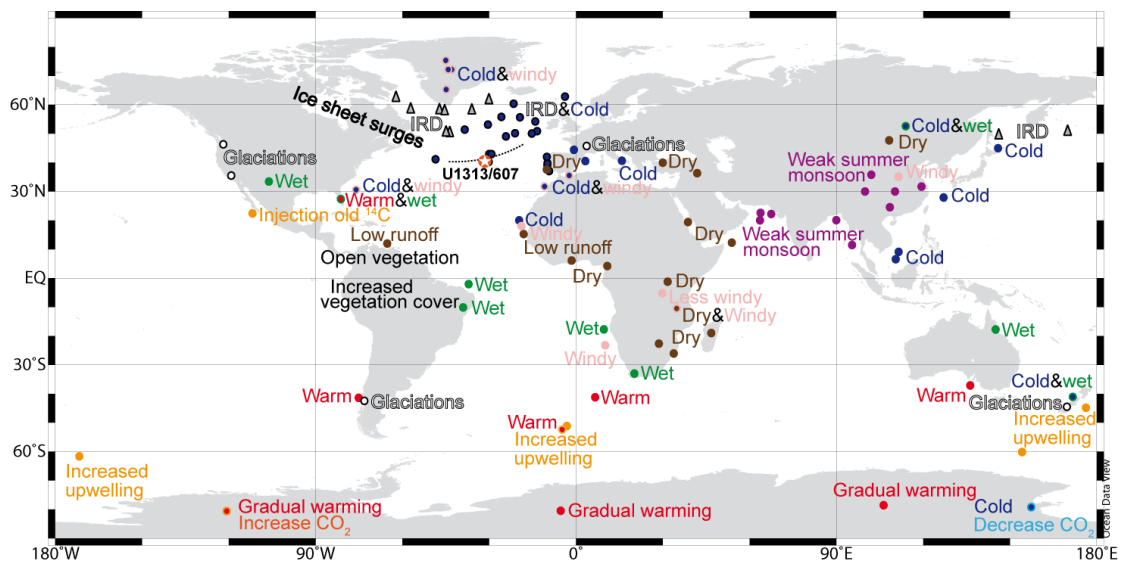
Figure 3; Overview of the impact of Heinrich events

Compilation of the impact of Heinrich events on climate across the globe based on data for all Heinrich events of the last glacial cycle, with a bias towards data from Heinrich event H1. In general the region of the North Atlantic cooled, Europe is characterized by colder and drier climate, the East Indian and Asian summer monsoon weakened, the ITCZ moved southwards, and the Southern Hemisphere warmed during Heinrich events. **Review papers**: [Leuschner and Sirocko, 2000; Voelker, 2002; Hemming, 2004; Denton *et al.*, 2010; Hessler *et al.*, 2010; Stager *et al.*, 2011]; **Greenland:** [Dansgaard *et al.*, 1993; Mayewski *et al.*, 1994; Grootes *et al.*, 2001; NGRIP members, 2004]; **Antarctica:** [Jouzel *et al.*, 1987; Blunier and Brook, 2001; EPICA Community Members, 2006]; **Atlantic**: [Andrews and Tedesco, 1992; Broecker *et al.*, 1992; Bond *et al.*, 1993; Andrews *et al.*, 1994; Keigwin *et al.*, 1994; Bond and Lotti, 1995; Robinson *et al.*, 1995; Zhao *et al.*, 1995; Cortijo *et al.*, 1997; Rosell-Melé *et al.*, 1997; Villanueva *et al.*, 1997; Andrews, 1998; Arz *et al.*, 1998; McManus *et al.*, 1999; Bard *et al.*, 2000; Peterson *et al.*, 2000; Rosell-Melé *et al.*, 2000; de Abreu *et al.*, 2003; McManus *et al.*, 2004;

Expedition 303 Scientists, 2006; López-Martínez *et al.*, 2006; Rashid and Grosjean, 2006; Jullien *et al.*, 2007; Martrat *et al.*, 2007; Peck *et al.*, 2007; Rashid and Boyle, 2007; Mulitza *et al.*, 2008; Hodell *et al.*, 2010; Penaud *et al.*, 2010; Voelker and de Abrue, 2010]; **Southern Ocean:** [Sachs and Anderson, 2005; Calvo *et al.*, 2007; Anderson *et al.*, 2009; Barker *et al.*, 2009]; **Pacific:** [Kotilainen and Shackleton, 1995; Li *et al.*, 2001; Sakamoto *et al.*, 2005; Harada *et al.*, 2006; Lamy *et al.*, 2007]; **Mediterranean:** [Cacho *et al.*, 2000]; **Arabian Sea:** [Reichart *et al.*, 1998; Schulz *et al.*, 1998]; **China Sea:** [Kiefer and Kienast, 2005]; **Asia:** [Wang *et al.*, 2001; Cheng *et al.*, 2009]; **South America:** [Lowell *et al.*, 1995; Wang *et al.*, 2004]; New Zealand: [Whittaker *et al.*, 2011]; **Australia:** [Muller *et al.*, 2008]; **Europe**: [Thouveny *et al.*, 1994; Ivy-Ochs *et al.*, 2006]; **North American:** [Phillips *et al.*, 1996; Grimm *et al.*, 2006; Asmerom *et al.*, 2010]; **Africa:** [Stager *et al.*, 2002; Brown *et al.*, 2007; Tierney and Russell, 2007].

Crucial is that Heinrich events affected one of the most climatically sensitive regions in the world; the North Atlantic. The expansion of polar/arctic water masses and sea-ice into the North Atlantic due to the severe cooling of surface waters during Heinrich events led to a southward displacement of the major weather fronts such as the Intertropical convergence zone and Southern Hemisphere westerlies [e.g., Dahl *et al.*, 2005], which influenced climate in South America [Arz *et al.*, 1998], Africa [Hessler *et al.*, 2010], Asia [Cheng *et al.*, 2009], and increased wind-driven upwelling in the Southern Ocean [Anderson *et al.*, 2009]. In addition, the freshening of surface waters and expansion of sea-ice severely reduced deep-water formation in the northern North Atlantic [e.g., Rahmstorf, 2002; McManus *et al.*, 2004], which triggered increased overturning in the Southern Ocean [Sigman *et al.*, 2007] and reduced northward heat transport that led to the built-up of warm and salty waters directly south of the IRD-belt and in the South Atlantic [Schmidt *et al.*, 2006; Benway *et al.*, 2010]. In its turn, the increased overturning and upwelling in the Southern ocean during Heinrich events led to a warming of ocean temperatures in the Southern Hemisphere [Barker *et al.*, 2009] (the bipolar seesaw) and release of ancient CO_2 from the deep-ocean [Marchitto *et al.*, 2007]. Due to these feedback mechanisms in the Southern Ocean, Heinrich event 1 appears to be crucial to start the last glacial termination [e.g., Denton *et al.*, 2010; Sigman *et al.*, 2010]. In addition, Chinese speleothem records indicate that similar a similar process took place during early terminations and highlights the importance of the North Atlantic in driving global climate [Cheng *et al.*, 2009].

4 Materials and methods

4.1 Study material

Marine sediments form one of the best archives of climate change as they continuously accumulate over millions of years. Most of the knowledge of long-term changes in North Atlantic climate comes from Deep Sea Drilling Project (DSDP) Sites 607 and 609 [Ruddiman *et al.*, 1987b; Ruddiman *et al.*, 1989; Raymo *et al.*, 1990; Raymo *et al.*, 1992], drilled during Leg 94 in 1983 [Ruddiman *et al.*, 1987a]. However, the drilling during DSDP Leg 94 preceded the advent of shipboard capability for construction of composite records, preventing the reconstruction of continuous high-resolution records. In 2005 during Integrated Ocean Drilling Program (IODP) Expedition 303/306 both sites were thus re-drilled to obtain long and continuous high-resolution records of the last 5 Ma from the North Atlantic [Channell *et al.*, 2006; Stein *et al.*, 2006].
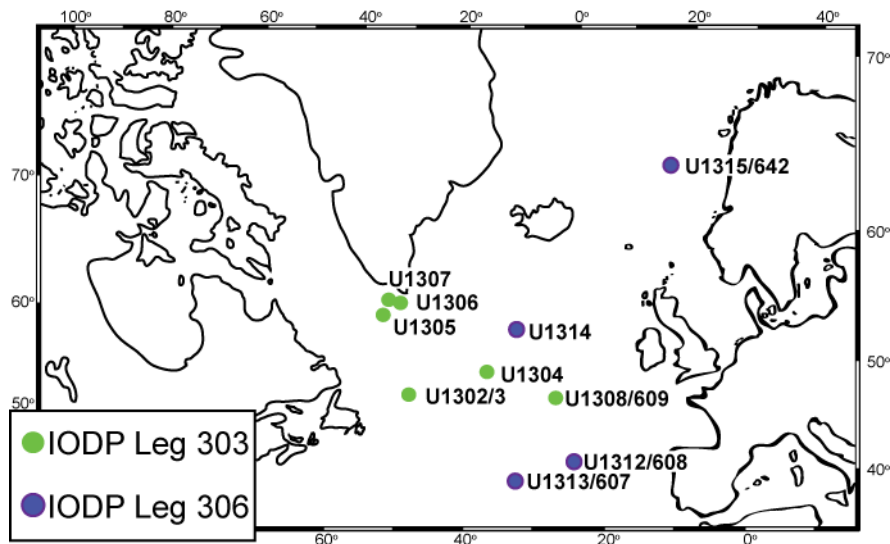
Figure 4; IODP Expeditions 303/306

Overview of the different sits drilled during IODP Expeditions 303/306 in the North Atlantic [Channell *et al.*, 2006].

This thesis uses samples from IODP Expedition 306 Site U1313 to reconstruct the long-term evolution of variations in surface water characteristics in the North Atlantic. Site U1313 is located at 41.00 ºN; 32.57 ºN in the North Atlantic and is a re-drill of Deep Sea Drilling Project (DSDP) Leg 94 Site 607 [Ruddiman *et al.*, 1987a]. Site 607/U1313 is located at one of the most climatically sensitive regions in the world as, 1) bottom water masses alternated between North Atlantic Deep Water (NADW) and AntArctic Bottom Water (AABW) on a glacial/interglacial bases [Raymo et al., 1990; Raymo et al., 1992], 2) it is located within the ice-rafted debris (IRD) belt [Ruddiman, 1977], where large variations in surface water

characteristics occurred during IRD-events [Bard et al., 2000; Rosell-Melé et al., 2002], 3) it is located close to the most southern position of the Arctic Front (AF), which is characterized by a steep gradient in sea-surface temperatures (SSTs) [Pflaumann et al., 2003], and 4) it is located under the direct influence of the westerly winds, receiving aeolian material from the North American continent. Site 607 has therefore proven to be the benchmark site for studies of the long-term evolution of North Atlantic palaeoceanography [e.g., Raymo et al., 1989; Ruddiman et al., 1989; Raymo et al., 1990; Raymo et al., 1992; Sosdian and Rosenthal, 2009; Lawrence et al., 2010]. With the re-drilling of Site 607, Site U1313 now provides the rare opportunity of a continuous high-resolution sediment record covering the complete period from the Pliocene to the Pleistocene at this climatic sensitive location.
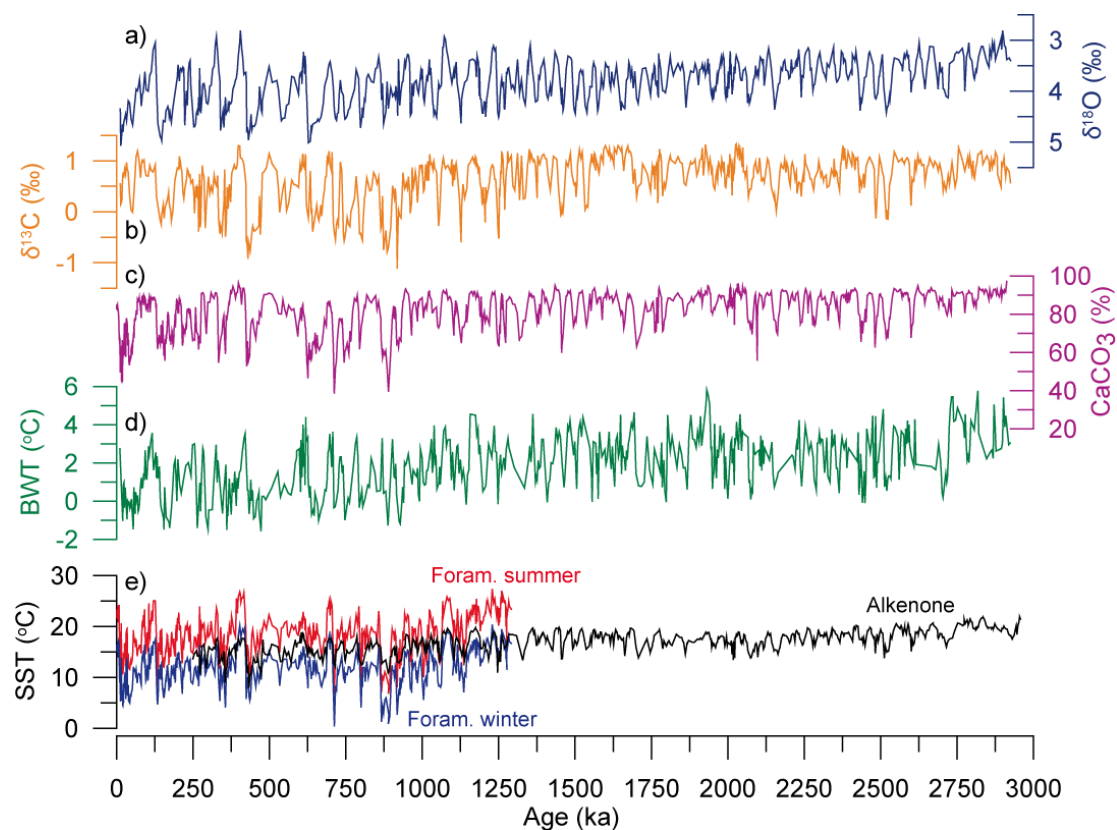
Figure 5; DSDP Site 607

Overview of the different climatic records obtained using material from DSDP Site 607 that made Site 607 the benchmark site for studies of the long-term evolution of North Atlantic palaeoceanography. **a,b**) Benthic foraminiferal $\delta^{18}O$ and $\delta^{13}C$ [Raymo *et al.*, 1989; Ruddiman *et al.*, 1989; Raymo *et al.*, 1990; Raymo *et al.*, 1992], **c**) carbonate content [Ruddiman *et al.*, 1989], **d**) Bottom water temperatures [Sosdian and Rosenthal, 2009], **e**) Summer and winter SSTs based on planktonic foraminiferal assemblages [Ruddiman *et al.*, 1989] together with alkenone-based SSTs [Lawrence *et al.*, 2010].
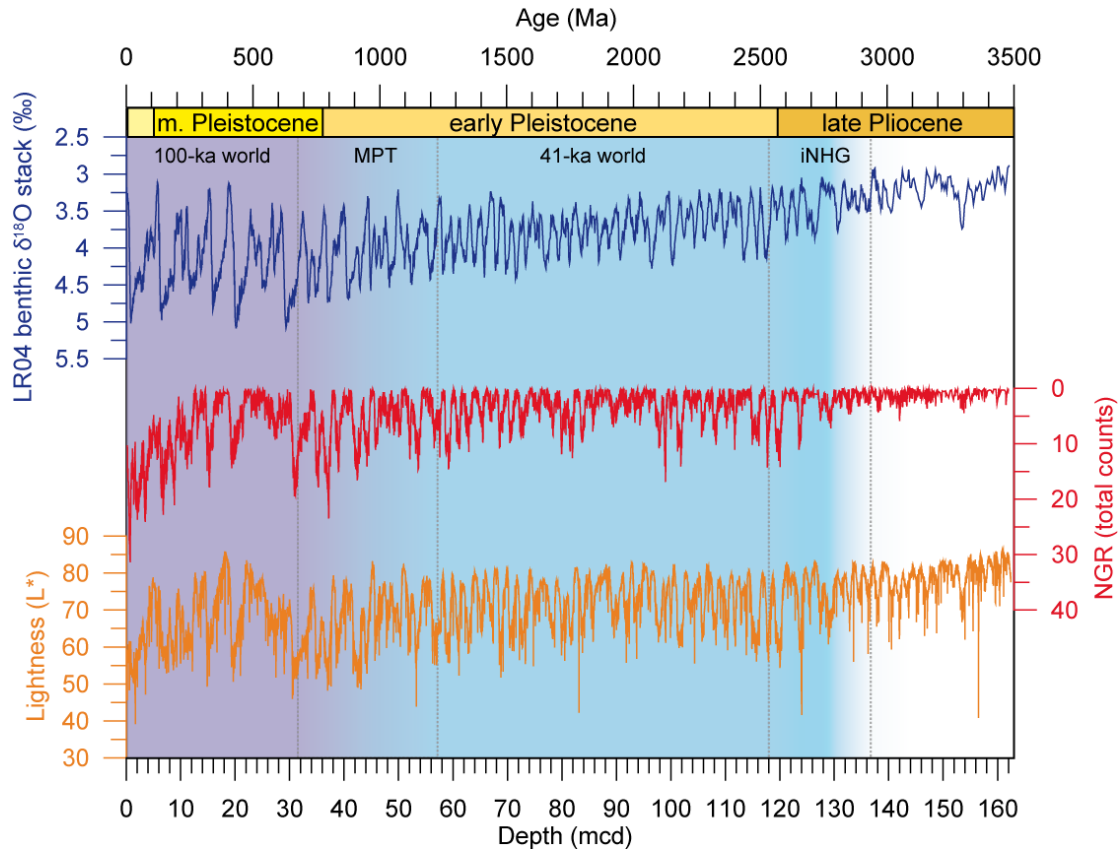
Figure 6; Shipboard data from IODP Site U1313

Lightness and Natural Gamma Radiation (NGR) for the primary splice of Site U1313 versus depth together with the LR04 benthic foraminiferal $\delta^{18}O$ stack [Lisiecki and Raymo, 2005]. Due to the very constant sedimentation rates at U1313, the records versus depth can easily be correlated to the LR04 stack [Channell *et al.*, 2006]. These records already show the large glacial/interglacial changes that characterize the upper 130 mcd of Site U1313 and demonstrate that the first manifestation of these changes occurred during the intensification of Northern Hemisphere glaciation in the late Pliocene [after Stein *et al.*, 2006].

Sampling of IODP Site U1313 was predominantly carried out during the IODP sampling party in 2005. The data in this thesis is almost exclusively obtained using samples from the primary splice, which consists of Holes B and C. The top 41 meter below sea floor (mbsf) of Site U1313, representing the last 1 Ma, was sampled using a 2 cm resolution. Given the extremely constant sedimentation rates at Site U1313 [Stein *et al.*, 2006], this translates into a temporal resolution of between 400 and 500 years. The remaining 260 mbsf of Site U1313, reaching back into the Miocene, was sampled using a 20 cm resolution and hence, temporal resolution between 4 and 5 ka.

4.2 Methods

The main part of this thesis is based on data produced by using organic geochemistry. Since organic geochemistry was first used to study past climate in the 1960s a wide variety of organic proxies have been developed. In this thesis, a selection of organic proxies is used to reconstruct surface characteristics (e.g., sea surface temperatures, surface water productivity, etc.) at the study site. Below, each proxy is briefly explained to provide a general background for the work discussed in *Chapters 5-7*.

4.2.1 Analytical techniques

Samples were freeze-dried directly after sampling and stored at 4 ºC until further processing took place. To obtain the soluble organic fraction that can be used to determine the various organic proxies, bulk samples were extracted with dichloromethane using an accelerated solvent extraction (ASE 200, DIONEX). Organic compounds were then identified and quantified using a gas chromatograph, coupled to a time of flight mass-spectrometer (GC/TOF-MS). The main advantage of this method above the classical GC/FID method is that using the GC/TOF-MS significantly reduces instrumental time, while collecting full-range spectra at high data rates, and allows the reconstruction of long high-resolution records. A range of standards was used to quantify the different organic compounds. A validated procedure was used to convert GC/TOF-MS C_{37} alkenone ratios to calibrated GC/FID values [Hefter, 2008]. To quantify the abundance of long-chain *n*-alkan-1-ols, samples were derivatized with N,O bis(trimethylsilyl) trifluoroacetamide shortly before analysis.
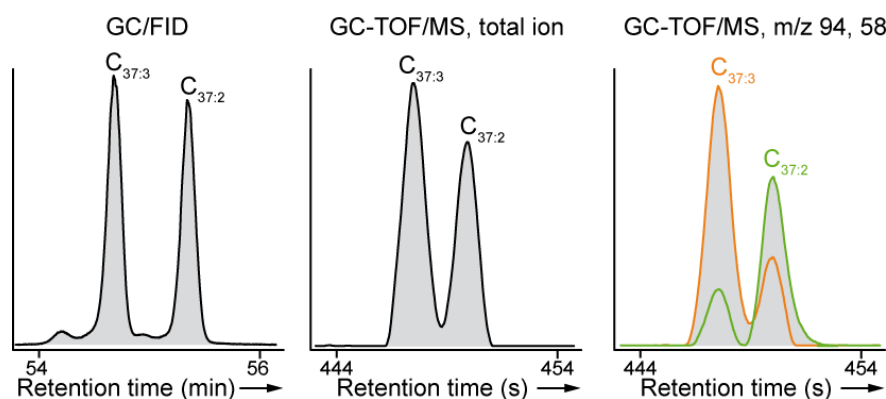
Figure 7; GC-methods

Comparison between the classical GC/FID method to determine the alkenone unsaturation index and the GC-TOF/MS method used in this study. All chromatograms were obtained using the same standard. $C_{37:3}$ and $C_{37:2}$ indicate the di- and tri-unsatureated alkenones used in the alkenone unsaturation index, determined using the m/z 58 and 94 respectively [Hefter, 2008]. Note the significantly reduced instrumental time for the GC-TOF/MS method.

4.2.2   Sea surface temperatures ($U_{37}^{k}{}'$)

Alkenones are highly resistant organic compounds, long-chain mono-ketones to be more exact (Figure 8), that are produced by members of the class *Prymnesiophyceae*, primarily the coccolithophores (single-celled phytoplankton) *Emiliania huxleyi* as well as *Gephyrocapsa oceanica* [e.g., Volkman *et al.*, 1980; Volkman *et al.*, 1995]. After alkenones were found to be tracers for predominantly *E. huxleyi* [Volkman *et al.*, 1980]*,* Brassel et al., [1986] discovered that these algae change the degree of unsaturation of the C_{37} alkenones according to the temperature of the medium they grow in. This led to the development of the now widely used alkenone unsaturation index ($U_{37}^{k}{}'$), which uses the relative abundance of the di- and tri-unsatured alkenones and together with the global core-top calibration can be used to accurately reconstruct mean annual sea surface (0m) temperatures:

$$U_{37}^{k}{}' = \frac{C_{37:2}}{C_{37:2} + C_{37:3}} \qquad \text{[Prahl and Wakeham, 1987]}$$

$$U_{37}^{k}{}' = 0.033 \bullet SST + 0.044 \qquad \text{[Müller \textit{et al.}, 1998]}$$

In which $C_{37:2}$ and $C_{37:3}$ represent the abundance of the di- and tri-unsatured alkenone and SST stands for Sea Surface Temperatures. However, although alkenones are widely used in paleoceanographic studies, 30 years after their discovery the exact function of these organic compounds in coccolithophores is still unknown. Originally alkenones were proposed to play a role in regulating membrane fluidity, but lately it appears more likely they function for energy storage within the cell [see Eltgroth *et al.*, 2005 and references therein]. Even so, alkenone measurements are now considered routine and widely applied to accurately reconstruct SSTs [e.g., Rosell-Melé *et al.*, 2001].
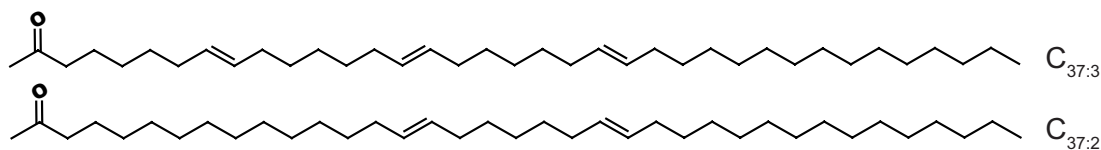
Figure 8: Alkenones

Molecular structure of the di- and tri-unsatured alkenone that is used in the alkenone unsaturation index ($U_{37}^{k}{}'$).

4.2.3   Surface water productivity (alkenone abundance)

As stated above, since the 1980s alkenones are known to be indicative for the occurrence of *E. huxleyi* [Volkman *et al.*, 1980]. *E. huxleyi* is a cosmopolitan phytoplankton specie that is found from the sub-polar to the tropical ocean and is important for total primary productivity in the world oceans. In the North Atlantic, for example, the phytoplankton community is dominated by coccolithophores, predominantly the alkenone producer *Emiliania huxleyi* [Gregg and Casey, 2007]. In sediment trap data from the North Atlantic the total flux of alkenones therefore tracks productivity in the overlying surface water mass [Rosell-Melé *et al.*, 2000]. Significant (± one order of magnitude) variations in the total flux of C_{37} alkenones to the sea floor are thus indicative for changes in the dominant phytoplankton group and can be used to determine changes in marine surface productivity [Lawrence *et al.*, 2007].

Figure 9; Emiliania huxleyi bloom south of Cornwall (UK). Landsat image from 24th July 1999, courtesy of Steve Groom, Plymouth Marine Laboratories

Source: http://www.nhm.ac.uk/hosted_sites/ina/galleries/ colourcoccos/source/z00-1_bloom_summer_99_.html

4.2.4   Aeolian input of terrestrial material (abundance and $\delta^{13}C$ of long-chain odd-numbered *n*-alkanes and even-numbered *n*-alkan-1-ols)

Besides using alkenones to reconstruct SSTs and marine productivity, the extractable organic fraction of marine sediments can also be used to determine the input from terrestrial sources. The most commonly used biomarkers for this purpose are the odd-numbered long-chain (C_{25}-C_{33}) *n*-alkanes and, to a lesser extent, even-numbered long-chain (C_{26}-C_{32}) *n*-alkan-1-ols. Both of these organic compounds are regular constituents of the epicuticular waxes of leafs of terrestrial higher plants and are normally not produced in marine settings [Eglinton and Hamilton, 1967; Bianchi, 1995]. Their presence is mainly related to aeolian input as they can easily be removed from the leaf surface by wind or rain, especially by sandblasting during dust storms, or entrained as part of soil and transported over large distances. They form a major component of dust, even in remote ocean areas [Conte and Weber, 2002]. Various studies therefore used the abundance of odd-numbered long-chain *n*-alkanes and even-

numbered long-chain *n*-alkan-1-ols in marine sediments to infer variation in the aeolian input of terrestrial material [e.g., López-Martínez *et al.*, 2006].

However, although the abundance of odd-numbered long-chain *n*-alkanes and even-numbered long-chain *n*-alkan-1-ols in marine sediments suggests the input of terrestrial material, it does not allow for further determination of the source. For this purpose in this thesis, the stable carbon isotopic composition ($\delta^{13}C$) of the two biomarkers is used. The $\delta^{13}C$ of both long-chain *n*-alkanes and *n*-alkan-1-ols is a well-established proxy to distinguish the input of different sources [Schefuss *et al.*, 2003b]. This is based on the fact that plants can photosynthesis in different ways. In general two types are distinguished; C_3 and C_4-plants, although a third type also exists (CAM-plants). C_3 plants (trees, shrubs, and cool-climate grasses) are the most abundant (95% of total plants) and are the dominant species in forested regions and high latitude grasslands. C_4 plants (notably tropical grasses) on the other hand have a more efficient water use than C_3-plants because they can internally concentrated CO_2 and are dominant in semi-arid regions. The different photosynthetic pathways of C_3 and C_4-plants results in an isotopic offset between the two [O'Leary, 1981], which is in the order of 10-15 ‰ for $\delta^{13}C$.
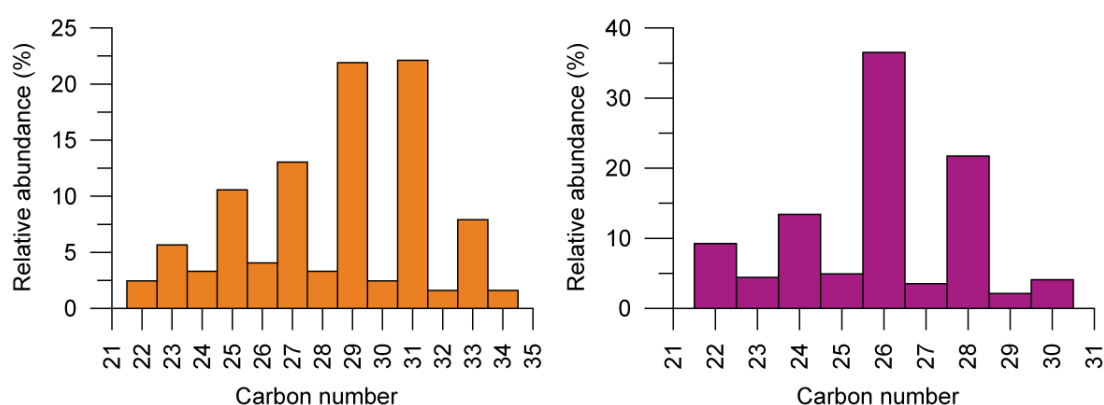
Figure 10; *n*-alkanes and *n*-alkan-1-ols

Relative abundance of the long-chain *n*-alkanes (orange) and *n*-alkan-1-ols (purple) in a sample from IODP Site U1313. The odd-numbered *n*-alkanes clearly dominate the *n*-alkane fraction with a carbon preference index (CPI) of 5.5, while the even-numbered compounds dominate the *n*-alkan-1-ol fraction. Such distributions are indicative for the input of terrestrial higher plant material.

4.2.5   Source and occurrence of ice-rafting events (ancient organic matter)

Besides *n*-alkanes and *n*-alkan-1-ols to infer the input of "fresh" organic matter from terrestrial higher plants, the abundance of so-called petrogenic compounds can be used to infer the input of ancient organic matter. Petrogenic compounds (benzohopans, palaerenieratane, mono- and triaromatic steroids, etc) are normally absent in recent marine

sediments. They are formed over long periods of time during diagenesis of organic matter and are found in the various ancient sedimentary rocks that surround the North Atlantic. As some of these rock formations outcrop in areas that were covered by continental ice sheets during glacials, rock fragments could get incorporated into the ice sheets as these flowed towards the continental margins. When ice-rafting events then occurred these fragments and petrogenic compounds could be carried large distances before being deposited in the open ocean as the icebergs melted in warmer surface waters. The occurrence of petrogenic compounds in marine sediments can therefore be used to track the input of ancient organic matter by ice-rafting events [Rosell-Melé *et al.*, 1997; Rashid and Grosjean, 2006]. Because the distribution of these compounds is highly specific for the age and type of source rock, the comparison between the biomarker distribution in marine sediments and possible source rocks can be used as correlation tool and to infer information about the origin of ice-rafting events.

4.2.6   Source and occurrence of ice-rafting events (detrital input)

In addition to the organic biomarkers, the input of detrital material is classically used as indicator for ice-rafting events [e.g., Heinrich, 1988; Hemming, 2004]. More over, the characteristics of the detrital material can be used to gain more information about the source of the IRD. For examples, the abundance of detrital carbonate in sediments from the North Atlantic is widely used as indicator for ice-rafted debris (IRD) originating from the Paleozoic carbonates in the Hudson area [e.g., Andrews and Tedesco, 1992; Bond *et al.*, 1992; Ji *et al.*, 2009; Stein *et al.*, 2009]. In this thesis, IRD was identified using X-Ray Diffraction (XRD) to distinguish material originating from different source areas. Following previous work from IODP Site U1313, Quartz was used as a general proxy for continental-derived material, reflecting input from different circum-Atlantic ice sheets (e.g., Canadian Shield, Greenland, Scandinavia, Great Britain), while dolomite was used as an indicator for ice-rafted debris (IRD) originating from the Paleozoic carbonates in the Hudson area [Stein *et al.*, 2009].
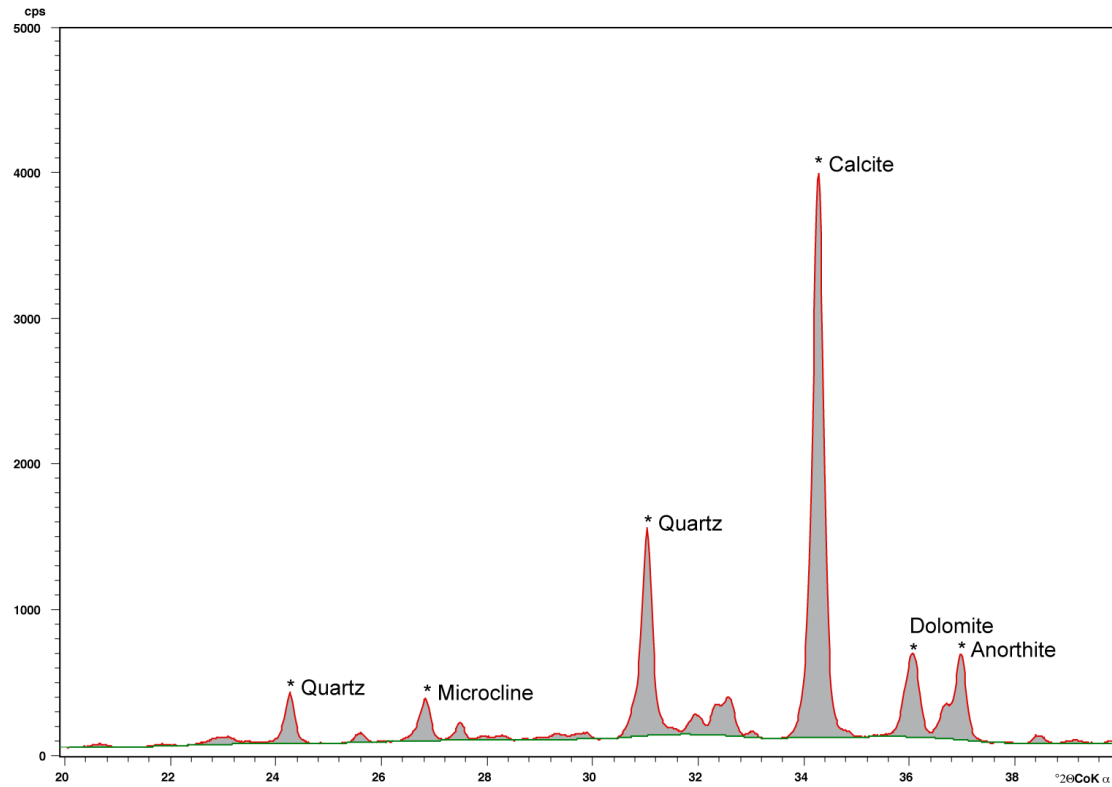
Figure 11; X-ray diffraction spectra

Example of X-ray diffraction spectra of a sample from Heinrich Layer 2 at Site U1313 that shows the abundance of dolomite and quartz. These minerals are brought to this open ocean as IRD during ice-rafting events. These minerals are absent in samples outside the Heinrich Layers.

5   Late Pliocene changes in the North Atlantic Current

B.D.A. Naafs, R. Stein, J. Hefter, N. Khélifi, S. De Schepper, and G.H. Haug

During the late Pliocene global climate changed drastically as the Northern Hemisphere glaciation (NHG) intensified. It remains poorly understood how the North Atlantic Current (NAC) changed in strength and position during this time interval. Such changes may alter the amount of northward heat transport and therefore have a large impact on climate in the circum-North Atlantic region and the growth of Northern Hemisphere ice sheets. Using the alkenone biomarker we reconstructed orbitally resolved sea surface temperature (SST) and productivity records at Integrated Ocean Drilling Project (IODP) Expedition 306 Site U1313 during the late Pliocene and early Pleistocene, 3.68 – 2.45 million years ago (Ma). Before 3.1 Ma, SSTs in the mid-latitude North Atlantic were up to 6 ℃ higher than present and surface water productivity was low, indicating that an intense NAC transported warm, nutrient-poor surface waters northwards. Starting at 3.1 Ma, surface water characteristics changed drastically as the NHG intensified. During glacial periods at the end of the late Pliocene and beginning of the Pleistocene, SSTs decreased and surface water productivity in the mid-latitude North Atlantic increased, reflecting a weakened influence of the NAC at our site. At the same time the increase in surface productivity suggests the Arctic Front (AF) reached down into the mid-latitudes. We propose that during the intensification of the NHG the NAC had an almost pure west to east flow direction in glacials and did not penetrate into the higher latitudes. The diminished northward heat transport would have led to a cooling of the higher latitudes, which may have encouraged the growth of large continental ice sheets in the Northern Hemisphere.

5.1   Introduction

The Pliocene epoch[1] is the most recent period in geological history when global temperatures were several degrees higher than today [e.g., Dowsett et al., 2009; Haywood et al., 2009]. Atmospheric pCO_2 was approximately 100 ppm higher than pre-industrial levels [Pagani et al., 2010] and ice sheets in the Northern Hemisphere were relatively small. The general surface current system was similar to the present one [Dowsett et al., 2009], but sea surface temperatures (SSTs) in the North Atlantic Ocean were up to 10 ºC warmer compared to the present as an intense North Atlantic Current (NAC) led to a reduced meridional SST gradient [e.g., Cronin, 1991; Dowsett et al., 1992; Robinson, 2009].

During the late Pliocene these warm conditions terminated as the Northern Hemisphere Glaciation (NHG) intensified and the Quaternary-style climate that characterizes the Pleistocene epoch developed. The exact timing of the intensification of NHG is not well constrained and differs between studies and site locations. In benthic foraminiferal $\delta^{18}O$ records, a measure for high latitude temperature and continental ice volume, the increase started around 3.6 Ma, indicating the built-up of continental ice sheets in the Northern Hemisphere [Mudelsee and Raymo, 2005]. However, the threshold towards full glacial/interglacial conditions is located near 2.7 Ma during Marine Isotope Stage (MIS) G6 when the amplitude of the 41-ka component increased [Ruggieri et al., 2009]. Around the same time ice-rafted debris (IRD) became widespread in sediments from the higher latitudes [e.g., Shackleton et al., 1984; Maslin et al., 1998; Kleiven et al., 2002]. MIS G6 is therefore considered as the first intense glacial period with large Northern Hemisphere ice sheets.

Various hypotheses such as a change in orbital configuration, a decrease in atmospheric pCO_2 via polar ocean stratification, and/or changes in oceanic and atmospheric heat transport, possibly related to the closing of the Central American Seaways (CAS), have been proposed as cause for the intensification of the NHG [Driscoll and Haug, 1998; Haug and Tiedemann, 1998; Maslin et al., 1998; Haug et al., 1999; Haywood et al., 2000; Ravelo et al., 2004; Bartoli et al., 2005; Haug et al., 2005; Mudelsee and Raymo, 2005; Lawrence et al., 2009; Sarnthein et al., 2009; Seki et al., 2010]. So far, none of these have given a complete satisfactory explanation and the ultimate cause remains an enigma. Nevertheless, recent studies suggest that cooling of the higher latitudes and increase in meridional SST gradient were crucial for the intensification of NHG [Berger and Wefer, 1996; Lunt et al., 2008; De Schepper et al., 2009; Brierley and Fedorov, 2010]. This means that the NAC, by which the excess in heat from the tropics was transported northwards during the Pliocene, had to weaken and/or change its path during the intensification of the NHG in order to allow the

---

[1] Please note we use the updated definitions of the early Pliocene (5.332 – 3.6 Ma), late Pliocene (3.6 – 2.588 Ma), and early Pleistocene (2.588 – 0.781 Ma) [Gibbard et al., 2009]

higher latitudes to cool and the meridional SST gradient to increase. This contradicts other hypotheses in which an increase in northward heat transport, related to closure of the CAS, and associated feedback mechanisms are suggested as main cause for the intensification of the NHG [e.g., Driscoll and Haug, 1998; Haug and Tiedemann, 1998; Bartoli et al., 2005].

Therefore reconstructing the influence of the NAC on the North Atlantic during the late Pliocene is crucial for a better understanding of the mechanisms behind the intensification of the NHG. At present, only one study discussing variations in northward heat transport is available for the complete late Pliocene [Lawrence et al., 2009]. However, that study used samples from Ocean Drilling Project (ODP) Site 982. This site is located at the northern end of the NAC and probably does not reflect major variations in the position and strength of the main branch of the NAC. This is obvious in view of the high-amplitude SST variability, which is most likely related to short-term variability in the most northern position of the NAC [Lawrence et al., 2009]. More important, the age model of Site 982 for the late Pliocene might require revision [Khélifi and Sarnthein, 2010]. Therefore, this study is based on sediment samples from the more southerly located Integrated Ocean Drilling Project (IODP) Expedition 306 Site U1313. The main objective of this paper is to reconstruct variations in the NAC and the subsequent change in northward heat transport during the late Pliocene, when the NHG intensified.

5.2 Regional Setting

The North Atlantic is characterized by a continuous northward flow of warm and salty surface water that constitutes the upper part of the meridional overturning circulation (Figure 12). At the origin of the surface current system is the Gulf Stream, which continues as the North Atlantic Current (NAC) and finally the North Atlantic Drift Current in the northeast North Atlantic. We use the term NAC to refer to the whole warm surface current that continues after the Gulf Stream into the northeast North Atlantic. The NAC forms the transition zone between the two different regimes: in the higher latitudes the cold and productive Arctic waters, in the subtropics the warm and oligotrophic waters from the subtropical gyre (Figure 12). The region of high surface water productivity just north of the NAC is associated with the location of the Artic Front (AF), which is characterized by high eddy activity that promotes surface water productivity.

Various studies showed that surface water characteristics in the (mid-latitude) North Atlantic mainly depend on the strength and position of the NAC, which in turn determines the position of oceanic fronts [e.g., Versteegh *et al.*, 1996; Calvo *et al.*, 2001; Villanueva *et al.*, 2001; Lawrence *et al.*, 2009; Robinson, 2009; Stein *et al.*, 2009]. High SSTs

indicate an intense NAC transporting warm surface waters northwards across the mid-latitude North Atlantic, where as cooler SSTs reflect a weakened influence of the NAC.
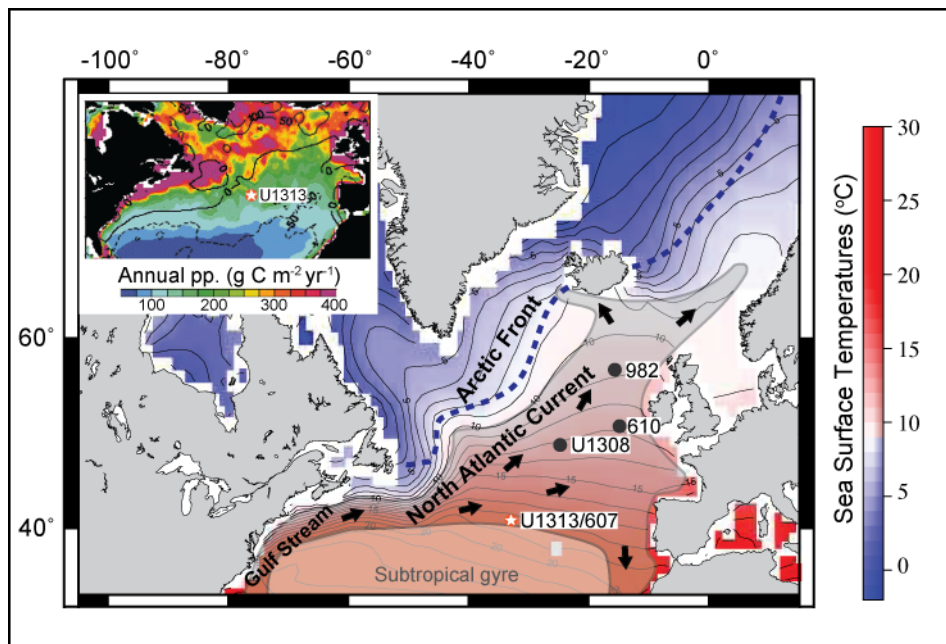
Figure 12; Map of the North Atlantic Ocean showing modern mean annual SSTs at the surface [Locarnini *et al.*, 2006] together with the position of the Gulf Stream and North Atlantic Current (NAC). Dashed line shows the position of the Arctic Front (AF), which separates warm Atlantic waters in the mid-latitudes from cold subpolar waters in the higher latitudes [Swift, 1986; Pflaumann *et al.*, 2003]. Insert shows annual primary productivity (pp.) in the North Atlantic [modified from Williams and Follows, 1998]. The NAC forms the transition zone between warm and oligotrophic waters of the subtropical gyre to the south and cold and productive Arctic waters associated with the AF in the north. In this study we used samples from IODP Site U1313, a re-drill of DSDP Site 607, which at present is located under the direct influence of the NAC. Other sites discussed in the text are also shown.

Alkenone ARs provide a second measure of variability in the NAC. Both coccolith carbonate and alkenone abundance have been used to track the movement of the high productivity zone associated with the AF during the middle and late Pleistocene [e.g., McIntyre *et al.*, 1972; Villanueva *et al.*, 2001; Stein *et al.*, 2009]. These studies showed that during glacials the productivity maximum moved southwards as the AF shifted into the mid-latitude North Atlantic, cold polar waters expanded to lower latitudes, and the NAC did not influence the higher latitudes in the northeast Atlantic. A reconstruction of SSTs for the Last Glacial Maximum depicts this almost purely west to east flow direction of warm surface waters and southern position of the AF between 37 and 45 ºN [Pflaumann et al., 2003], which

led to increased surface water productivity in the mid-latitude North Atlantic [Villanueva et al., 2001].

Since surface water characteristics are so different to the north and the south of the NAC, a change in position of the NAC as described above can lead to large changes in SSTs and productivity at Site U1313, which at present is located under the direct influence of the NAC. Records of surface water characteristics at site U1313 are therefore well suited to reconstruct changes in position and strength of the NAC.

5.3   Materials and Methods

5.3.1   Age model Site U1313

Site U1313 is a re-drill of Deep Sea Drilling Project (DSDP) Site 607 and is located at the base of the upper western flank of the Mid-Atlantic Ridge (3426 m water depth, latitude 41º00'N, longitude 32º57'W). Four holes were drilled at Site U1313 to obtain a continuous sedimentary record [Expedition 306 Scientists, 2006]. Using the holes U1313B and U1313C a complete spliced stratigraphic section was obtained. The original meter composite depth (mcd)-scale was updated to an adjusted, so-called amcd-scale, to improve the overall correlation of distinct features in the lightness, susceptibility, and paleomagnetic data between the holes. Slight adjustments were made to the mcd-scale of Hole U1313C, which was tied to the mcd-scale for Hole U1313B [G. Acton, personal communication]. We obtained an age model for the period between 3.65 and 2.45 Ma by improving and extending the preliminary shipboard age model for Site U1313 [Expedition 306 Scientists, 2006]. The age model is based on tuning the lightness record of the primary splice to the global benthic foraminiferal $\delta^{18}O$ LR04 stack [Lisiecki and Raymo, 2005], using the Match 2.0 software [Lisiecki and Lisiecki, 2002]. We assumed that the variability in lightness, caused by changing carbonate content due to variations in terrestrial input, mimicked changes in benthic foraminiferal $\delta^{18}O$ without any temporal offset during the late Pliocene and early Pleistocene [Expedition 306 Scientists, 2006]. This assumption is supported by data from DSDP Site 607 where changes in carbonate content, hence lightness, are in phase with benthic foraminiferal $\delta^{18}O$ at the obliquity rhythm [Ruddiman et al., 1989]. Depth-age tie-points were based on the magnetostratigraphy of Site U1313 [Expedition 306 Scientists, 2006] and visual correlation between the two records. The resulting sedimentation rates vary between 2 and 10 cm/ka (Figure 13). The ages obtained for magnetic reversals at Site U1313, which can clearly be identified in the inclination record (Figure 13), all match the ages as given by Lisiecki and Raymo [2005] within the error margin.
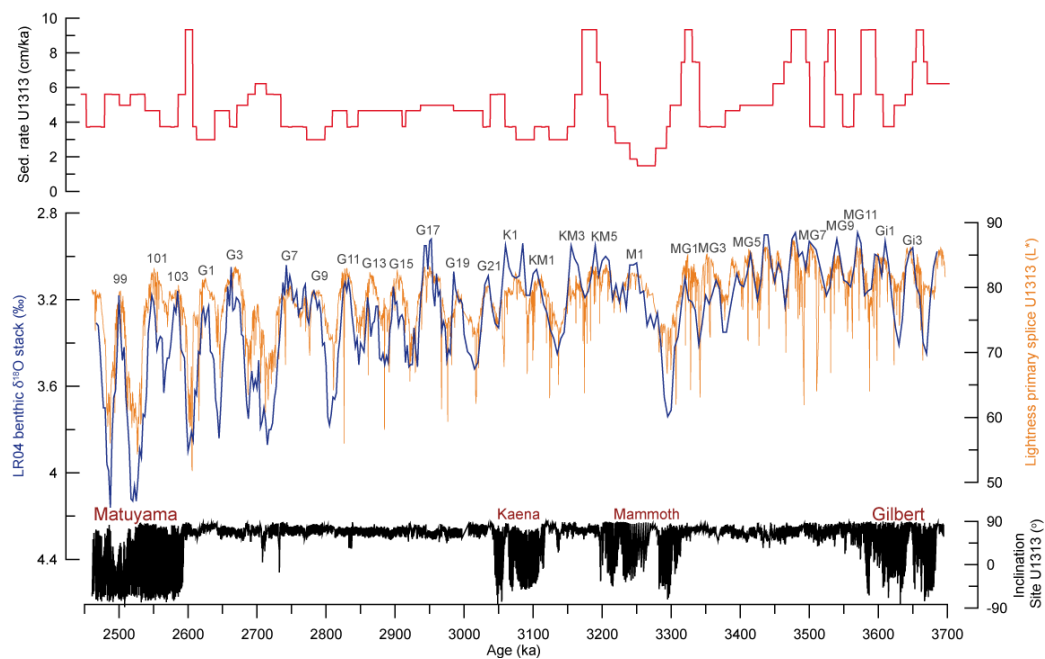
Figure 13; Age model for Site U1313. The age model is based on tuning of the lightness of the primary splice (orange) to the global benthic foraminiferal $\delta^{18}O$ stack (blue) [Lisiecki and Raymo, 2005]. The resulting sedimentation rates vary between 2 and 10 cm/ka (red). Also shown are the inclination data for the primary splice of Site U1313 (black) and matching polarity chrons.

5.3.2 Sample preparation and methods

Samples of 10cc were taken from the primary splice at a 20 cm ($\pm$ 4 ka) resolution. Between 2.78 and 2.65 Ma (MIS G9 – G3) sampling resolution was 10 cm ($\pm$ 2 ka). All samples were freeze-dried after sampling and stored at 4 ºC until further processing.

A LECO Pegasus III GC/TOF-MS system was used to measure biomarker content of the sediment samples. This method has recently been established as alternative for alkenone analyses and has the advantage over classical GC/FID methods that it significantly reduces instrumental time and has a higher sensitivity [Hefter, 2008]. Full details of the methods applied are discussed elsewhere [Hefter, 2008; Stein *et al.*, 2009]. In short, organic compounds were obtained from around 6 grams of freeze-dried and homogenized sediment using dichloromethane and accelerated solvent extraction (ASE 200, DIONEX, 5 min. at 100 ºC and 1000 psi). For quantification purposes, 2.1435 µg of n-hexatriacontane (*n*-C$_{36}$ alkane) were added to each sample as standard prior to extraction. Total extracts were concentrated, dried under a nitrogen flow and then re-dissolved in 0.5 ml hexane before being measured by the GC/TOF-MS system. The alkenone unsaturation index ($U^{k'}_{37}$) was used together with the global core-top calibration [Prahl and Wakeham, 1987; Müller et al., 1998] to reconstruct mean annual temperatures at the surface (top 10 meters). Total C$_{37}$ alkenone (C$_{37:2}$ + C$_{37:3}$)

accumulation rates (ARs) in ng/cm^2/ka were calculated using linear sedimentation rates (Figure 13), biomarker concentrations obtained by GC/TOF-MS system, and dry bulk densities (DBD), calculated from shipboard measured wet bulk densities (WBD) using DBD = – 1.6047 + 1.5805 * WBD [Expedition 306 Scientists, 2006; Stein *et al.*, 2009].

5.3.3   Reliability of $U_{37}^{k'}$ in the late Pliocene

In the modern ocean alkenones are produced by members of the class *Prymnesiophyceae*, primarily *Emiliania huxleyi* as well as *Gephyrocapsa oceanica* [e.g., Volkman et al., 1995]. Both species first appeared in the mid-latitude North Atlantic during the (middle) Pleistocene [Expedition 306 Scientists, 2006], but alkenones are found in much older sediments. Then, other extant and extinct members of the class *Prymnesiophyceae* presumably produced the alkenones. Although the alkenone producers changed over time, previous work has shown that $U_{37}^{k'}$ and global core-top calibration are applicable beyond the first occurrence of *E. huxleyi* [Villanueva et al., 2002; McClymont et al., 2005]. In recent years the alkenone thermometer was therefore used to produce several long-term SST records [e.g., Dekens et al., 2007; Lawrence et al., 2009], showing the capability to provide reliable temperature estimates for at least the last 5 Ma.

In the mid-latitudes seasonal fluctuations in alkenone production most likely cause only a small bias in SSTs reconstructions towards the temperature of the growing season [Müller et al., 1998; Conte et al., 2006]. Therefore our SST record is interpreted to reflect mean annual temperatures. This is supported by an alkenone-derived SST of 18.2 ºC from our core-top sample, within the error identical to the modern mean annual SST of 18.3 ºC at Site U1313 [Locarnini et al., 2006]. Even so, recent work has suggested that at least during the interglacials of the late Pleistocene, alkenone-based SSTs in the mid-latitude North Atlantic reflect spring temperatures [Leduc et al., 2010]. If this was also the case in the late Pliocene then the increase in Pliocene SSTs compared to modern is underestimated (compare Pliocene SSTs with modern spring SST instead of annual mean SST in figure 14).

The input of allochthonous alkenones likely did not significantly affect our biomarker records from the mid-latitude North Atlantic since this is more important in the higher latitudes such as the Nordic Seas [Bendle et al., 2005] or at sites located on or close to continental margins [e.g., Mollenhauer et al., 2005].

5.4 Results
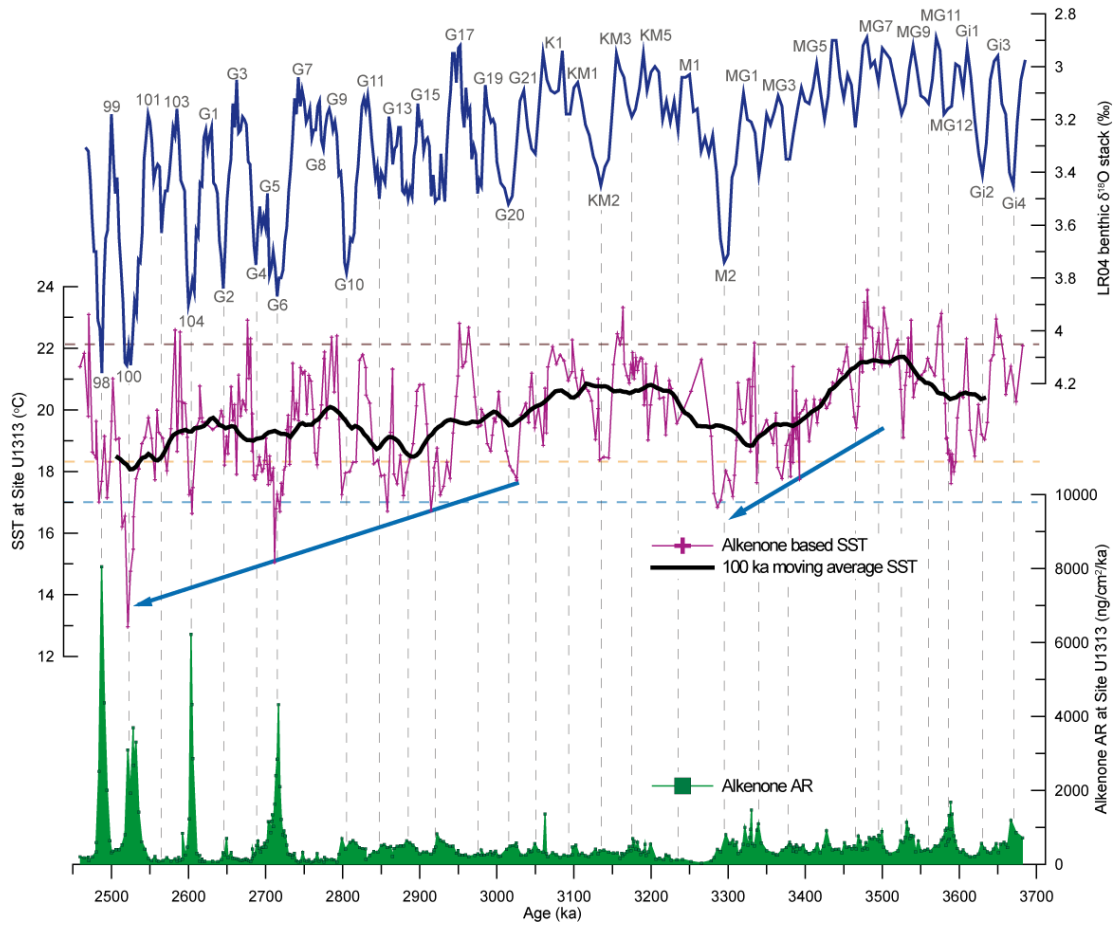
Figure 14; Sea surface temperatures (purple) and alkenone accumulation rates (green) from Site U1313 together with the global benthic foraminiferal $\delta^{18}O$ stack (blue) and marine isotope taxonomy [Lisiecki and Raymo, 2005]. To obtain the 100 ka moving average of the SST record, the data was re-sampled on a 4 ka interval after which a 100 ka smoothing filter was applied. Dashed lines represent modern mean summer (JAS, in dark brown), annual (in orange), and spring (AMJ, in blue) SST at Site U1313 [Locarnini *et al.*, 2006].

The SST record from Site U1313 ranges from 3.65 to 2.45 Ma and demonstrates both long- and short-term variability during this period (Figure 14). SST variability is similar to the global benthic foraminiferal $\delta^{18}O$ stack [Lisiecki and Raymo, 2005]. Intervals of low benthic foraminiferal $\delta^{18}O$ coincide with periods of increased SSTs at Site U1313 and vice versa. During most of the late Pliocene, SSTs were higher than present with interglacial temperatures occasionally as high as 24 ºC, in accordance with the general consensus of a warm North Atlantic Ocean during the late Pliocene [see Lawrence et al., 2009 and references therein]. SSTs decreased between 3.5 and 3.3 Ma by 5 ºC, culminating in MIS M2 with values as low as 17 ºC. The Pliocene Research Interpretation and Synoptic Mapping

(PRISM)-interval between 3.29 and 2.97 Ma [Dowsett et al., 2009], is characterized by high SSTs with both glacial and interglacial values higher than present. From 3.1 Ma onwards SSTs got progressively lower. Especially glacial SSTs decreased by several degrees at the end of our record with the lowest SSTs found during MIS G6 (15 ºC) and 100 (13 ºC).

Alkenone ARs are generally low and show little variation during most of our record with typical values of around 500 $ng/cm^2/ka$. The exception is during MIS G6, 104, 100, and 98 when intense cooling of surface waters coincides with an increase in alkenone ARs by one order of magnitude, reaching values as high as 8000 $ng/cm^2/ka$ (Figure 14).

5.5   Discussion

Variations in the surface water characteristics at Site U1313 are interpreted to reflect changes in the influence of the NAC. The shift from warm and oligotrophic conditions at our site towards cold and more productive surface waters during the latest Pliocene and early Pleistocene (Figure 14) suggest a process comparable to that of glacials of the late Quaternary when the NAC had a almost purely west to east flow direction and the AF was located close to our study site. Below we discuss the changes in surface water characteristics at Site U1313 and, hence, influence of the NAC for different time intervals of the late Pliocene and early Pleistocene.

5.5.1   Period between 3.68 and 3.45 Ma: warm beginning of the late Pliocene

High SSTs and low alkenone ARs during this period suggest that throughout this interval an intense NAC transported warm waters northwards, keeping the higher latitudes warm. SSTs at Site 982 in the northern North Atlantic also record warm surface waters during this interval [Lawrence et al., 2009], suggesting that the entire North Atlantic was influenced by an intense NAC. At that time, Site U1313 was likely bathed with waters from the subtropical gyre since this gyre likely expanded in the warm Pliocene. The NAC then may have followed a more northern pathway compared to present, keeping the high productivity region associated with the AF far to the north of our study site.
A short alkenone-based SST record form DSDP Site 607 [Lawrence et al., 2009], of which U1313 is a re-drill, is in good agreement with our record. The only difference is the low SSTs at Site U1313 during MIS MG12 (± 3.59 Ma). At Site 607 lowest SSTs occur during MIS Gi2 (± 3.63 Ma). Lowest SSTs during MIS Gi2 seem to better fit benthic foraminiferal $\delta^{18}O$, with heavier values during MIS Gi2 [Lisiecki and Raymo, 2005]. However at Site U1313 the excellent resolved inclination data (Figure 12) shows that the Guass/Gilbert magnetic

boundary coincides with these low SSTs. The Gauss/Gilbert boundary in the LR04 stack has an age of 3.588 Ma and is placed within MIS MG12 [Lisiecki and Raymo, 2005]. We are therefore certain that the low SSTs at Site U1313 occur during MIS MG12. At Site 607 identification of magnetic polarity chrons is problematic in this interval, preventing us to be certain the SST records are truly different. Possibly future benthic oxygen isotope stratigraphy at Site U1313 can help to resolve this.

5.5.2   Period between 3.45 and 3.29 Ma: Towards MIS M2

Decreasing SSTs during this period suggest the influence of the NAC, and hence northward heat transport, weakened prior to MIS M2. Low alkenone ARs suggest that despite the weakening of the NAC, it was still strong enough to prevent nutrient rich waters and the AF to reach the core site. This is supported by data of IRD, which is recorded only at sites north of 50 ºN [Kleiven et al., 2002]. The absence of IRD in more southern sites suggests that warm surface waters were still influencing the mid-latitude North Atlantic and prevented icebergs from reaching further south.

Although covering only a small time interval around MIS M2, Mg/Ca based SST and dinoflagellate cyst assemblages from the northern North Atlantic (DSDP Site 610 and IODP Site U1308) also show a reduction in northward heat transport during this time period [De Schepper et al., 2009]. In agreement with our interpretation, the palynological records at Sites 610 and 1308 suggest that the AF moved southward during MIS M2, but still remained to the north of 53 ºN [De Schepper et al., 2009]. Our results show a long-term weakening in the influence of the NAC is preceding MIS M2 and the development of a more glacial-like surface circulation in the North Atlantic. This points to a long (> 100 ka) and gradual process, which might have crossed a threshold during MIS M2, as a cause for this global cooling event.

5.5.3   Period between 3.29 and 2.94 Ma: warm interval

Warm and oligotrophic conditions quickly returned at Site U1313 after MIS M2, suggesting that northward heat transport by the NAC was increased and the AF located far north of our site. This period includes the well-studied PRISM interval between 3.29 and 2.97 Ma [e.g., Dowsett et al., 2009]. Numerous studies using sites in the North Atlantic demonstrate increased northward heat transport by an intensified NAC during this period [e.g., Cronin, 1991; Dowsett et al., 1992; Haywood and Valdes, 2004; Robinson, 2009].

These reconstructions use "snap-shots" and represent warm peak averages [Robinson, 2009], making comparison with our SST record difficult.

Multi-proxy SST records, including alkenone based-SST, obtained from several sites in the North Atlantic (e.g., DSDP Sites 607 and 610) also show higher SSTs for the PRISM-interval compared to the present [Robinson et al., 2008]. Although the age model and SST-calibration are slightly different, our SST estimates agree very well with the short alkenone-based SST from Site 607 for the PRISM-interval in both absolute values and trend.

The only other continuous SST record for the late Pliocene in the North Atlantic comes from ODP Site 982 [Lawrence et al., 2009]. However for this interval the record differs significantly from that at Site U1313. Site 982 records a continuous cooling of surface waters that started already at 3.5 Ma, suggesting a decrease in strength of the NAC from the beginning of the late Pliocene onwards. The interval between 3.29 and 2.94 Ma is characterized by decreasing SSTs with values occasionally as low as those during MIS M2 and G6, both major global cooling events. Especially the lack of high SST during MIS KM5 and KM3 at Site 982, both characterized by very light benthic foraminiferal $\delta^{18}O$, is different from our findings. The SST record from Site 982 might reflect a shift in position of the northern end of the NAC and decrease in heat transport to the northern North Atlantic since 3.5 Ma [Lawrence et al., 2009], in agreement with other studies that suggested the built-up of continental ice sheets in the Northern Hemisphere began as early as 3.7 Ma [Mudelsee and Raymo, 2005; Meyers and Hinnov, 2010]. However, a detailed revision of composite depths and magnetostratigraphy, and renewed fine-tuning of the benthic foraminiferal $\delta^{18}O$ record at Site 982 led to a significant revision of the SST record of Lawrence et al., [2009] by 20 to 120 ka [Khélifi, 2010; Khélifi and Sarnthein, 2010]. These authors suggested that the age of the benthic foraminiferal $\delta^{18}O$ signal formally assigned to MIS KM2 (± 3.135 Ma) is replaced by the age of MIS G20 (± 3.015 Ma). The possible absence of the Kaena subchron in the sediment sequence of Site 982 may explain the discrepancies with our SST record.

5.5.4   Period between 2.94 and 2.45 Ma: intensification of the NHG

Although alkenone ARs can be influenced by various factors, we interpret the order of magnitude increase in alkenone ARs during MIS G6, 104, 100, and 98 as an increase in total surface water productivity. Because the modern North Atlantic phytoplankton community is dominated by coccolithophores, predominantly the alkenone producing *Emiliania huxleyi* [Gregg and Casey, 2007], variations in the alkenone ARs reflect changes in the dominant phytoplankton group. Secondly, other studies showed that alkenone abundances in sediment cores and sediment traps track surface productivity in the North Atlantic [Rosell-

Melé et al., 2000; Villanueva et al., 2001; Incarbona et al., 2010]. Moreover, our alkenone ARs agree with a palynological study from Site 607 for the period between 2.85 and 2.3 Ma [Versteegh et al., 1996]. That study displays increased concentrations of dinoflagellate cysts during MIS G6, 104, 100, and 98, also suggesting increased mixed layer productivity during these glacial periods.

A more than ten-fold increases in alkenone ARs is considered too large to be explained by preservation alone [Lawrence et al., 2007]. Nevertheless, preservation of organic matter, including dinoflagellate cysts, can be influenced by oxygenation of the bottom waters and sediment [Versteegh and Zonneveld, 2002; Zonneveld et al., 2010]. Therefore it could be argued that a decrease in bottom water ventilation during glacial periods could account for the observed increase in alkenone ARs and dinoflagellate cyst concentrations. During MIS 104, 100, and 98 benthic foraminiferal $\delta^{13}C$ values were approximately 1 ‰ lower than during interglacials [Raymo et al., 1992], reflecting increased influence of less ventilated Antarctic bottom waters at our core site. However, when a reduction in bottom water ventilation caused the increase in alkenone ARs in the North Atlantic, we would expect low benthic foraminiferal $\delta^{13}C$ during all glacial periods with increased alkenone ARs. This is not the case in for example MIS G6, which is characterized by high alkenone ARs, when benthic foraminiferal $\delta^{13}C$ remained high. If bottom water ventilation plays a role, then Heinrich(-like) events in the North Atlantic during the middle and late Pleistocene should also be characterized by and increase in alkenone ARs. During these events North Atlantic deep-water formation came to a halt and the deep North Atlantic basin was poorly ventilated [Vidal et al., 1997]. Published alkenone records demonstrate the opposite with periods of low alkenone abundances during Heinrich(-like) events, reflecting a collapse of the phytoplankton community due to harsh surface water conditions [Villanueva et al., 1997; Stein et al., 2009]. Recent high-resolution work from the Iberian Margin also shows no major influence of changes in bottom water ventilation on alkenone concentrations during the last 70 ka [Incarbona et al., 2010].

The increased surface water productivity together with cooler SST during MIS G6, 104, 100, and 98 at Site U1313 suggests that at the end of the Pliocene the influence of the NAC weakened. The NAC then likely had a more west to east flow direction and the AF was located closer to our site (Figure 15), comparable to the glacial conditions of the middle and late Pleistocene [McIntyre et al., 1972; Villanueva et al., 2001; Stein et al., 2009]. Such interpretation is supported by evidence from Site 607 with (1) an increase in IRD during glacials from MIS G16 onwards [Kleiven et al., 2002, updated to LR04 ages], (2) the appearance of larger sized IRD during MIS 100 and 98 [Raymo et al., 1989], and (3) occurrence of Heinrich(-like) events during MIS 100 [Becker et al., 2006]. This all indicates

that during peak glacial conditions icebergs could travel as far south as 41 °N and accounts for a changed North Atlantic surface circulation, including a weakened influence of the NAC and proximity of the AF at Site U1313 during glacial periods.
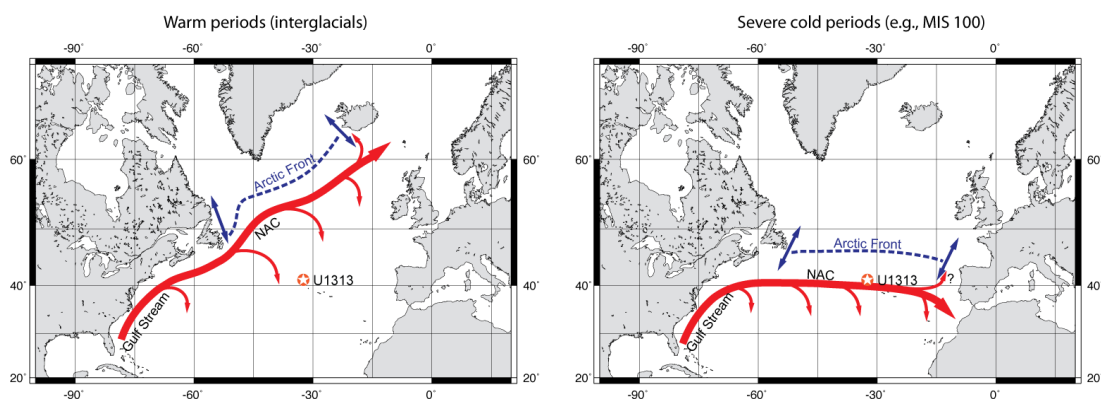
Figure 15; a, schematic representation of suggested position of the Gulf Stream, North Atlantic Current (NAC), and Arctic Front (AF) during warm interglacials and, **b,** severe glacial periods of the late Pliocene and early Pleistocene (e.g., MIS 100). Records of SSTs and surface water productivity at Site U1313 show the influence of cold and nutrient-rich surface waters during these glacials, suggesting proximity of the AF to Site U1313 and an almost purely west to east flow direction of the NAC.

5.5.5   Implications of changing NAC during the intensification of the NHG

Our study demonstrates a close correspondence between the influence of the NAC at Site U1313 and the size of Northern Hemisphere ice sheets. Periods of intense NAC at U1313 coincide with periods of small ice sheets (light benthic foraminiferal δ^{18}O) and absence of IRD in the North Atlantic [Kleiven et al., 2002]. On the other hand, the influence of the AF at Site U1313 together with a weak NAC is observed for the first time during MIS G6, when the amplitude of benthic foraminiferal δ^{18}O increased as continental ice volume grew larger and IRD became widespread in sediments from the North Atlantic [Kleiven et al., 2002; Ruggieri et al., 2009].

Changes in surface water characteristics in the North Atlantic led changes in ice volume (benthic foraminiferal δ^{18}O) by a few ka during the late Pliocene and early Pleistocene [Versteegh et al., 1996; De Schepper et al., 2009; Lawrence et al., 2009]. This suggests that changes in the NAC and subsequent decrease in northward heat transport were a cause for the intensification of NHG rather then a result. This agrees with recent modeling results [Lunt et al., 2008; Brierley and Fedorov, 2010], which show that cooling of the higher latitudes was a necessity for the development of large continental ice sheets in the Northern Hemisphere. Although closing of the CAS might have led to a more intense northward heat

transport in the early Pliocene [e.g., Haug and Tiedemann, 1998], our results show that during the late Pliocene northward heat transport diminished as continental ice volume increased. Our results support the long-standing proposal, dating back to James Croll [1875], that the eastward diversion of the NAC and a positive ice-albedo feedback played a central role in the growth of Northern Hemisphere ice sheets during the Pleistocene. Moreover, the changes in polar ocean conditions such as would result from the observed NAC changes have the potential to alter ocean storage of carbon dioxide, introducing an additional dimension of climate feedback [Haug et al., 1999; Sigman et al., 2010].

5.5.6   Cause for variability in NAC

Our record of late Pliocene surface water characteristics suggests that an intense NAC transported warm tropical waters northwards, leading to a reduced meridional SST gradient during most of the late Pliocene. How such increased northward heat transport was maintained together with a weak meridional SST gradient remains controversial. Intense Atlantic deep-water circulation during the Pliocene has been proposed as a cause for increased northward heat transport [Cronin, 1991; Dowsett et al., 1992; Robinson, 2009]. However, changes in surface water characteristics lead the changes in deep-water formation and ice volume by a few ka [Versteegh et al., 1996; De Schepper et al., 2009; Lawrence et al., 2009]. Thus, changes in deep-water formation could only have acted as positive feedbacks for the intensity of the NAC.

Lawrence et al. [2009], similar to Versteegh et al., [1996], proposed that increased wind forcing, as modeled for the late Pliocene [Haywood et al., 2000], was responsible for maintaining the increased advection of warm surface water northwards. In their concept orbitally driven changes in solar insolation, possibly amplified by changes in sea-ice extent, altered the strength and latitudinal position of the strongest westerly winds. This would influence the position and strength of the NAC and subsequent northward heat transport. Such mechanism agrees with recent observations in which a link was found between the strength of North Atlantic pressure systems and the intensity and northward extent of the NAC on decadal [Flatau et al., 2003] and millennial time scales [Giraudeau et al., 2010].

Possibly the Northern Hemisphere ice sheets provided a positive feedback to the initial changes in wind forcing. When the ice sheets grew large enough they could start to interact with atmospheric circulation. Together with changes in deepwater formation and an increase in sea-ice formation as positive feedbacks, this could have led to the observed shift in the position of the NAC. Future work should focus on testing such hypothesis by

palaeorecords of variations in wind strength from the mid-latitude North Atlantic, e.g. grain sizes of detrital sediments.

5.6   Conclusions

We obtained new SST and marine productivity records from the mid-latitude North Atlantic (IODP Site U1313) for the period between 3.68 and 2.45 Ma. Changes in surface water characteristics at Site U1313 provide new insights into the variations of the NAC during this critical time period. Warm SSTs and low alkenone ARs during the period between 3.65 and 2.94 Ma indicate the presence of an intense NAC in the mid-latitude North Atlantic, transporting warm tropical waters northwards. The final cooling of SSTs in the mid-latitude North Atlantic started around 3.1 Ma as the influence of the NAC weakened. This is later than previously suggested for the northern North Atlantic [Lawrence et al., 2009]. During peak glacial conditions at the end of the Pliocene and beginning of the Pleistocene (MIS G6, 104, 100, and 98) the NAC transported less heat to the north due to a more west to east flow direction and the AF had a closer location to our study site. Surface water characteristics at our site during these glacials were similar to glacials of the late Pleistocene [Stein *et al.*, 2009]. Our results argue against an increase in northward heat transport in the North Atlantic during the intensification of NHG [Bartoli et al., 2005]. The observed weakening of the NAC and subsequent decrease in northward heat transport during the late Pliocene and early Pleistocene would have led to a cooling of the higher latitudes, a condition necessary for the growth of large continental ice sheets surrounding the North Atlantic.

5.7   Acknowledgements

reviewer, and the editor improved the manuscript and are gratefully acknowledged. Data supplement is available online at http://doi.pangaea.de/10.1594/PANGAEA.744483.

6 Strengthening of North American dust sources during the late Pliocene (2.7 Ma)

B.D.A. Naafs, J. Hefter, G. Acton, G.H. Haug, A. Martínez-Garcia, R. Pancost, and R. Stein

Here we present orbitally-resolved records of terrestrial higher plant leaf wax inputs to the North Atlantic over the last 3.4 million years, based on the accumulation of long-chain *n*-alkanes and *n*-alkanl-1-ols at IODP Site U1313. These lipids are a major component of dust, even in remote ocean areas, and thus have a predominantly aeolian origin in distal marine sediments. The results show that around 2.7 million years ago (Ma), coinciding with the intensification of the Northern Hemisphere glaciation (NHG), the aeolian input of terrestrial material to the North Atlantic increased drastically. Since then, during every glacial of the Quaternary the aeolian input was up to 30 times higher than during interglacials. The close correspondence between aeolian input to the North Atlantic and other dust records indicates a globally uniform response of dust sources to Quaternary climate variability, although the amplitude of variation differs among areas. We suggest that the increased aeolian input at Site U1313 during glacials is predominantly related to the episodic appearance of continental ice sheets in North America and the associated strengthening of glaciogenic dust sources. Evolutional spectral analyses of the *n*-alkane records were used to determine the dominant astronomical forcing in North American ice sheet advances. These results demonstrate that during the early Pleistocene North American ice sheet dynamics responded predominantly to variations in obliquity (41-ka), which argues against previous suggestions of precession-related variations in Northern Hemisphere ice sheets during the early Pleistocene.

6.1 Introduction

Small rock fragments, soils particles, and pollen can easily be entrained by the wind and transported over large distances through the atmosphere [Ridgwell, 2002]. This heterogeneous mixture of aerosols, i.e. dust, plays an important role in global climate [Maher *et al.*, 2010] as it influences the radiative forcing of the atmosphere [Mahowald *et al.*, 2006b], and can be a source of nutrients to the open ocean that can lead to a strengthening of the biological pump [Fung *et al.*, 2000; Mills *et al.*, 2004]. In addition, dust particles influence cloud formation by providing cloud condensation nuclei [Mahowald and Kiehl, 2003], and can affect the albedo of ice sheets [Ridgwell, 2002].

Globally distributed climate records show that the global emission of dust was significantly higher during the most recent glacials than during interglacials such as the present [e.g., Maher *et al.*, 2010; McGee *et al.*, 2010; Mahowald *et al.*, 2011]. For example the analysis of dust particles in ice cores from the Antarctic continent show that throughout the last 800 ka the dust flux to Antarctica was 25 times higher during glacials than during interglacials [Lambert *et al.*, 2008]. Although dust deposition in the low-latitudes was also higher during glacials [Tiedemann *et al.*, 1994; deMenocal, 1995; Winckler *et al.*, 2008; McGee *et al.*, 2010], it was lower than the glacial flux in the higher latitudes of the Southern Hemisphere [Lambert *et al.*, 2008; Martìnez-Garcia *et al.*, 2009]. The 5 to 8 times higher dust deposition during glacials in the Southern Ocean has been explained by the effect of continental ice sheets in Patagonia that act as an amplifying mechanism for dust emission in the higher latitudes [Ridgwell and Watson, 2002; Winckler *et al.*, 2008; Sugden *et al.*, 2009], while the even greater increase seen in Antarctic dust fluxes is attributed to a more efficient transport mechanism during glacials [Lambert *et al.*, 2008].

Continental ice sheets are effective dust sources. The grinding of rocks by continental ice sheets produces large amounts of glaciogenic dust that is transported by melt waters towards glacial outwash plains where it can easily be entrained by wind [e.g., Mahowald *et al.*, 2006a; Ganopolski *et al.*, 2010; Maher *et al.*, 2010]. The presence of extensive loess deposits between 45 and 35 °N in the interior of North America [Bettis *et al.*, 2003] indicates that the North American ice sheets were a major dust source during the last glacial. Studies using the accumulation of organic terrestrial biomarkers in marine sediments from the northern North Atlantic, downwind from the North American continent, demonstrate similar results with increased input of terrestrial material during the last glacial cycle [Madureira *et al.*, 1997; López-Martínez *et al.*, 2006]. Several long-term dust records exist from the eastern subtropical Atlantic and indicate an increase in aeolian input during the intensification of the Northern Hemisphere glaciation (NHG) during the late Pliocene [e.g., Stein and Sarnthein, 1984; Stein, 1985; Tiedemann *et al.*, 1994; deMenocal, 1995]. However, these records reflect

changes in the African dust sources. Virtually nothing is known about variations in dust deposition in the northern North Atlantic over the Plio-Pleistocene.

Climate models show that the effect of dust on Northern Hemisphere ice sheets is crucial for simulating a complete glacial cycle [Ganopolski *et al.*, 2010]. Furthermore, changes in dust emission over the Southern Ocean during the most recent glacial/interglacial cycles may cause part of the observed 90 ppm change in atmospheric CO_2 during glacials via stimulation of the biological pump [e.g., Watson *et al.*, 2000]. In this context, determining the long-term evolution of dust accumulation in the northern North Atlantic is crucial to understand the mechanisms that drove Quaternary climate.

Using material from Integrated Ocean Drilling Project (IODP) Expedition 306 Site U1313, here we report the first orbitally-resolved long-term record of changes in aeolian input from the northern North Atlantic. We focus on the last 3.4 million years to investigate whether changes in aeolian input were associated with the intensification of the NHG around 2.7 Ma and/or the Mid-Pleistocene Transition (MPT) around 800 ka, two major steps in global climate towards more intense glacial conditions [e.g., Ruggieri *et al.*, 2009].
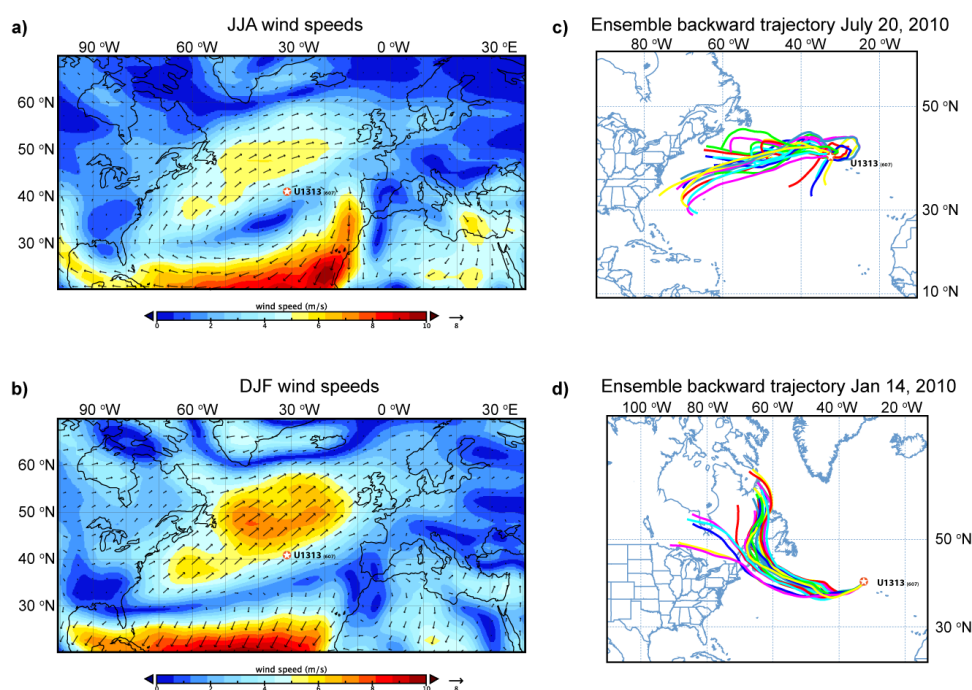
Figure 16; Study area

Average wind direction and speeds at the surface over the North Atlantic during boreal summer; June, July, and August (**a**) and boreal winter; December, January, and February (**b**). Data obtained using NCEP/NCAR reanalysis data from http://www.esrl.noaa.gov/psd/. In addition the five-day ensemble atmospheric backward trajectories at 50 m for Site U1313 during summer (**c**) and winter (**d**) are shown, calculated using HYSPLIT, available at http://www.arl.noaa.gov/. Backward trajectories are similar for different altitudes (not shown).

6.2   Regional Settings

Samples come from IODP Site U1313, located in the North Atlantic (41.00°N; 32.57°W), at the same latitude as the extensive loess deposits in the North American continent [Bettis *et al.*, 2003]. Site U1313 (3426 m water depth) is a re-drill of Deep Sea Drilling Project (DSDP) Leg 94 Site 607, which represents a benchmark site for Quaternary paleoceanography [e.g., Raymo *et al.*, 1989; Ruddiman *et al.*, 1989]. The drilling of DSDP Site 607 in the 1980s preceded the advent of the shipboard capability for construction of composite sections and pass-through magnetometers for continuous measurement of magnetic parameters. With the re-drilling of Site 607, Site U1313 now provides the rare opportunity of a continuous high-resolution sediment record covering the complete period from the Pliocene to the Pleistocene at one of the most climatically sensitive locations in the world [Expedition 306 Scientists, 2006].

The westerlies are the dominant winds between 60 and 30°N during both boreal summer and winter, blowing from the high-pressure cell in the subtropics to the low-pressure cell associated to the atmospheric polar front. In general the winds are stronger during winter due to a weakening of the low-pressure cell. Located at 41°N, Site U1313 is thus predominantly influenced by the westerlies that transport air masses from the North American continent over the North Atlantic (Figure 16).

Surface ocean circulation in the mid-latitude North Atlantic is dominated by the influence of the Gulf Stream and North Atlantic Current (NAC) that transport oligotrophic and warm surface waters northwards. The annual mean sea surface temperature (SST) at Site U1313 is 18.3 °C [Locarnini *et al.*, 2006]. During glacials, however, surface ocean circulation in the North Atlantic was radically different as high-latitude waters migrated southwards [e.g., Pflaumann *et al.*, 2003] and massive armadas of ice-bergs episodically filled the North Atlantic north of 40 °N [Ruddiman, 1977]. Bottom waters in the North Atlantic basin nowadays are influenced by North Atlantic Deep Water (NADW). In contrast, during the most recent glacials poorly ventilated Antarctic Bottom Water (AABW) filled the deep North Atlantic basin (> 2 km deep) and influenced the study site [Raymo *et al.*, 1990; Raymo *et al.*, 1992] as deep water formation in the northern North Atlantic shifted southwards [Rahmstorf, 2002].

6.3   Sampling Strategy

Four holes were drilled at Site U1313 from which two complete spliced stratigraphic sections for the Pleistocene were constructed by correlating physical properties between the holes [Expedition 306 Scientists, 2006]. For this study, we further refine the correlation to ensure that we have sampled a complete and continuous stratigraphic section for Site U1313. In this process, the original meter composite depth (mcd)-scales from Holes U1313A, C, and D were updated by tying them to the mcd-scale for Hole U1313B, providing what we call an adjusted mcd (amcd) depth scale. Creating a common depth scale allows data from different holes to be combined and compared and resolves conflicts in stratigraphic depth between holes that exist in the mcd scale. Site U1313B was selected as the master hole because it is one of the deepest continuously cored holes and it is part of the primary splice that is being studied by many others. Because of this choice, amcd = mcd for Hole U1313B, with the mcd scales adjusted for the other three holes. The adjustments are based on simultaneously correlating the lightness (L*), magnetic susceptibility (X), and paleomagnetic data (inclination and intensity) between the four holes. These records were resampled every 1 cm down to 200 mcd and correlated using the AnalySeries software [Paillard *et al.*, 1996]. Besides the upper 40 cm, correlation between holes is consistently better than ± 5 cm down to 158 amcd (~3.4 Ma), but becomes more uncertain further down section because of the lack of variations in physical properties. The tie-points for the new amcd-depths for all holes are given in Table 1 of the supplementary information.

In this study, samples from the primary splice, consisting of Holes U1313B and U1313C, were used. From the upper 160 amcd of Site U1313 (representing the last 3.4 million years) samples of 10 cm^3 were taken from the primary splice at a 20 cm (± 4 ka) resolution. A higher resolution (up to 2 cm) was used for the last one million years (Marine Isotope Stage (MIS) 26 - 1) and between 2.78 and 2.65 Ma (MIS G9 - G3). In total around 2450 samples were used in this study. All samples were freeze-dried after sampling and stored at 4 ºC until further processing took place.

6.4   Chronology

For the largest part of the record we used the shipboard age model [Expedition 306 Scientists, 2006], based on tuning of the lightness (L*) from the primary splice to the global benthic foraminiferal $\delta^{18}O$ stack [Lisiecki and Raymo, 2005]. This method assumes that changes in lightness, caused by changing carbonate content due to variations in terrestrial input, mimicked changes in benthic foraminiferal $\delta^{18}O$ without any temporal offset [Expedition 306 Scientists, 2006]. For the late Pliocene and early Pleistocene this assumption

holds and the shipboard age model is not significantly different from an age model based on benthic foraminiferal $\delta^{18}O$ for the late Pliocene [Bolton *et al.*, 2010]. However during the last 1 Ma, variations in carbonate content at Site U1313, hence lightness, occasionally lagged changes in benthic foraminiferal $\delta^{18}O$ by several ka [Stein *et al.*, 2009]. For the last 1 Ma a new age model was therefore constructed based on the combination of benthic foraminiferal $\delta^{18}O$ and lightness that accurately captures the glacial terminations [Naafs *et al.*, submitted]. Even so, future high resolution studies from Site U1313 using benthic foraminiferal $\delta^{18}O$ combined with paleo-intensities will improve this age model. Based on our age model, the sedimentation rates over the whole record vary between 2 and 9 cm/ka, but overall are constant throughout the last 3.4 Ma (Figure 18).

6.5   Methodology

6.5.1   Mass accumulation rates of *n*-alkanes and *n*-alkan-1-ols

The mass accumulation rates (MAR) of the odd-carbon-numbered C_{27}-C_{33} *n*-alkanes and C_{26}-alkan-1-ol at Site U1313 were used to reconstruct changes in aeolian input. Long-chain *n*-alkanes (C_{21}-C_{33}) with a clear odd over even predominance and *n*-alkan-1-ols (C_{22}-C_{32}) with a clear even over odd predominance are common constituents of the epicuticular waxes of terrestrial higher plants [Eglinton and Hamilton, 1967; Bianchi, 1995]. They are a major component of modern dust even in remote ocean areas [Simoneit *et al.*, 1977; Gagosian *et al.*, 1981; Conte and Weber, 2002; Conte *et al.*, 2003] as they can easily be removed from the leaf surface by wind or rain, especially by sandblasting during dust storms, or entrained as part of soil and transported over large distances. Numerous studies therefore used the accumulation of these lipids in marine sediments far from major fluvial inputs to infer changes in aeolian input to the open ocean [e.g., Madureira *et al.*, 1997; López-Martínez *et al.*, 2006; Martìnez-Garcia *et al.*, 2009].

In order to differentiate odd numbered long-chain *n*-alkanes from higher plant material and the minor input of long-chain *n*-alkanes without odd over even predominance from other potential sources, we followed the approach developed by Villanueva *et al.*, [1997]. This approach assumes that all of the even-numbered long-chain *n*-alkanes (C_{20}-C_{34}) in marine sediments reflect microbial input or reworking of odd-numbered *n*-alkanes and thus an equal amount of odd numbered long-chain *n*-alkanes does not originate from terrestrial higher plant material. Therefore, the sum of the odd-numbered C_{27} to C_{33} *n*-alkane homologues was corrected for the input of reworked *n*-alkanes by subtracting the sum of the even-numbered C_{26} to C_{34} *n*-alkane homologues by using:

$$A_{plant} = \sum_{i=0}^{2} \overset{odd}{C_{(27+2i)}} - \sum_{i=0}^{2} C_{(28+2i)} - \tfrac{1}{2}\left(C_{26}+C_{34}\right) \text{[Modified from Villanueva \textit{et al.}, 1997]}$$

where A_{plant} is the total amount of higher plant (non-reworked) n-alkanes for each sample in ng/g and C_{26}-C_{34} the abundance of the individual n-alkanes in ng/g. The Carbon Preference Index (CPI), which is used to identify the input of terrestrial higher plant material, was calculated following Bray and Evans, [1961]:

$$CPI = \tfrac{1}{2}\left[\left(\frac{C_{25}+C_{27}+C_{29}+C_{31}+C_{33}}{C_{24}+C_{26}+C_{28}+C_{30}+C_{32}}\right) + \left(\frac{C_{25}+C_{27}+C_{29}+C_{31}+C_{33}}{C_{26}+C_{28}+C_{30}+C_{32}+C_{34}}\right)\right]$$

where C_{24} - C_{34} indicate the concentration of the individual n-alkanes.

Mass accumulation rates of the biomarkers in ng/cm^2/ka were calculated using linear sedimentation rates, biomarker concentrations (A_{plant} for the n-alkanes), and dry bulk densities (DBD), calculated from shipboard measured wet bulk densities (WBD) using DBD = - 1.6047 + 1.5805 * WBD [Expedition 306 Scientists, 2006; Stein \textit{et al.}, 2009].
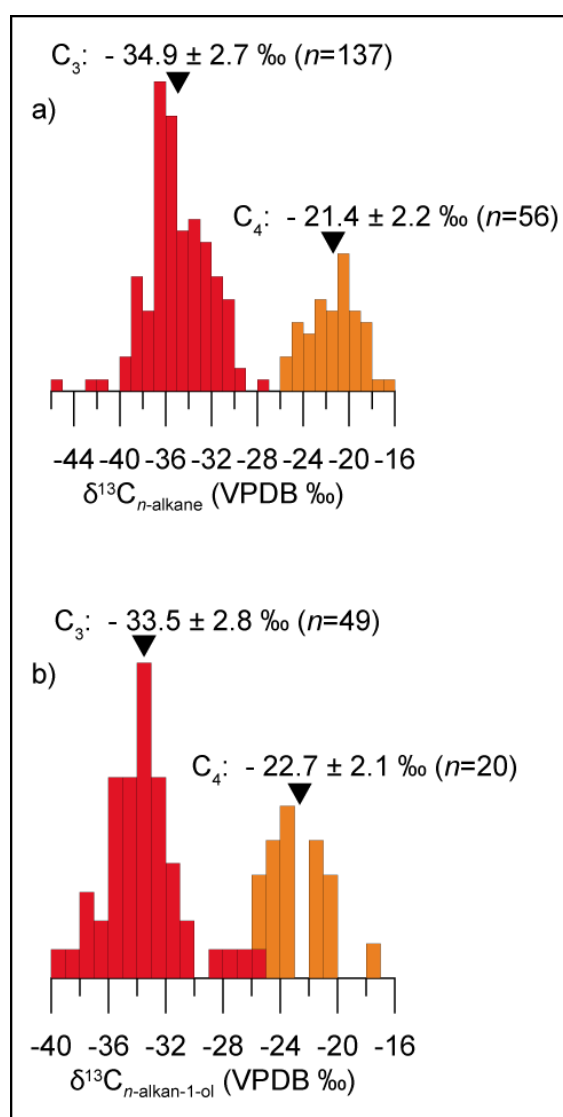
Figure 17; Histograms of modern δ^{13}C values in n-alkanes and n-alkan-1-ols

Compilation of all available literature δ^{13}C values of modern plant wax n-alkanes (C_{29} + C_{31}) **a)** and n-alkan-1-ols (C_{26} + C_{28}) **b)** in C$_3$ (red) and C$_4$-plants (orange).
[Data compiled from Rieley \textit{et al.}, 1991; Collister \textit{et al.}, 1994; Lockheart \textit{et al.}, 1997; Chikaraishi and Naraoka, 2003; Chikaraishi \textit{et al.}, 2004; Bi \textit{et al.}, 2005; Chikaraishi and Naraoka, 2006; Rommerskirchen \textit{et al.}, 2006; Pedentchouk \textit{et al.}, 2008; Vogts \textit{et al.}, 2009].

6.5.2 δ^{13}C long-chain *n*-alkanes and *n*-alkan-1-ols

Plants can photosynthesize in different ways. In general two types of photosynthetic pathways are distinguished, C_3 and C_4-plants, although a third type also exists (CAM-plants). C_3 plants (trees, shrubs, and cool-climate grasses) are the most abundant (95% of total plants) and are the dominant species in forested regions and high latitude grasslands. C_4 plants (notably tropical grasses) on the other hand have more efficient water use than C_3-plants because they can internally concentrate CO_2 and are dominant in semi-arid regions. The different photosynthetic pathways of C_3 and C_4-plants results in an isotopic offset between the two [O'Leary, 1981]. The compound specific stable carbon isotope ratio (δ^{13}C) of plant wax *n*-alkanes (C_{29} + C_{31}) in C_3-plants is on average -34.9 ‰, while for C_4-plants it is -21.4 ‰ (Figure 17 and references in caption). For the *n*-alkan-1-ols (C_{26} + C_{28}) the values are -33.5 ‰ and -22.7 ‰, for C_3 and C_4-plants respectively. Determining the δ^{13}C value of *n*-alkanes, and to a lesser extent *n*-alkan-1-ols, accumulating in marine sediments is therefore a well-established proxy to distinguish between the input from C_3 and C_4-plants [e.g., Schefuss *et al.*, 2003a; Tipple and Pagani, 2010] and infer information about the source of these lipids in marine sediments [López-Martínez *et al.*, 2006].

6.5.3   Sea surface temperatures

Annual mean SSTs (0m) at Site U1313 were calculated using the modified alkenone unsaturation index ($U_{37}^{k'}$) and the global core-top calibration [Prahl and Wakeham, 1987; Müller *et al.*, 1998].

6.5.4   Spectral analysis

The evolutionary spectra were computed using the short-time Fourier transform of overlapping segments with a 600,000-year Hamming window and 85% overlap. All the records were detrended, liniearly interpolated at 2 ka resolution and prewhitened before evolutionary spectral analysis. Prewhitening reduces the red spectral background noise arising from the nonlinear long-term evolution of climate records. Hence, it allows for a better resolution of the time series variability in the frequency range of obliquity (41ka) and precession (23 and 19 ka), but it also attenuates some of the spectral power concentrated in lower frequencies ($\geq$ 100 ka). Because high latitude dust deposition appear to be exponentially rather than lineally linked to climate [Lambert *et al.*, 2008; Martìnez-Garcia *et al.*, 2009], in the case of the *n*-alkane records the logarithm of both concentrations and mass accumulation rates were used to compute the evolutionary spectra.

Phase and coherency estimates between the different time series were computed using the iterative spectral feature of the Arand software package with a 500,000-year window and 1/2 lags. All the records were detrended and resampled at 2 ka resolution before cross-spectral analysis.

6.6 Analytical techniques

The biomarker records for Site U1313 were obtained using a gas chromatograph coupled to a LECO time of flight mass spectrometer (GC-TOF/MS). In total ± 2450 samples from the primary splice of U1313 were measured for $U_{37}^{k'}$ ratios and long-chain n-alkane concentrations. Extraction and details of the analytical methods for the $U_{37}^{k'}$-based SSTs and long-chain n-alkane records are explained elsewhere [Hefter, 2008; Stein *et al.*, 2009].

In 470 samples the concentration of the C_{26}-alkan-1-ol was measured. For this purpose the samples were derivatized with N,O bis(trimethylsilyl) trifluoroacetamide (200 μl, heated for 2 hours at 60 °C) shortly before analysis by GC/TOF-MS (using the same conditions as in Hefter, 2008). Concentrations of C_{26}-alkan-1-ol were determined from GC/TOF-MS peak areas (using *m/z* of 75), whereby a compound specific response factor was obtained from the calibration with an external C_{26}-alkan-1-ol standard (Fluka, Switzerland).

Compound specific $\delta^{13}C$ values were determined in 12 samples at the University of Bristol using a GC-isotope ratio mass spectrometer (GC-IRMS). Because of the general low concentration of higher plant waxes at Site U1313 and the current analytical limit for compound specific isotope analyses, it was not possible to get reliable $\delta^{13}C$ values from more samples although we did attempt this.

GC-IRMS methods are identical to those used elsewhere [Handley *et al.*, 2008]. $\delta^{13}C$ measurements were done in triplicate, and the $\delta^{13}C$ value for the long-chain odd numbered n-alkanes was calculated by taking the weighted average of the $\delta^{13}C$ value of the C_{29} and C_{31} n-alkane. For the long-chain even numbered n-alkan-1-ols the weighted average of the $\delta^{13}C$ value of the C_{26} and C_{28} n-alkan-1-ol was taken. Compound specific $\delta^{13}C$ values for the long-chain even numbered n-alkan-1-ols were then corrected for the derivatization process following Rieley et al., [1994]. Compound specific $\delta^{13}C$ values were not corrected for variations in $\delta^{13}C$ of atmospheric CO_2 over time, because these were assumed to be small for the time scale used in this study [e.g., Seki *et al.*, 2010]. $\delta^{13}C$ values are reported relative to the Vienna Pee Dee Belemnite (VPDB)-scale, calculated by comparison against a calibrated reference CO_2 gas.

6.7 Results

6.7.1 Mass accumulation rates of *n*-alkanes and *n*-alkan-1-ols

The results show that the MARs of both the C_{27}-C_{33} *n*-alkanes and C_{26}-alkan-1-ol are low during most of the late Pliocene[2] with values below 500 and 250 ng/cm^2/ka, respectively (Figure 18 and 19). Values were slightly higher during glacial than during interglacials of the late Pliocene. The MAR of terrestrial higher plant material increased significantly at Site U1313 during MIS G6 (~ 2.7 Ma) (Figure 19). Following MIS G6, every glacial is characterized by increased input of terrestrial higher plant material with maximum values of 2800 and 2100 ng/cm^2/ka for the *n*-alkanes and *n*-alkan-1-ol, respectively (Figure 18). During interglacials, the MAR of these terrestrial lipids is very low with values below 100 ng/cm^2/ka. The glacial/interglacial variations of aeolian input can be seen in both the accumulation rates and the concentrations of long-chain odd numbered *n*-alkanes and long-chain even numbered *n*-alkan-1-ol. A period of relatively lower aeolian input occurred during glacials between 2.1 and 1.3 Ma.

6.7.2 δ^{13}C long-chain n-alkanes and n-alkan-1-ols

Due to the low concentrations of higher plant waxes prior to 2.7 Ma and during interglacials, reliable δ^{13}C values were obtained for selected glacials only (Figure 18). δ^{13}C values of the long-chain *n*-alkanes and *n*-alkan-1-ols are relatively constant throughout the glacials of the last 2.7 Ma with a value of around -31 ‰.

---

[2] Please note we use the updated definitions of the Pliocene and Pleistocene [Gibbard et al., 2009].
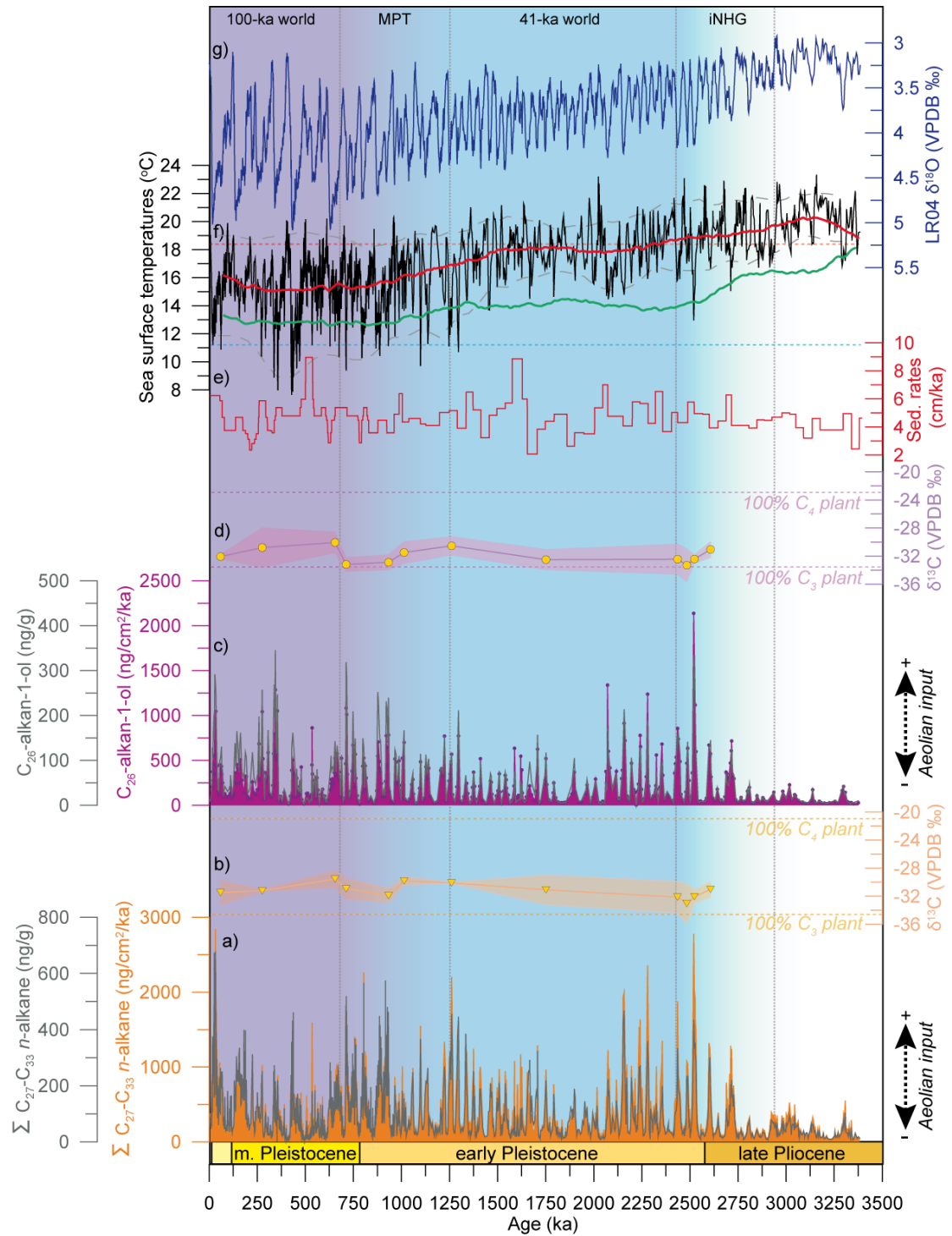
Figure 18; Biomarker records from Site U1313 covering the last 3.4 Ma

Accumulation rates and concentrations of the odd-numbered long-chain *n*-alkanes (**a**) and long-chain alkan-1-ol (**c**) together with the $\delta^{13}C$ values of the *n*-alkanes (C_{29} + C_{31}), and *n*-alkan-1-ols (C_{26} + C_{28}) (**b, d**). Shading in **b** and **d** indicates the error (1σ) associated with the $\delta^{13}C$ measurements. The modern C_3 and C_4-plant isotopic end-members are shown as dashed lines (see Figure 17). In addition, the sedimentation rates (**e**) and $U^{k'}_{37}$-based SST record from Site U1313 (black) and 400-ka moving averages of IODP Site U1313 (red) and ODP Site 982 (green), located at 57 ºN [Lawrence *et al.*, 2009]

(**f**) are shown together with the global benthic foraminiferal δ^{18}O record (**g**) for reference [Lisiecki and Raymo, 2005]. Coloured dashed lines in (**f**) indicate SSTs at present (red) [Locarnini *et al.*, 2006] and during the LGM (blue) at Site U1313. Grey dashed lines in (**f**) indicate average glacial and interglacial SSTs. iNHG = intensification of Northern Hemisphere Glaciation. MPT = Mid-Pleistocene Transition.

6.7.3   Sea surface temperatures

The SST record from Site U1313 demonstrates that surface waters in the mid-latitude North Atlantic were cooling during most of the early Pleistocene (Figure 18), continuing the long-term trend that began in the late Pliocene [Naafs *et al.*, 2010]. During the Pliocene, SSTs were generally warmer than present, even during glacials. Two major steps in the overall decrease of SSTs can be recognized; the late Pliocene (3.1-2.1 Ma) and early Pleistocene (1.5-0.3 Ma). Cooling was the most pronounced during glacials, especially during the last 1.5 Ma. Interglacial SSTs changed much less and present-day values were reached around 1 Ma. These results are almost identical to a lower resolution alkenone-based SST record from Site 607, of which U1313 is a re-drill, obtained using the traditional GC-FID method [Lawrence *et al.*, 2010].
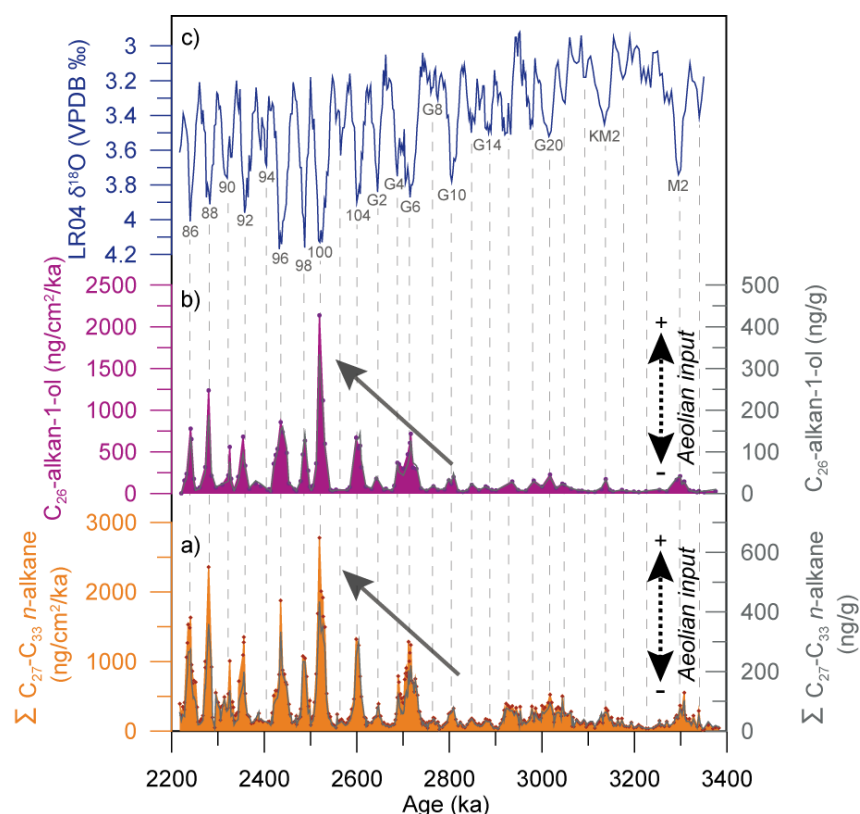

Figure 19; Intensification of the Northern Hemisphere glaciation

Accumulation rates and concentrations of long-chain odd-numbered *n*-alkanes (**a**) and even-numbered alkan-1-ol (**b**) for the period between 3.4 and 2.2 Ma. For reference the global benthic foraminiferal δ^{18}O record [Lisiecki and Raymo, 2005] is plotted together with the marine isotope stage taxonomy (**c**).

6.8   Discussion

6.8.1   Source higher plant material

Several lines of evidence suggest that both the odd-numbered C_{27}-C_{33} n-alkanes and C_{26}-alkan-1-ol that accumulated at Site U1313 during glacials are derived from aeolian input of higher plant waxes originating from the North American continent. First of all, fluvial input can be discarded as Site U1313 is located more then 1750 km from any continent.

Secondly, a hypothetical contribution from old organic material to the n-alkane signal can be considered negligible because the concentrations and distribution of the plant lipid waxes are not correlated with the occurrence of the ice-rafting events of the last glacial cycle (Figure 20). During the most recent glacial cycles the North Atlantic was characterized by episodes of massive ice-rafting events, originating from the ice sheets circum the North Atlantic [Heinrich, 1988]. As Site U1313 is located at the southern end of the ice-rafting debris (IRD)-belt [Ruddiman, 1977] it was also influenced by IRD-events during the Pleistocene [Stein *et al.*, 2009; Naafs *et al.*, submitted]. IRD contains a wide-range of organic compounds [Rosell-Melé *et al.*, 1997; Rashid and Grosjean, 2006; Naafs *et al.*, submitted] and could be a possible additional source of long-chain n-alkanes. However, in our record the abundance of odd-numbered long-chain n-alkanes and even-numbered long-chain n-alkan-1-ol is not correlated with the occurrence of the major IRD-events of the last glacial cycle (Figure 20). Especially the lag of correlation between the input of petrogenic compounds such as monoaromatic steroids, indicative for the input of ancient and organic rich material by IRD [Naafs *et al.*, submitted], and abundance of odd-numbered long-chain n-alkanes at Site U1313 indicates that IRD is not a major source for the higher plant waxes. This is also supported by the carbon preference indices (CPI) of the n-alkanes, which vary between 2 and 6 for the last glacial cycle (Figure 20). The n-alkane distribution of IRD derived organic material would be characteristic of a mature source and lead to a distribution of long-chain n-alkanes without odd over even predominance (CPI < 2.5) [Bray and Evans, 1961]. In addition, IRD for the first time started to influence the study area around 2.9 Ma [Kleiven *et al.*, 2002], more then 200 ka before the increase in aeolian input at Site U1313. Following other studies from the North Atlantic [Madureira *et al.*, 1997; López-Martínez *et al.*, 2006], we thus conclude aeolian input of higher plant waxes to be the dominant source of the long-chain n-alkanes and n-alkan-1-ols at Site U1313.

Lastly, the CPI values as well as the $\delta^{13}C$ values for the n-alkanes and n-alkan-1-ols are similar to those found at present in air masses originating from the North American continent [Conte and Weber, 2002; Conte *et al.*, 2003] and significantly different from those found in dust originating from Northern Africa [Huang *et al.*, 2000; Conte and Weber, 2002;

Schefuss *et al.*, 2003a], at present the largest source of dust in the world. The $\delta^{13}C$ values found at Site U1313 during glacials are also similar to those found in lipids accumulating during the last glacial cycle close to the American continent [López-Martínez *et al.*, 2006]. Moreover, the relatively constant $\delta^{13}C$ values over the last 2.7 Ma indicate a source that was continuously dominated by C_3-plants (Figure 18). A continuously dominant source of C_3-plants argues against both Africa and east Asia as main source for the aeolian material at Site U1313 as in those regions C_4-plants are more dominant and large variations in the dominant plant type, and hence $\delta^{13}C$, took place during the Pliocene and Quaternary [e.g., Schefuss *et al.*, 2003b; Zhisheng *et al.*, 2005; Yao *et al.*, 2010]. In line with the dominant westerly wind direction in the mid-latitude North Atlantic (Figure 16), we therefore assume that aeolian input of terrestrial higher plant material from the North American continent is the dominant source of the lipids accumulating at Site U13113.
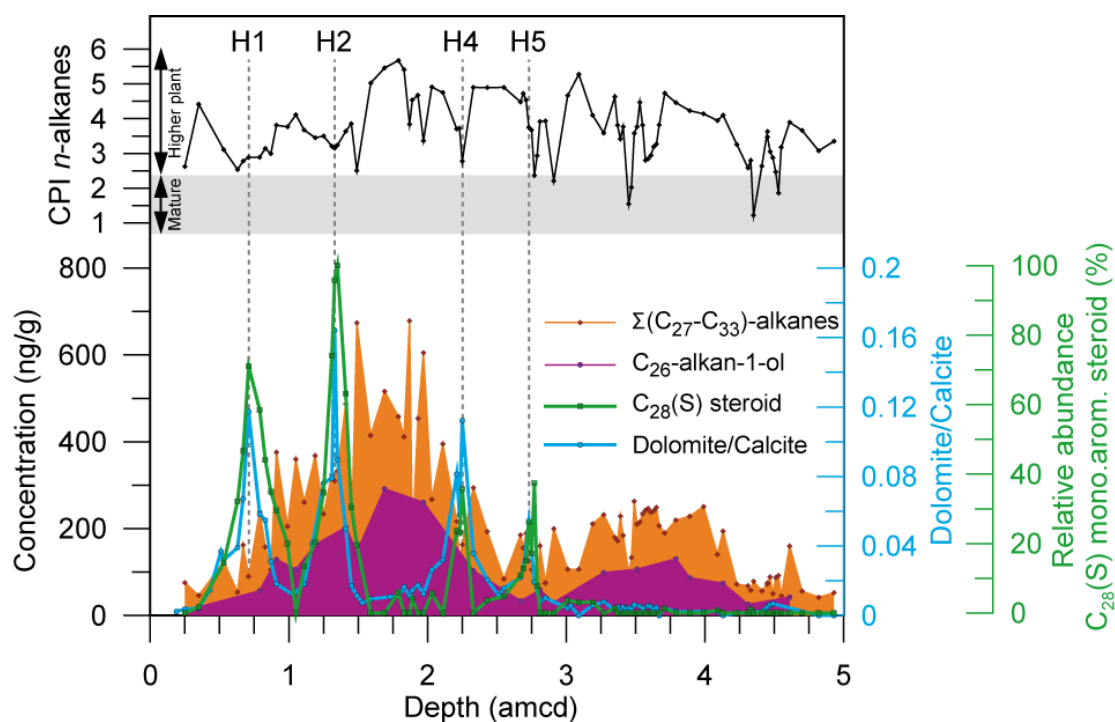
Figure 20; The last glacial cycle

Concentrations of the of long-chain odd *n*-alkanes (orange) and even *n*-alkan-1-ol (purple) together with the abundance of dolomite (blue) and $C_{28}(S)$ C-ring monoaromatic steroid (green) of the upper 5 adjusted meter composite depth (amcd) of IODP Site U1313, comprising the last 90 ka. The abundance of both dolomite and $C_{28}(S)$ steroids indicates the occurrence of IRD-events originating from the Laurentide ice sheet [Naafs *et al.*, accepted]. In addition, the CPI for the (C_{24}-C_{34})-alkanes (black) is shown. A CPI below ~ 2.5 indicates the input from a mature source, while higher values indicate higher plant waxes as source. H1-5 indicates Heinrich layers 1-5.

6.8.2 Variations in aeolian input

When the record of aeolian input from Site U1313 for the last 800 ka is compared to the dust flux in Antarctica [Lambert *et al.*, 2008], it becomes clear that the aeolian input of the North Atlantic is highly correlated with the dust flux in Antarctica (Figure 21), which beyond the differences in the magnitude of the glacial/interglacial change is correlated with the aeolian flux in the low-latitudes [Winckler *et al.*, 2008] and the Southern Ocean [Martìnez-Garcia *et al.*, 2009]. In addition, although few marine records of dust input extend back to the Pliocene, those available indicate a similar shift towards more aeolian input starting during the intensification of the Northern Hemisphere Glaciation [Dersch and Stein, 1991; Dersch and Stein, 1994; Tiedemann *et al.*, 1994]. This also coincides with the onset of loess accumulation in Asia [Yang and Ding, 2010]. These results thus suggest a global strengthening of dust sources in response to the intensification of glacial/interglacial climate variability through the Quaternary.
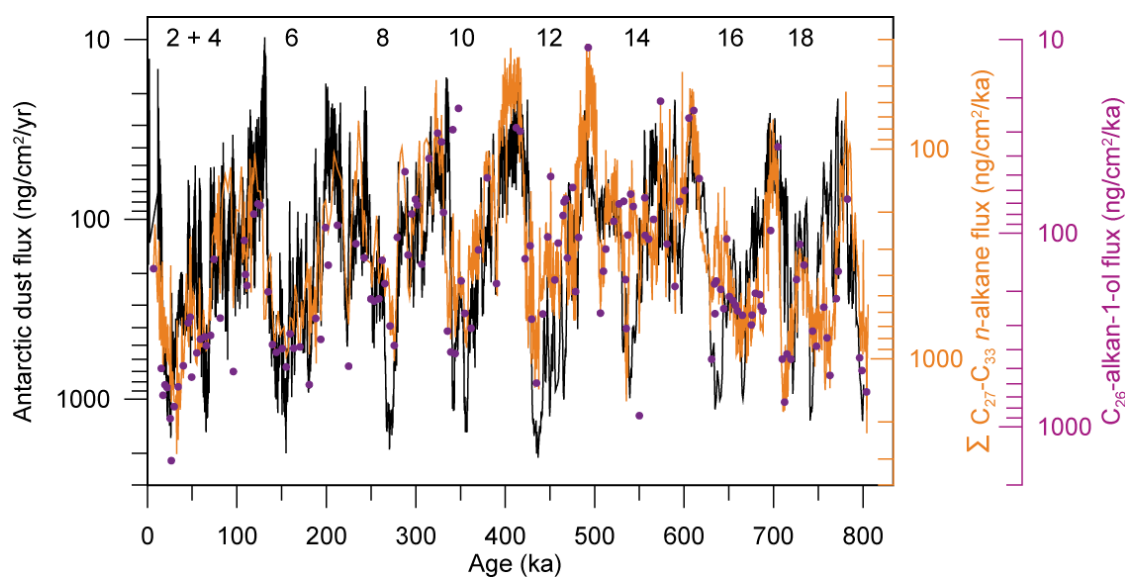
Figure 21; Aeolian input at Site U1313 compared to dust flux in Antarctica

Aeolian input at Site U1313 during the last 800 ka (orange for *n*-alkanes, pink for alkan-1-ol) and dust flux in Antarctica (black) [Lambert *et al.*, 2008]. Numbers on top indicate marine isotope stages associated to the different glacials.

The magnitude of 30 times increase in aeolian input to the North Atlantic during glacials of the Quaternary is also similar to observations from the Antarctic ice cores [Lambert *et al.*, 2008; Martìnez-Garcia *et al.*, 2009]. As Site U1313 is located in the middle of the North Atlantic it is likely that a large fraction of the aeolian material does not reach the study area and is deposited closer to the North American continent. Future long-term records that are taken from a position closer to the North American continent, therefore, will likely show even higher accumulation rates of terrestrial material during the glacials of the Quaternary. Classically, increased accumulation of terrestrial material in marine sediments during glacials is generally thought to result from a combination of process that involve the expansion of continental dust sources as a consequence of the increased glacial erosion and aridity, and a more efficient atmospheric transport of dust particles as a result of the reduced hydrological cycle, and increased wind intensity or gustiness during glacial stages [e.g., Yung *et al.*, 1996; McGee *et al.*, 2010; Mahowald *et al.*, 2011]. However, an overall increase in wind speed from the late Pliocene towards the present does not agree with modelling results for that time period that indicate stronger westerly winds during the late Pliocene warm period in the North Atlantic [Haywood *et al.*, 2000], or at most only little changes in atmospheric circulation north of ~ 40ºN [Brierley *et al.*, 2009].

However, the 30-fold increase of aeolian input observed at Site U1313 compared to the 2-4-fold increase observed at low-latitudes indicates the presence of an amplifying mechanism in our record that is probably related to the presence of continental ice sheets in the source region. In addition, the strengthening of storm tracks directly south of the large continental ice sheets [Pollard and Thompson, 1997] may have also contributed to the increased aeolian input during glacials.

Modelling results for the Last Glacial Maximum (LGM) demonstrate that the margins of the North American ice sheets were important glaciogenic dust sources [Ganopolski *et al.*, 2010]. This is also supported by studies of loess deposits in North America, which demonstrate that during the LGM loess was deposited on a large scale south of the maximum extent of the Laurentide ice sheet [Bettis *et al.*, 2003], and transported from the extensive glacial outwash plains by predominant (north)westerly winds [Muhs and Bettis, 2000]. It is likely that the higher plant material that accumulated at Site U1313 during glacials is transported in a similar way. The amplifying effect of glacial erosion in the generation of dust has also been suggested to explain the higher glacial/interglacial variability found in marine sediments from the Southern Ocean [Martìnez-Garcia *et al.*, 2009] compared to the low latitudes [Winckler *et al.*, 2008]. The 30 times increase in dust deposition in our record indicates that the process may have been more important than in high southern latitudes, and

suggest that dust deposition in IODP Site U1313 mainly reflect changes in glaciogenic dust generation associated with the advance and retreat of north American ice-sheets.

The appearance of continental ice sheets in the Northern Hemisphere during end of the late Pliocene can be concluded from the widespread appearance of IRD in sediments from the Northern Hemisphere [Shackleton *et al.*, 1984; Maslin *et al.*, 1998; Kleiven *et al.*, 2002], the appearance of glacial tills at 39 °N in the North America continent [Balco and Rovey, 2010], and the increase in the benthic foraminiferal δ^{18}O [Bintanja and van de Wal, 2008]. We therefore argue that sharp increase in glacial dust fluxes observed in our record at 2.7 Ma is related to the strengthening of North American dust sources as a consequence of the appearance of large continental ice sheets and glacial outwash plains in North America. The period of relatively reduced aeolian input during glacials between ~ 2.1 and 1.3 Ma roughly coincides with the absence of evidence for Laurentide Ice Sheet advances south of 45-47 ºN [Balco and Rovey, 2010].

6.8.3   Possible consequences of increased aeolian input

The increased aeolian input of terrestrial material to the northern North Atlantic during the late Pliocene might have had far reaching consequences. So far, most hypotheses that link dust deposition and the glacial/interglacial variations in atmospheric CO_2 through promoting primary productivity focus on the role of the Southern Ocean, which at present is iron limited [e.g., Martin, 1990; Watson *et al.*, 2000], and in particular in the Subantarctic zone where there is evidence of an increase in marine export production associated with the increased dust loads during glacial stages [Martìnez-Garcia *et al.*, 2009]. However, results from the eastern tropical North Atlantic indicate that at present aeolian mineral dust deposition from Northern Africa promotes nitrogen fixation by relieving co-limitation of iron and phosphorus [Mills *et al.*, 2004]. On geological timescales increased nitrogen fixation due to higher amounts of aeolian input can increase the nitrate inventory of the ocean and thereby-primary productivity [Mills *et al.*, 2004]. In addition, recent results showed that during summer even the northern North Atlantic is iron limited [Nielsdóttir *et al.*, 2009].

It is likely that the episodic increases in aeolian input of terrestrial material from the North American continent as reconstructed at Site U1313 fertilized the surface ocean with iron. This increase in iron supply may have affected marine ecosystems either by promoting nitrogen fixation or directly relieving iron limitation, a process that could have led to increased primary productivity in the North Atlantic Ocean during glacial stages, similar to those inferred in the Subantarctic Atlantic. This mechanism may have potentially contributed to the glacial/interglacial variations in atmospheric CO_2 providing an additional positive

feedback mechanism to the development of glacial conditions during the Quaternary. However, to test this hypothesis, long-term productivity records from the North Atlantic and reconstructions of atmospheric CO_2 that resolve glacial/interglacial variations during the early Pleistocene are required, together with an accurate estimate of its potential contribution to the glacial atmospheric CO_2 decrease using biogeochemical models.

6.8.4 Implications for the dynamics of the NH ice-sheets

The Milankovitchs theory predicts that variations in high-latitude summer solstice insolation were the primary forcing for the glacial/interglacial cycles of the Quaternary [Milankovitch, 1941]. A major problem for the standard orbital hypothesis is that although high-latitude summer insolation is mainly driven by changes in precession, records of early Pleistocene benthic foraminiferal $\delta^{18}O$ (reflecting predominantly variations in continental ice volume) varied mainly at the obliquity period [Raymo and Nisancioglu, 2003]. To explain this mismatch, it has been proposed that precession related changes in ice volume in both Hemispheres did occur but cancel out in globally integrated proxies such as benthic foraminiferal $\delta^{18}O$ [Raymo *et al.*, 2006]. Based on this hypothesis a simple ice sheet model that is sensitive to local (high-latitude) summer insolation was used to calculate Northern Hemisphere ice volume with a strong variance in the precession periods (23 and 19 ka) during the early Pleistocene [Raymo *et al.*, 2006]. The hypothesis of precession related changes in Northern Hemisphere ice volume during the early Pleistocene could potentially be tested if proxy data reflecting exclusively changes in Northern Hemisphere ice sheet dynamics was available and compared to the model output.

So far, it has been difficult to obtain long and continuous climate records indicative for Northern Hemisphere ice-sheet variability because ice sheet advances on a terrestrial margin are not recorded in most marine archives (e.g., IRD records), which demonstrate a strong 41-ka pacing [Raymo *et al.*, 2006]. As the record of aeolian input at Site U1313 is predominantly related to the dust production at active terrestrial glacial margins in North America, it provides a unique record to test the pacing of the advance and retreat of the North American ice-sheet through the Plio-Pleistocene.

Although the lack of a continuous benthic foraminiferal $\delta^{18}O$ record at Site U1313 during the Pleistocene prevents a detailed investigation of the evolution of the phasing between ice volume (benthic foraminiferal $\delta^{18}O$) and aeolian input (*n*-alkane record), a cross-spectral analysis was computed for the late Pliocene where benthic foraminiferal $\delta^{18}O$ data is available [Bolton *et al.*, 2010]. The results show that coinciding with the development of increased aeolian input during glacials, variations in aeolian input were in phase or slightly

lagged changes in global ice volume at the obliquity (41-ka) band (Figure 22). This is in-line with the suggestion of ice-sheet variability as the dominant control on changes in aeolian dust deposition at Site U1313. Therefore, evolutionary spectra of the *n*-alkane records were used to determine the dominant orbital control on North American ice-sheet dynamics and to test the hypothesis that significant precession related changes in ice volume in both Hemispheres did occur during the early Pleistocene.
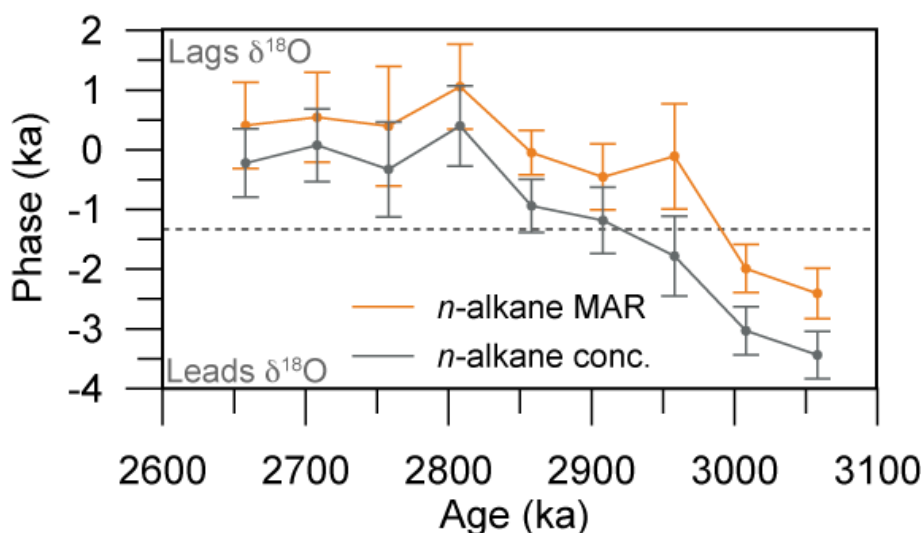
Figure 22; Phasing

Phase and coherency of the *n*-alkane concentrations (grey) and mass accumulation rates (orange) relative to benthic foraminiferal $\delta^{18}O$ at Site U1313 for the period between 3.1 and 2.6 Ma.

If ice volume in the Northern Hemisphere during the early Pleistocene would vary according to precession as previously suggested [Raymo *et al.*, 2006], the evolutionary spectra of the *n*-alkanes would be similar to that of the modelled Northern Hemisphere ice volume that assumes a strong variance in the precession periods. However, the evolutionary spectra of the *n*-alkane records and Northern Hemisphere ice volume are radically different (compare Fig. 23c-d with Fig. 23f). As expected, the evolutionary spectrum of the modelled Northern Hemisphere ice volume is dominated by strong precession periods (23 and 19 ka). In contrast, the evolutionary spectra of the *n*-alkanes clearly demonstrate that during the early Pleistocene variance in the obliquity period (41-ka) dominates aeolian input at Site U1313 (Figure 23c-d), similar to the benthic foraminiferal $\delta^{18}O$ stack and SSTs at Site U1313 (Figure 23a-b). Following the MPT, the frequencies shift towards a dominance of 100-ka cycles. Here we do not focus on the shift during the MPT, which has been studied intensively [e.g., Huybers and Wunsch, 2005; Bintanja and van de Wal, 2008], but on the dominance of the obliquity period during the early Pleistocene.

The absence of strong precession periods (23 and 19 ka) in the *n*-alkane records during the early Pleistocene suggest that the North American ice-sheet did not vary significantly as a response to precession during the early Pleistocene. These results are in good agreement with those obtained in other high-latitude SST records that all depict a dominance of obliquity during the early Pleistocene [e.g., Lawrence *et al.*, 2009; Lawrence *et al.*, 2010]. Thus, according to these results it is unlikely that strong precession related changes in ice volume in the Northern Hemisphere did occur but cancel out in globally integrated proxies such as foraminiferal δ^{18}O. Other mechanisms are needed to explain the strong dominance of the obliquity period during the early Pleistocene, possibly related to the role of integrated summer insolation in controlling the advance and retreat of northern hemisphere ice-sheets [Huybers, 2006].
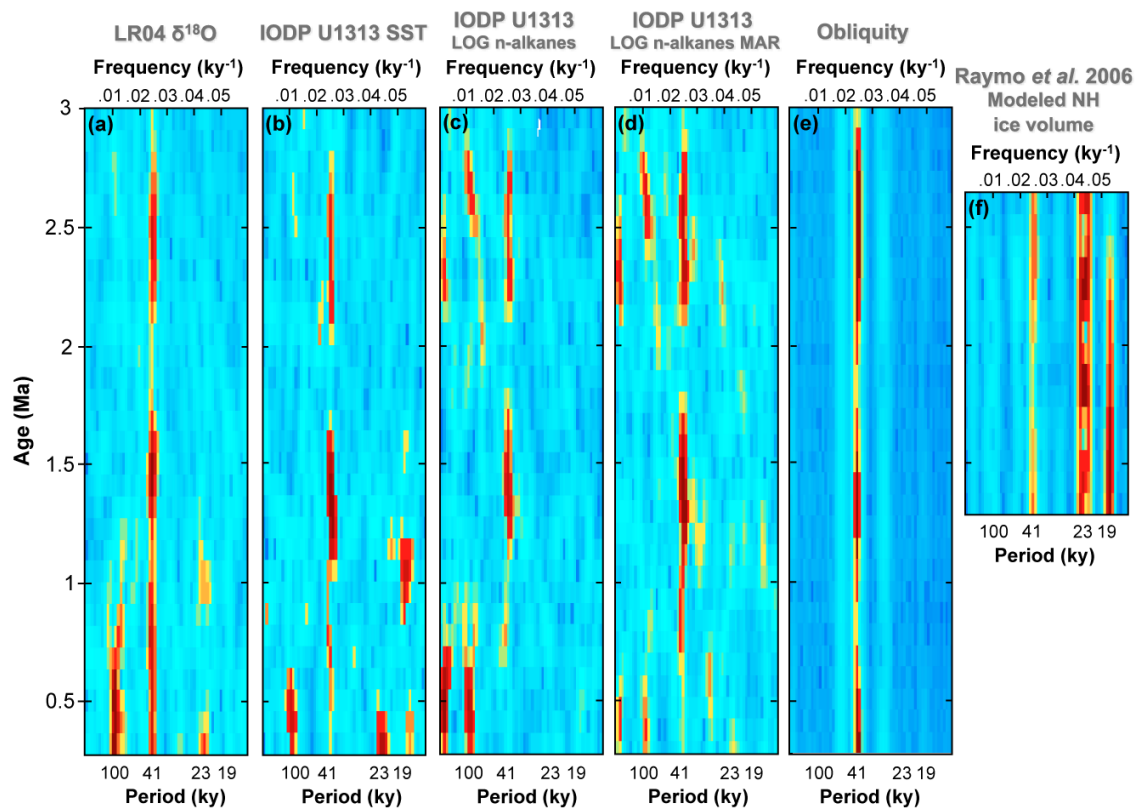
Figure 23; Evolutionary spectra

Evolutionary spectra of the global benthic foraminiferal δ^{18}O record [Lisiecki and Raymo, 2005] (**a**), Sea surface temperatures at Site U1313 (**b**), logarithm of the concentrations and mass accumulation rates of long-chain odd I-alkanes (**c** and **d**), obliquity (**e**), and modelled Northern Hemisphere ice volume by assuming a strong dependence on local summer insolation [Raymo *et al.*, 2006] (**f**).

6.9 Conclusions

In summary, the flux of aeolian derived terrestrial higher plant waxes to the North Atlantic increased significantly during glacial stages starting at 2.7 Ma. The characteristics of the lipids of higher plant waxes (CPI and $\delta^{13}C$ values) are similar as those found at present in air masses originating from North American continent and thus suggest this as main source for the aeolian material over the last 3.4 Ma. The timing of the onset of significant amounts of aeolian material accumulating in the North Atlantic coincides with the development of continental ice sheets at the North American continent. We suggest that the episodic development of glacial outwash plains associated with large continental ice sheets in North America was the main cause of the observed increase in aeolian input during glacials. This is in line with results of cross-spectral analysis between benthic foraminiferal $\delta^{18}O$ and *n*-alkane records from Site U1313, which indicate that variations in aeolian input are in phase or slightly lag changes in ice volume at the obliquity band. Evolutional spectral analysis of the *n*-alkane records demonstrates that throughout the early Pleistocene, variance in the obliquity period (41-ka) dominates aeolian input and hence North American ice sheet dynamics. This argues against suggestions of precession-related variations in Northern Hemisphere ice volume during the early Pleistocene and urges for other mechanisms to explain the dominance of the 41-ka period during the early Pleistocene.

So far the role of dust on long-term climate change has been largely neglected. Our results show that the increased dustiness that characterized the most recent glacial cycles has been a persistent feature of Quaternary climate. As we propose the increased aeolian input to the North Atlantic could have had a significant effect on global climate, future work should focus on more precisely determine the role of dust and associated feedback mechanisms in the development of Quaternary climate.

6.10 Acknowledgements

6.11 Supplementary material

6.11.1 Introduction

Multiple holes were cored at Site U1313 in order to provide sufficient material to build a complete stratigraphic section. No single drill hole can provide such a section because coring gaps commonly occur between cores and inevitably some intervals are affected by coring disturbance. Hence, a complete composite section is built by splicing cored intervals from the different holes together such that coring gaps or intervals affected by coring disturbance are excluded [e.g., Acton *et al.*, 2001]. Ultimately, an accurate composite depth scale allows data from the different holes to be combined and compared and for complete composite paleoceanographic, climatic, environmental, geomagnetic, and physical properties records to be constructed. In order to accomplish this task, the depths of coeval strata from one hole must be know relative to the depths in the other holes.

Core depths are initially measured in meters below seafloor (mbsf), which is based on a drill pipe measurement to the top of the cored interval. This establishes the depth to the top of the core, with the assumption that the top of any core material recovered was at this depth, even if core recovery was incomplete. Depths along the core are established by measuring along the core from the depth at the top of the core. Given tides, ship motion, and the relatively low precision of the drill pipe measurement, the mbsf depth for a stratigraphic interval in one hole is not equivalent to the mbsf depth in other holes at the site. Coeval strata may be offset my several meters in the mbsf scale from one hole to the next.

During Expedition 306, this first-order misalignment was addressed by creating a meters composite depth (mcd) scale, which aligns features (e.g., a susceptibility anomalies or ash layers) from one core in a hole to coeval features in a core from another hole, but without allowing compression or expansion of the within-core mbsf depth scales [Expedition 306 Scientists, 2006]. Thus, the mcd scale might align a feature between two holes perfectly at one position along the two cores being correlated but misalign other features elsewhere along these two cores. The misalignment is usually on the scale of a few centimeters up to about 60 cm over a 9.6-m-long core. Larger misalignments are rare but can occur if gaps or coring disturbed intervals occur in one or both of the cores being correlated.

The mcd scale can be improved upon by allowing the within-core depth scales to be adjusted by expanding or compressing them. This creates the new depth scale referred to as the adjusted meters composite depth (amcd) scale. Importantly, the second-order correlations used in the amcd scale are built upon the first-order correlations used in the mcd scale, which limits the compression or expansion to within a core rather than over longer intervals.

The correlation is done by wiggle matching, where the wiggles are physical, chemical, lithologic, or magnetic properties data that have been collected continuous along the cores. The precision of the correlation is thus limited to the resolution of these data and to how precisely the position of each core section can be attained in the various track systems that do the measurements. Data used for the amcd are measured every 2 to 5 cm along the core, and core sections are positioned in track systems with a precision of a couple of centimeters. Thus, the Site U1313 amcd scale correlates features to better than about 5 cm. Given that sedimentation rates average ~5 cm/k.y. at this site and that the correlation extends to a depth of 200 amcd, this amounts to misfits between holes of ≤1 k.y. over a section that spans the past 4.3 Ma.

6.11.2 Method

The amcd scale was built by simultaneously correlating color reflectance, susceptibility, and paleomagnetic data from one of the holes at Site U1313 to the mcd scale of a selected master hole. We chose Hole U1313B as the master hole because it is (1) one of the deepest holes, (2) one of the more complete records, and (3) one of the two holes in the primary splice, with the other hole being U1313C. Based on IODP sampling policy, both the archive and working halves of the primary splice can be sampled, which makes the primary splice the focus of most post-cruise studies. The choice of which hole to use for the master hole is not that significant as long as the hole has fairly good recovery and spans the interval of interest. For this study, we sought to extend the amcd to 200 meters depth (~4.3 Ma) in order to include the full transition through the onset of Northern Hemisphere glaciation, the mid-Pleistocene transition, and multiple geomagnetic reversals. Hole U1313D was not a good choice because it was only cored to 152 mbsf. Hole U1313A was not as good a choice as Hole B because many whole-round samples were collected from it for pore-water analysis prior to making color, susceptibility, and paleomagnetic measurements, and so more data gaps exist for Hole A than the other holes.

Because Hole U1313B is the master hole, its mcd scale is equivalent to the amcd scale. The mcd scales of the other three holes are adjusted relative to the Hole B mcd, and the new scale is then referred to as amcd for clarity. It is worth noting that the procedure used in building the mcd scale, results in expansion of that scale by about 10% to 15% relative to the mbsf depth scale. This results from curation practices, core decompression, and coring deformation as discussed in Acton and Borton [2001]. The amcd scale is likewise expanded since it is derived from the mcd scale. The expansion can easily be removed by compressing the amcd scale based on comparison of the amcd scale with the original mbsf depths for each

core. Such compression is of course unnecessary for most studies that are interested in chronostratigraphic relationships whereby the amcd is converted directly to age using an appropriate age model.

The specific data used for correlation are the lightness (L*) component of the color reflectance data, the whole-core susceptibility data, and the paleomagnetic inclination (I) and intensity (J) measured on the archive halves of the cores following alternating field (AF) demagnetization at 20 mT. All these data were collected during Expedition 306 [Channell et al., 2006] and are available on the IODP database (http://iodp.tamu.edu/janusweb/links/links_all.shtml). They were cleaned using the same procedure as used during the cruise for the mcd scale, in which data from disturbed intervals (Table T28 from Expedition 306 Scientists, 2006) and obvious spurious measurements are deleted. In addition, inclination and intensity data from U-channel samples (150 cm x 2 cm x 2 cm) from the upper 120 mcd of Holes B and C (G. Acton, unpublished data) were used to fine-tune the correlation between these two holes. Beside the continuous data sets, two discrete turbidite layers were recovered (at 160.37 and 197.79 mcd in Hole B) that are used as tie points.

Signal correlation was accomplished using the program AnalySeries [Palliard et al., 1996; version 2.0.3]. Data were uploaded into AnalySeries and resampled every 1 cm down to 200 amcd. The L*, susceptibility, inclination, and intensity data for Holes A, C, and D were then simultaneously compared and correlated with the same type of data from Hole B. Improvements in the fit are noted both visually and by an increase in the correlation coefficient.

6.11.3 Results

The L* data provide the strongest constraint of the long wavelength and sometimes short wavelength correlation. As noted by Expedition 306 Scientists [2006], the L* values are generally high (= lighter intervals) during warmer periods (interglacials) when biogenic carbonate content is high, whereas L* values are lower (= darker intervals) during colder periods (glacials) when the clay content increases. The characteristic L* signal is easily correlated between holes and can also be readily correlated to the LR04 oxygen isotope stack of Lisiecki and Raymo [2005] to obtain an age model [Expedition 306 Scientists, 2006; Stein et al., 2006].

The stratigraphic section becomes very light in color below about 158 amcd (before the onset of Northern Hemisphere glaciation) and the L* signal is less distinctive and harder to correlate. Susceptibility and intensity provide characteristic peaks that are strong

constraints in the upper part of the record. Below 120 amcd, the whole core susceptibility record is very noisy and no longer provides any reliable constraint and the intensity has only rare peaks that are of use. The inclination can be correlated well down to about 175 amcd but provides weaker correlation further downhole. The two turbidites at 160.37 and 197.79 amcd provide two additional tie points. Some other general observations on the quality of correlation are:

- The upper 40 cm is not well correlated between any of the holes. This soupy core interval is possibly disturbed by coring or subsequent core recovery in at least three if not all four of the holes.

- Except for the upper 40 cm, the between-hole correlation is very good down to 158 amcd and from 190-200 amcd.

- Correlation of Hole A to B between 175-185 amcd is relatively poor.

- Correlation of Hole C to B between 170-200 amcd is relatively poor.

- The lower 4 m of Hole D (164-168 mcd) is relatively poorly correlated to Hole B.

- The poorest overall correlation occurs between 178 and 185 amcd, with the possibility that as much as a full precession cycle is duplicated or missed in one or more of the cores within this interval.
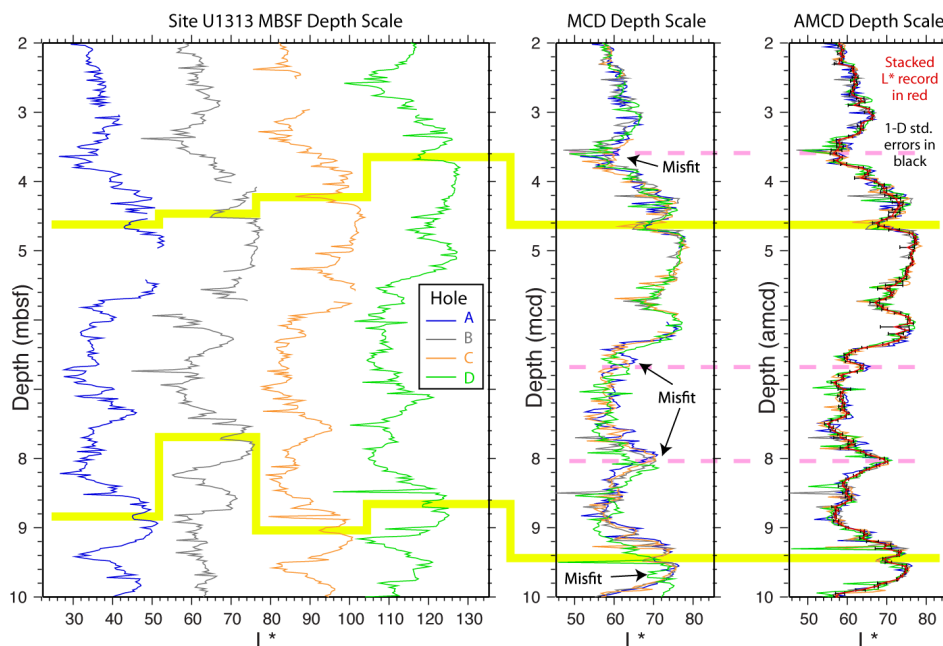
Figure S1; Example of the depth adjustments required to create the amcd depth scale and to align distinct variations in the lightness (L*) of the sediment. For the mbsf scale, the L* values for Holes A, C, and D have been offset from their measured values by -25, +25, and +50, respectively. Red curve in the amcd scale is the stack (average values) of L* from all four holes and the black error bars give the 1-D standard errors. Yellow and light purple lines illustrate the positions of a few of the distinct anomalies that are misaligned in the mbsf and mcd depth scales and that are aligned well in the amcd scale.

After completing the correlation between Hole B and each of the other holes, the L* data from all four holes were stacked as described below. Data from each hole were then compared with the stack and several slight adjustments were made to the depths of Holes A, C, and D to ensure that the correlation was consistent between all the holes. Final fine-scale adjustments were made in the correlation of the upper 120 amcd of Hole C to Hole B by using the inclination and intensity measured every 1 cm along U-channel samples. This final amcd is given in Table 1. An example of the evolution of the depth scale from mbsf to mcd to amcd is illustrated in Figure S1. Adjustments to the depths of tie points used in the amcd scale relative to their depths in the mcd scale were most commonly <10 cm (the mode in Figure S2) and 95% of the tie points were adjusted <60 cm. The largest adjustment is 1.97 m.

Distance Between Tie Points
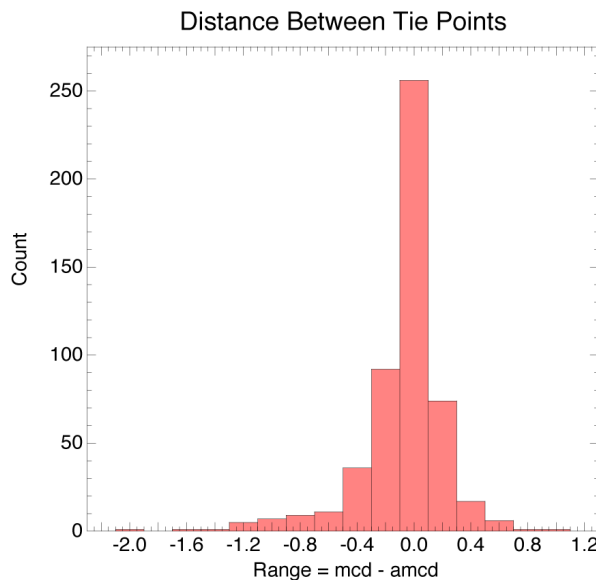
Figure S2; Distance between tie points in mcd necessary for construction of the amcd scale. The mode falls within the ±10 cm bin and 95% of the tie points fall within ± 60 cm. The largest adjustment is 1.97 m.

6.11.4 Stacked Data Sets

Stacked L* and susceptibility datasets were created by first placing all the data from the four holes into the amcd scale, combining the data by type, and then averaging them every 5 cm downhole with a window that is ±2.5 cm. Thus, each average datum is independent of its neighbors. Outliers are removed where an outlier is defined as any datum that is more than four standard errors from the mean for a specific interval being averaged. Arithmetic averages are used in computing the mean values for both the L* and susceptibility data sets.

The resulting stacked records are somewhat smoother than the records for the individual holes but the noise should be reduced by about a factor of two (the standard error in a mean observation is the reciprocal of the square root of the number of observations used in computing the mean) and potential outliers should be absent or very rare. An example of

the stacked L* record and its standard error is shown for a short interval (Figure S1) along with the L* data from all four holes. As noted above, this record correlates very well with LR04 and so has a very similar power spectrum with peaks at Milankovitch frequencies.

Table S1; Tie-points for the newly constructed amcd depth-scale

Tie Points A-->B		Tie points C-->B		Tie Points D-->B	
1313A-mcd	1313B-mcd	1313C-mcd	1313B-mcd	1313D-mcd	1313B-mcd
0,000	0,000	0,000	0,000	0,000	0,000
0,555	0,662	0,200	0,200	1,429	1,357
0,792	0,910	0,562	0,672	2,345	2,251
1,351	1,338	1,297	1,317	3,603	3,554
1,770	1,792	1,792	1,684	4,460	4,374
2,076	2,115	2,307	2,242	4,684	4,669
2,484	2,437	3,586	3,437	5,902	5,897
3,640	3,550	4,144	4,088	7,956	7,857
3,860	3,810	4,668	4,609	9,531	9,334
4,638	4,595	5,385	5,436	10,198	9,959
7,590	7,770	5,690	5,733	10,964	10,569
7,710	7,860	7,747	7,853	11,197	11,136
7,970	8,040	8,444	8,428	11,649	11,588
8,384	8,423	8,665	8,698	14,300	14,261
9,120	9,180	9,461	9,468	16,996	16,916
9,450	9,460	10,547	10,579	19,510	19,352
10,030	10,000	11,010	11,019	22,649	22,647
10,650	10,580	11,332	11,379	23,041	22,951
10,897	10,783	11,579	11,583	24,184	24,149
11,507	11,389	12,140	12,151	25,687	25,774
11,797	11,581	14,287	14,265	26,522	26,782
12,114	11,918	14,909	14,873	26,758	26,982
12,400	12,150	15,848	15,784	30,668	30,670
12,740	12,540	17,001	16,972	33,215	32,990
13,398	13,092	18,704	18,723	34,236	34,093
13,500	13,240	19,326	19,314	35,150	35,041
14,560	14,250	20,972	20,961	35,602	35,462
15,430	15,050	21,107	21,142	37,149	37,068
16,490	16,910	21,376	21,376	38,302	38,333
16,760	17,160	22,563	22,621	38,438	38,437
18,490	18,720	22,962	23,041	38,745	38,747
19,190	19,210	26,056	26,094	40,628	40,795
19,990	19,890	28,025	28,177	41,132	41,385
20,750	20,580	28,507	28,564	41,555	41,748
21,290	20,930	30,003	30,134	44,651	44,902
21,520	21,160	30,885	30,890	45,075	45,377
21,790	21,400	31,760	31,695	45,445	45,664
22,300	21,860	32,172	32,160	45,705	45,919
24,230	23,650	32,944	32,895	48,806	49,218
25,190	24,710	33,267	33,212	51,726	51,557
25,780	25,240	36,442	36,263	52,203	52,104
30,822	30,790	36,694	36,603	52,487	52,336
31,718	31,711	37,129	37,064	53,067	52,897
32,860	32,970	37,485	37,354	54,909	54,856
34,177	34,429	37,741	37,734	55,459	55,409
34,480	34,720	38,723	38,777	55,918	55,769

36,740	37,170	38,963	39,001	56,297	56,252
36,985	37,356	41,141	41,188	57,310	57,289
37,540	38,040	41,676	41,737	58,545	58,554
39,250	38,350	42,434	42,465	59,458	59,393
39,392	38,755	43,783	43,759	61,924	61,843
39,567	39,303	44,496	44,487	63,251	63,229
40,004	40,366	45,513	45,529	63,569	63,668
40,830	41,190	46,161	46,418	66,504	66,425
41,480	41,820	46,393	46,836	67,339	67,422
42,210	42,450	46,521	47,005	68,452	68,556
43,850	43,920	46,859	47,212	70,318	70,409
45,590	45,600	47,475	47,805	73,456	73,503
46,121	46,119	48,943	49,211	73,663	73,687
46,952	46,947	49,077	49,337	74,939	75,459
47,756	47,719	50,555	50,502	75,122	75,679
50,107	50,338	52,436	52,133	75,227	75,870
51,896	51,794	53,245	52,872	75,775	76,370
52,121	51,935	54,503	54,205	76,449	77,176
52,508	52,347	57,719	57,694	76,887	77,635
53,289	53,152	58,128	58,094	78,392	79,279
53,544	53,405	59,054	59,034	79,841	80,779
56,190	56,270	60,004	60,063	80,064	81,101
57,500	57,799	62,184	62,070	81,445	81,932
62,168	62,059	63,079	62,883	81,971	82,240
62,802	62,864	63,322	63,211	83,083	82,785
63,577	63,564	65,684	65,579	83,342	83,327
64,533	64,582	68,558	68,544	83,486	83,487
65,194	65,243	70,421	70,474	85,810	85,774
65,531	65,610	73,154	73,224	88,289	88,264
66,799	66,770	74,790	74,772	89,878	89,907
67,293	67,380	75,916	75,883	91,491	91,500
67,832	67,950	78,063	79,014	91,791	91,852
70,330	70,360	78,434	79,413	93,696	93,639
71,111	71,322	79,783	80,791	94,094	93,999
72,032	72,264	79,946	81,085	94,352	94,431
73,083	73,281	81,405	81,889	95,881	95,925
73,413	73,479	82,216	82,356	99,058	99,029
74,236	74,196	83,130	82,788	99,895	99,848
74,422	74,395	83,540	83,483	100,431	100,339
74,717	74,584	84,236	84,207	101,120	101,071
76,148	75,948	84,389	84,358	102,560	102,390
78,975	78,773	84,538	84,562	104,660	104,432
79,355	79,243	84,727	84,744	106,228	106,063
79,698	79,549	85,382	85,387	107,023	106,784
80,116	80,048	85,609	85,734	107,169	107,064
80,816	81,068	88,910	88,616	107,647	107,725
81,407	81,909	91,419	91,370	108,269	108,436
83,119	82,787	91,813	91,772	109,349	109,463
83,348	83,317	94,405	94,454	109,532	109,852
84,696	84,734	95,292	95,490	109,732	110,098
85,640	85,770	95,911	95,926	109,967	110,375
90,610	91,037	96,230	96,224	110,232	110,586
92,267	92,240	97,185	97,266	111,809	112,381
92,435	92,449	98,005	98,094	114,138	114,340
93,348	93,369	100,034	100,039	114,921	114,897
93,910	93,901	100,852	100,814	117,662	117,686
94,460	94,450	101,184	101,193	118,852	118,888

96,090	96,074	101,432	101,411	119,220	119,383
96,568	96,465	106,226	106,089	119,557	119,626
97,318	97,256	108,338	108,412	122,315	122,373
99,110	99,040	110,206	110,495	123,087	123,046
101,230	101,190	111,084	111,531	123,204	123,142
103,738	103,507	111,521	112,090	123,929	124,198
104,810	104,580	111,835	112,374	125,255	125,282
106,162	105,962	114,858	114,879	125,480	125,567
108,478	108,432	115,203	115,242	127,534	127,416
109,715	109,774	116,192	116,112	127,760	127,801
110,223	110,267	116,363	116,324	129,081	129,148
110,502	110,587	117,431	117,389	131,591	131,701
111,400	111,550	118,048	117,856	132,734	132,857
111,824	112,222	119,344	119,192	132,968	133,002
112,198	112,462	119,401	119,357	133,449	133,563
113,794	114,272	120,478	120,334	136,062	135,996
114,640	114,870	122,334	122,391	137,864	137,826
115,034	115,244	123,068	123,067	138,832	138,966
116,000	116,110	124,042	124,195	139,731	139,915
117,317	117,385	124,307	124,524	141,625	141,959
117,661	117,607	124,866	124,957	142,156	142,593
118,078	118,029	125,476	125,574	142,717	143,173
119,297	119,151	127,317	127,413	143,092	143,556
119,437	119,266	128,273	128,500	146,496	146,366
119,508	119,418	129,103	129,144	147,288	147,088
119,746	119,581	131,704	131,701	149,703	149,625
120,482	120,216	132,821	132,852	150,755	150,772
122,190	122,101	136,692	136,611	151,790	151,713
122,908	123,148	137,846	137,816	153,154	153,103
123,480	123,513	138,028	138,027	155,488	155,597
123,962	124,193	139,634	139,809	156,453	156,597
125,983	125,643	139,843	140,053	157,768	158,090
127,448	126,960	141,392	141,806	160,434	160,395
128,133	127,630	141,822	142,318	164,146	164,441
129,108	128,469	142,171	142,617	164,340	164,791
130,393	129,737	142,622	143,157	165,577	167,141
131,619	130,785	143,424	144,034	166,646	168,612
133,339	133,435	143,747	144,537	168,145	169,618
134,274	134,544	147,087	147,100		
134,569	134,714	148,878	148,834		
136,125	135,993	149,673	149,617		
138,034	138,019	151,826	151,798		
139,786	139,892	153,180	153,169		
139,911	140,044	155,037	155,201		
140,428	140,635	155,486	155,611		
141,650	141,829	156,039	156,177		
141,992	142,202	156,157	156,340		
143,631	143,914	156,444	156,555		
146,008	145,935	156,705	156,888		
146,369	146,367	157,568	157,811		
147,141	147,234	159,016	159,218		
149,546	149,511	160,085	160,370		
150,726	150,800	160,120	160,405		
152,007	152,035	162,466	162,602		
152,278	152,385	163,974	164,317		
153,065	153,121	164,075	164,485		
155,235	155,337	166,217	166,070		

155,507	155,592	167,132	167,132
156,436	156,582	168,812	168,596
157,932	158,081	169,166	168,847
158,610	158,683	170,152	170,125
159,429	159,586	171,083	171,113
160,400	160,370	173,250	173,117
160,430	160,405	174,687	174,692
160,941	161,102	175,239	175,186
162,439	162,601	176,050	177,218
166,877	166,788	177,050	178,197
167,308	167,127	178,025	179,157
171,169	171,069	179,816	180,658
173,388	173,517	181,307	182,168
173,985	174,293	182,773	182,894
176,917	178,200	183,301	183,380
179,084	180,034	183,950	184,004
180,641	181,551	189,033	189,029
181,390	182,151	191,136	191,331
182,231	182,865	191,592	191,601
182,921	183,677	192,152	192,217
187,505	187,469	193,753	193,643
189,042	189,031	194,817	194,532
190,189	190,125	195,118	195,122
191,692	191,629	196,635	196,598
193,205	193,131	197,810	197,790
194,692	194,608	197,940	197,840
197,950	197,790	199,966	199,938
198,040	198,840		
198,214	197,810		
199,261	199,110		

7 Sea surface temperatures did not control the first occurrence of Hudson Strait Heinrich Events during MIS 16

B.D.A. Naafs, J. Hefter, P. Ferretti, R. Stein, and G.H. Haug

Hudson Strait (HS) Heinrich Events, ice-rafting events in the North Atlantic originating from the Laurentide ice sheet (LIS), are among the most dramatic examples of millennial-scale climate variability and have a large influence on global climate. However, it is debated as to whether the occurrence of HS Heinrich Events in the (eastern) North Atlantic in the geological record depends on greater ice discharge, or simply from the longer survival of icebergs in cold waters. Using sediments from Integrated Ocean Drilling Program (IODP) Site U1313 in the North Atlantic spanning the period between 960 and 320 ka, we show that sea surface temperatures (SSTs) did not control the first occurrence of HS Heinrich(-like) Events in the sedimentary record. Using mineralogy and organic geochemistry to determine the characteristics of ice-rafting debris (IRD), we detect the first HS Heinrich(-like) Event in our record around 643 ka (Marine Isotope Stage (MIS) 16), which is similar as previously reported for Site U1308. However, the accompanying high-resolution alkenone-based SST record demonstrates that the first HS Heinrich(-like) Event did not coincide with low SSTs. Thus, the HS Heinrich(-like) Events do indicate enhanced ice discharge from the LIS at the end of the Mid-Pleistocene Transition, not simply the survivability of icebergs due to cold conditions in the North Atlantic.

7.1 Introduction

In the 1980s Heinrich discovered that sediments from the Dreizack Seamounts in the North Atlantic covering the last glacial cycle contained several layers that were rich in ice-rafted debris (IRD) [Heinrich, 1988]. These layers that now bear his name [Broecker *et al.*, 1992] have been found at many sites between ~ 40 and 55 ºN in the North Atlantic and have received much attention from the paleoclimate community over the past two decades [e.g., Hemming, 2004]. Besides the high flux of IRD, Heinrich layers have anomalously high magnetic susceptibility values and low abundance of foraminifera [e.g., Broecker *et al.*, 1992; Grousset *et al.*, 1993; McManus *et al.*, 1998]. Although six layers were originally identified for the last glacial cycle (H1-6) [Bond *et al.*, 1992], it is debated whether H3 and 6 are truly ice-rafting events (at least in the eastern North Atlantic) and are not the result from low accumulation of foraminifera [Gwiazda *et al.*, 1996; Hemming, 2004]. The IRD of Heinrich layers 1, 2, 4, and 5 shares a set of characteristics that is consistent with an origin from Paleozoic carbonates in the Hudson area of Canada [Hemming, 2004]. This subgroup is termed Hudson Strait (HS) Heinrich Events and is related to instabilities of the Laurentide ice sheet (LIS) [Hemming, 2004; Hodell *et al.*, 2008]. As the LIS formed the largest ice sheet in the Northern Hemisphere during glacials it is reasonable to suggest that the HS Heinrich Events indicate the most intense periods of ice-rafting in the mid-latitude North Atlantic. This is also supported by the higher flux of IRD during these four events in the eastern North Atlantic [McManus *et al.*, 1998; Hemming, 2004].

The massive input of icebergs from the LIS during (HS) Heinrich Events led to severe cooling and freshening of surface waters in one of the most sensitive regions of the world: the North Atlantic [Bard *et al.*, 2000; Rosell-Melé *et al.*, 2002]. Based on the most recent glacial cycle, a set of related hypotheses have arisen for a feedback by which the HS Heinrich Events in the North Atlantic initiate deglaciations [Marchitto *et al.*, 2007; Sigman *et al.*, 2007; Anderson *et al.*, 2009]. During and possibly just prior to HS Heinrich Events, perhaps resulting from insolation-driven melting of and/or internal instabilities in the Northern Hemisphere ice sheets [Hemming, 2004], North Atlantic overturning terminates [e.g., McManus *et al.*, 2004; Pisias *et al.*, 2010]. It has been suggested that this termination of North Atlantic overturning induced increased overturning and warming in the Southern Ocean [e.g., Sigman *et al.*, 2007; Barker *et al.*, 2009], yielding the observed abrupt rises in the Antarctic temperature and most likely atmospheric CO_2 [Jouzel *et al.*, 2007; Lüthi *et al.*, 2008]. Although the HS Heinrich Events thus appear to have been important during the last glacial termination and are the most dramatic examples of millennial-scale climate variability, little is known about the occurrence of HS Heinrich(-like) Events in older glacials especially when boundary conditions were different (e.g., across the Mid-Pleistocene Transition (MPT)).

One recent study suggested that the occurrence of HS Heinrich(-like) Events at Integrated Ocean Drilling Program (IODP) Site U1308, a re-drill of DSDP Site 609 that played an important role for the discovery of Heinrich Events [e.g., Bond *et al.*, 1992; Bond and Lotti, 1995], was restricted to the "100-ka world" of the Pleistocene with the first HS Heinrich(-like) Event occurring during MIS 16 [Hodell *et al.*, 2008], the first prolonged glacial following the MPT [Clark *et al.*, 2006]. Although HS Heinrich(-like) Events were also found during MIS 16 at IODP Site U1313, this record ended at 650 ka [Stein *et al.*, 2009], so whether the onset of HS Heinrich(-like) Events at U1308 during MIS 16 represents a basin-wide signal remained unknown. More importantly, the possibility that the occurrence of HS Heinrich(-like) Events at U1308 was driven by a long-term decrease in SSTs in the eastern North Atlantic could not be ruled out [Hodell *et al.*, 2008]. Here we thus extended both the SST and IRD record from IODP Site U1313 to 960 ka to investigate the correlation between the first occurrence of HS Heinrich(-like) Events and SSTs in the North Atlantic.
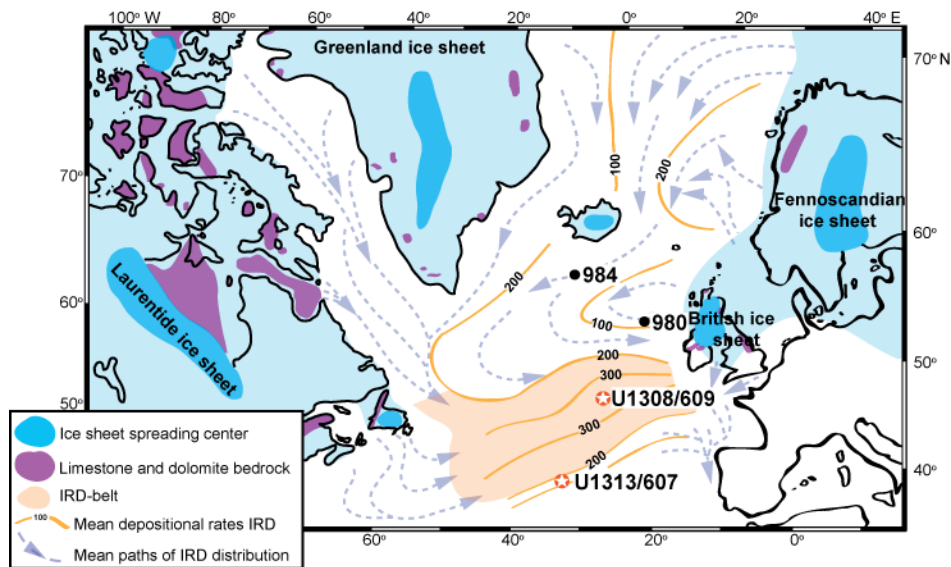
Figure 24; Study Area

Map of the North Atlantic showing the location of IODP Site U1308 (re-drill of DSDP Site 609), IODP Site U1313 (re-drill of DSDP Site 607), and ODP Sites 980 and 984 together with the IRD accumulation for the last glacial period [Ruddiman, 1977]. The occurrence of Paleozoic carbonates around the North Atlantic, the source of dolomite, is highlighted with purple [Bond *et al.*, 1992]. This study uses samples from IODP Site U1313.

7.2   Study Material

In this study sediment from IODP Site U1313 was used. Site U1313, a re-drill of Deep Sea Drilling Project (DSDP) Site 607, is located in the North Atlantic (latitude 41º00'N, longitude 32º57'W) at the southern boundary of the IRD-belt [Ruddiman, 1977] (Fig. 24). At present Site U1313 is predominantly influenced by the warm and oligotrophic surface waters of the North Atlantic Current, leading to present-day mean annual SSTs of 18.3 ºC [Locarnini *et al.*, 2006]. During glacials however the surface water circulation in the North Atlantic was significantly different and colder conditions prevailed in the North Atlantic as the Arctic Front (AF) was located further south [Pflaumann *et al.*, 2003].

During IODP Expedition 306 four holes were drilled at Site U1313 (3426 m water depth) from which two complete spliced stratigraphic sections for the Pleistocene were constructed [Expedition 306 Scientists, 2006]. Holes U1313B and U1313C were used for the primary splice, while U1313A and U1313D formed the secondary splice. The original meter composite depth (mcd)-scales from U1313A, U1313C, and U1313D were updated by tying them to the mcd-scale for Hole U1313B. Hereby an adjusted so-called amcd-scale was created that improved overall correlation of distinct features in the lightness, susceptibility, and paleomagnetic data between the holes [G. Acton, personal communication 2010]. For this study samples from the primary splice were used to obtain biomarker, XRD, and part of the foraminiferal δ^{18}O data. Samples from the secondary splice were used to reconstruct the Mg/Ca record and the remainder of the foraminiferal δ^{18}O data.

7.3   Chronology

The chronology of Site U1313 between 14.5 and 46 amcd partly relies on benthic foraminiferal δ^{18}O data (Fig. 25). In addition to the benthic foraminiferal δ^{18}O data from the secondary splice, which were previously published [Stein *et al.*, 2009; Ferretti *et al.*, 2010; Voelker *et al.*, 2010], we measured δ^{18}O on the benthic foraminifera *Cibicidoides wuellerstorfi* from Holes U1313B and U1313D across terminations IV, V, and X (4 cm sampling resolution) as well as during MIS 16 (10 cm sampling resolution). In total 123 new samples were measured.

All benthic foraminiferal δ^{18}O data from U1313 for the interval between 960 and 320 ka were tuned to the LR04 stack [Lisiecki and Raymo, 2005]. At the same time the lightness of the primary splice (L*) from U1313 was tuned to the carbonate content of DSDP Site 607 [Ruddiman et al., 1989], which is part of the LR04 stack. Lightness at Site U1313 is mainly controlled by variations in terrestrial input and is highly correlated with carbonate content at Site U1313 [Stein *et al.*, 2009]. The tuning was done using the Match 2.0 software [Lisiecki

and Lisiecki, 2002]. Using our age model sedimentation rates vary between 2 and 10 cm/ka and the Bruhnes/Matuyama magnetic boundary is identified at 783 ka (Fig. 25). The B/M boundary was not used as age-depth tie-point in order to give the Match 2.0 software more freedom to find the optimal correlation. Future high-resolution studies from Site U1313 using a continuous benthic foraminiferal $\delta^{18}O$ record combined with paleo-intensities will undoubtedly improve this age model.
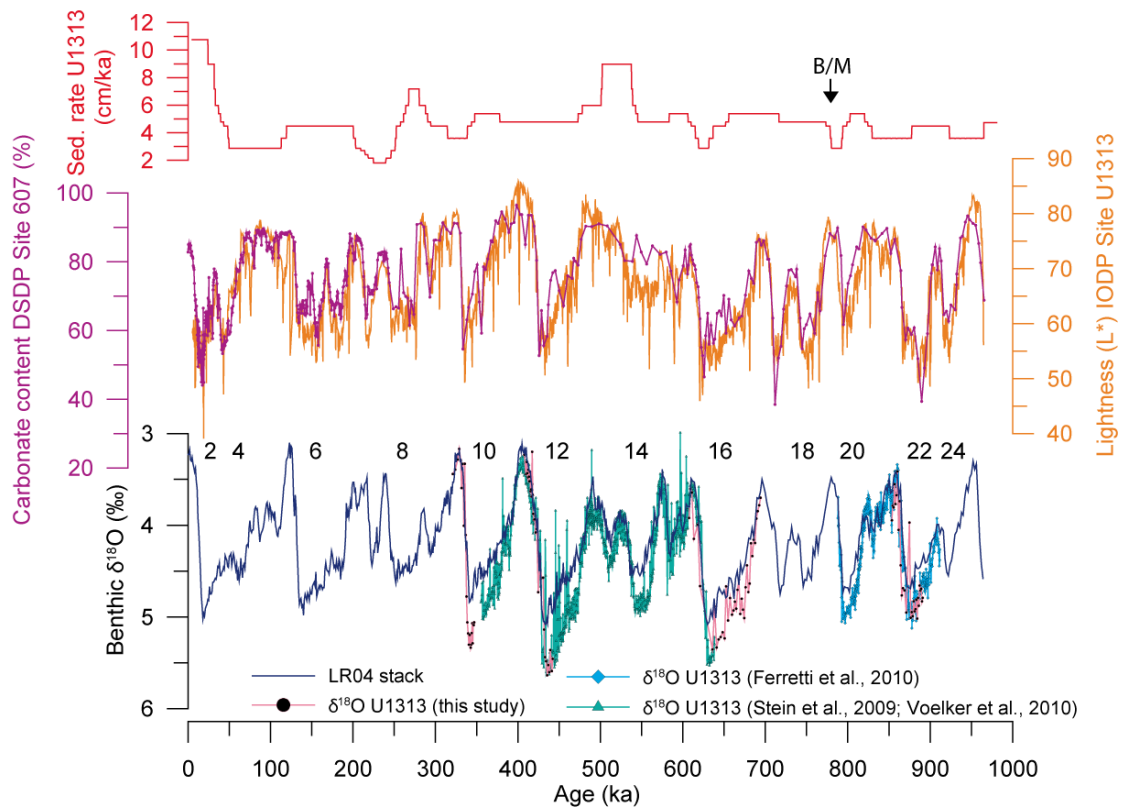
Figure 25; **Chronology of Site U1313.**

Sedimentation rates at U1313 (red), carbonate content of DSDP Site 607 [Ruddiman et al., 1989] (purple) together with lightness of the primary splice from U1313 (orange), and benthic $\delta^{18}O$ of Site U1313 [this study; Stein *et al.*, 2009; Ferretti *et al.*, 2010; Voelker *et al.*, 2010] together with the global benthic $\delta^{18}O$ stack [Lisiecki and Raymo, 2005]. Arrow with B/M indicates the position of the Bruhnes/Matuyama boundary.

7.4 Methodology

7.4.1 Sea surface temperatures (SSTs)

Mean annual SSTs were calculated using the alkenone unsaturation index ($U_{37}^{k'}$) and the global core-top calibration [Prahl and Wakeham, 1987; Müller *et al.*, 1998]. The relative abundance (%) of the $C_{37:4}$ alkenone was used to reconstruct the influence of cold and less saline polar/arctic waters at Site U1313 [Bendle *et al.*, 2005].

7.4.2 Ice-rafted debris (IRD) characteristics

IRD was identified using X-Ray Diffraction (XRD) to distinguish material originating from different source areas. Quartz was used as a general proxy for continental-derived material, reflecting input from different circum-Atlantic ice sheets (e.g., Canadian Shield, Greenland, Scandinavia, Great Britain) [Grousset *et al.*, 2001; Stein *et al.*, 2009]. Following previous studies from the North Atlantic [e.g., Andrews and Tedesco, 1992; Ji *et al.*, 2009; Stein *et al.*, 2009] dolomite was used as an indicator for ice-rafted debris (IRD) originating from the Paleozoic carbonates in the Hudson area [Bond et al., 1992] and thus HS Heinrich Events.

In addition to the detrital component, Heinrich layers in the North Atlantic are characterized by an increased abundance of so-called petrogenic organic compounds that are normally absent in recent sediments. These include hopanes and steroids and their aromatic counterparts, as well as palaerenieratane and isorenieratane and their derivatives, which indicate the input of ancient and organic rich material [Rosell-Melé et al., 1997; Rashid and Grosjean, 2006]. Like the detrital component, the biomarker distribution points to a Paleozoic bedrock source in the Hudson area as the source for the organic material during Heinrich events [Rashid and Grosjean, 2006]. The most abundant petrogenic compound accumulating at Site U1313 during the four HS Heinrich events of the last glacial cycle is the C_{28}(S) C-ring monoaromatic steroid. Although the exact mechanism for the formation of C_{28}(S) C-ring monoaromatic steroids is not clear, it is an aromatization product of sterols (derived from eukaryotes) that forms during diagenesis. It is therefore normally absent in recent sediments, but common in source rocks and oils. The abundance of the C_{28}(S) C-ring monoaromatic steroid was thus used as a proxy for the input of ancient and organic rich material and hence IRD.

7.5 Analytical techniques

Approximately 1500 sediment samples from the primary splice of Site U1313 were analyzed for biomarkers at the AWI-Bremerhaven using a LECO Pegasus III GC/TOF-MS system. Samples were taken at 2-cm resolution, corresponding to a temporal resolution of on average less then 500 years. Organic compounds were extracted from ± 6 gram of homogenized and freeze-dried sediment using dichloromethane and Automated Solvent Extraction (ASE 200, DIONEX, 5 min. at 100 ºC and 1000 psi). Total extracts were analyzed using a LECO Pegasus III (LECO Corp., St. Joseph, MI), interfaced to an Agilent 6890 GC. The gas chromatograph (GC) was equipped with a 15m x 0.18mm i.d. Rtx-1MS (Restek Corp., USA) column (film thickness: 0.10μm) with an integrated 5 meter guard column. The GC oven was initially held at 60 °C for 1 min, then heated at 50 °C min^{-1} to 250 °C and at 30 °C min^{-1} to 310 °C (held 2.5 min), resulting in an analysis time of 9.3 min per sample.

The occurrence and distribution of alkenones was monitored using the diagnostic *m/z* 94, 81, 79, 67, and 58 ionization fragments [Hefter, 2008]. A validated procedure was used to convert GC/TOF-MS C_{37} alkenone ratios to calibrated GC/FID values [Hefter, 2008]. The input of ancient and organic rich material was monitored using the diagnostic *m/z* 253 ionization fragment for C-ring monoaromatic steroids. Down core variations of the $C_{28}S$-triaromatic steroid are expressed semi quantitatively by normalizing the respective peak areas to the maximum area per gram sediment detected.

XRD measurements were carried out at the AWI-Bremerhaven following the methods described by Stein et al., [2009], although here relative intensities of dolomite and quartz abundance were normalized to calcite. Between 660 and 320 ka, samples were measured for XRD at 2-cm (~ 500 years) resolution. For the remainder of the record, samples were measured for XRD at 10-cm (~ 2.5 ka) resolution, although during terminations a 2-cm (500 years) resolution was used to fully captured the IRD events.

To obtain benthic foraminiferal $\delta^{18}O$ values, on average 5 specimens of *C. wuellerstorfi* were handpicked from the fraction larger than 250 μm and measured for $\delta^{18}O$ at the AWI-Bremerhaven, primarily using a Kiel carbonate device interfaced with a ThermoFinnigan MAT251 mass spectrometer. Some samples that contained only a few specimens of *C. wuellerstorfi* were measured using a ThermoFinnigan MAT253 mass spectrometer, which needs less material. Analytical precision was 0.09 and 0.07 ‰ for $\delta^{18}O$ using the MAT251 and MAT253 mass spectrometer, respectively. $\delta^{18}O$ values were calibrated to the NBS-19 (National Bureau of Standards) and reported relative to the Vienna Pee Dee Belemnite (VPDB) standard. *C. wuellerstorfi* $\delta^{18}O$ was adjusted to equilibrium by adding 0.64 ‰.

Paired measurements of Mg/Ca and $\delta^{18}O$ in planktonic foraminifera were predominantly performed in samples from the secondary splice of Site U1313. *G. ruber* was selected from the larger than 250 μm coarse fraction of sediment samples. Around 20 *G. ruber* specimens per sample were measured for $\delta^{18}O$ at the AWI-Bremerhaven. *G. bulloides* was selected from the 315-355 μm coarse fraction of sediment samples, and on average 80 specimens were picked for isotope and minor element analyses in order to reduce statistical variability. All $\delta^{18}O$ and minor element analyses on *G. bulloides* were carried out at the Analytical Service Unit of the University of Barcelona using a ThermoFinnigan MAT 252 mass spectrometer linked online to a single acid bath CarboKiel-II carbonate preparation device and a Perkin Elmer Elan 6000 quadrupole ICP-MS respectively. The Mg/Ca cleaning process is after Pena *et al.*, [2005] and involved the following steps. 1) Clay removal: crushed samples were rinsed and briefly ultrasonicated in ultrahigh quality water (UHQ H_2O) five times, in methanol (Aristar grade) twice, and then in UHQ H_2O again to remove clays and fine-grained carbonates. 2) Reductive cleaning: to remove a variety of contaminants phases, such as Mn–Fe oxides, a reductive reagent composed by a mixture of hydrazine hydroxide, citric acid and ammonia hydroxide was used in a hot (c. 100 ºC) ultrasonic bath for fifteen minutes with brief intervals of ultrasonication, followed by rinsing. 3) Oxydative cleaning: to remove organic matter, samples were then reacted with an oxidizing reagent (alkali buffered (NaOH) hydrogen peroxide (H_2O_2) 1% solution) in a boiling water bath for ten minutes with brief intervals of ultrasonication, followed by rinsing. 4) Samples were then checked under the microscope for coarse grained-silicates and any particles that were not apparently carbonate were removed using a fine brush. 5) Weak acid leach: to remove any remaining contaminant phase or particle that could be still attached to the foraminifera walls, samples were reacted with a weak acid (0.001 M HNO_3) and were rinsed in UHQ H_2O. 6) Finally, cleaned samples were dissolved the day of analysis in ultra-pure HNO3 (1%), ultrasonicated to promote dissolution, centrifuged in order to settle out any of the less soluble impurities, and then transferred to clean vials to prevent possible leaching from residual particles. Mg/Ca ratios were converted to temperatures using the calibration from Elderfield and Ganssen [2000].

7.6　Results

Based on the increased abundance of dolomite and $C_{28}(S)$ C-ring monoaromatic steroids during the last glacial cycle, HS Heinrich Events 1, 2, 4, and 5 can easily be identified at Site U1313 (Fig. 26). Heinrich Events 3 and 6 are absent in the dolomite/calcite record, suggesting that no IRD from the LIS reached the study location in the eastern North Atlantic during these events.
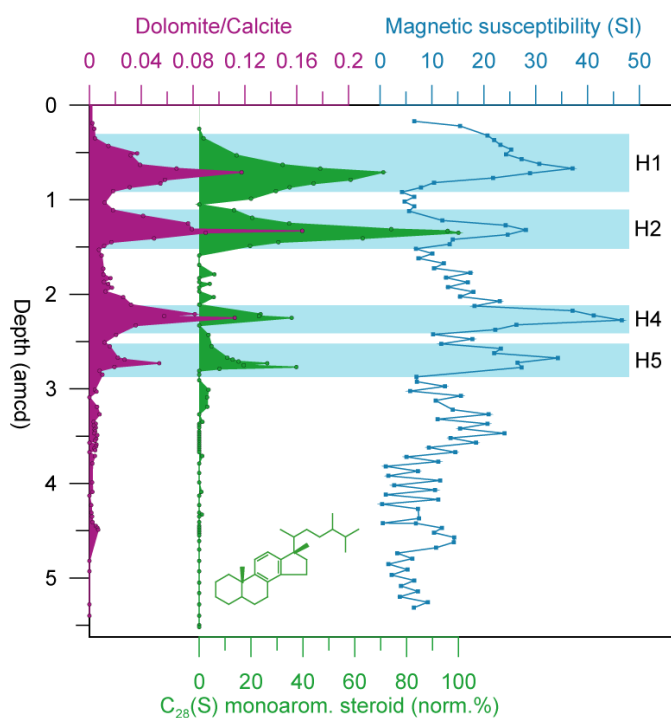
Figure 26; Dolomite and $C_{28}(S)$ abundance during the most recent glacial cycle.

a, dolomite/calcite (purple) **b**, Relative abundance of the monoaromatic steroid $C_{28}(S)$ (green) and **c**, Magnetic susceptibility (blue) at Site U1313 for the upper 5 amcd. Dolomite/calcite and $C_{28}(S)$ abundance are high during Heinrich layers 1,2,4, and 5; the four HS Heinrich events [Hemming, 2004].

For the period between 960 and 320 ka, periods of increased quartz deposition characterize glacials, especially glacial terminations (Fig. 27h). These events are associated with severe cooling of surface waters and expansion of arctic/polar waters into the mid-latitude North Atlantic (Fig. 27d-e). During glacial terminations (TX, TVIII, and TIV), minima in SSTs occasionally lag benthic foraminiferal $\delta^{18}O$ by several ka (Fig. 28). Dolomite/calcite is below or just above detection limits prior to MIS 16. At 643 ka (MIS 16) dolomite becomes abundant for the first time in the sediment, followed by high abundance during termination VII. After MIS 16, dolomite became abundant in the sediment during the later stages of MIS 12 and 10, but remained low during MIS 14 [Stein *et al.*, 2009]. The abundance of the $C_{28}(S)$ C-ring monoaromatic steroid is highly correlated with the occurrence of dolomite, not only during the last glacial cycle (Fig. 26), but also throughout the period between 960 and 320 ka (Fig. 27f-g). The $C_{28}(S)$ C-ring monoaromatic steroid was thus absent before MIS 16 and abundant during the later stages of MIS 16, 12, and 10.
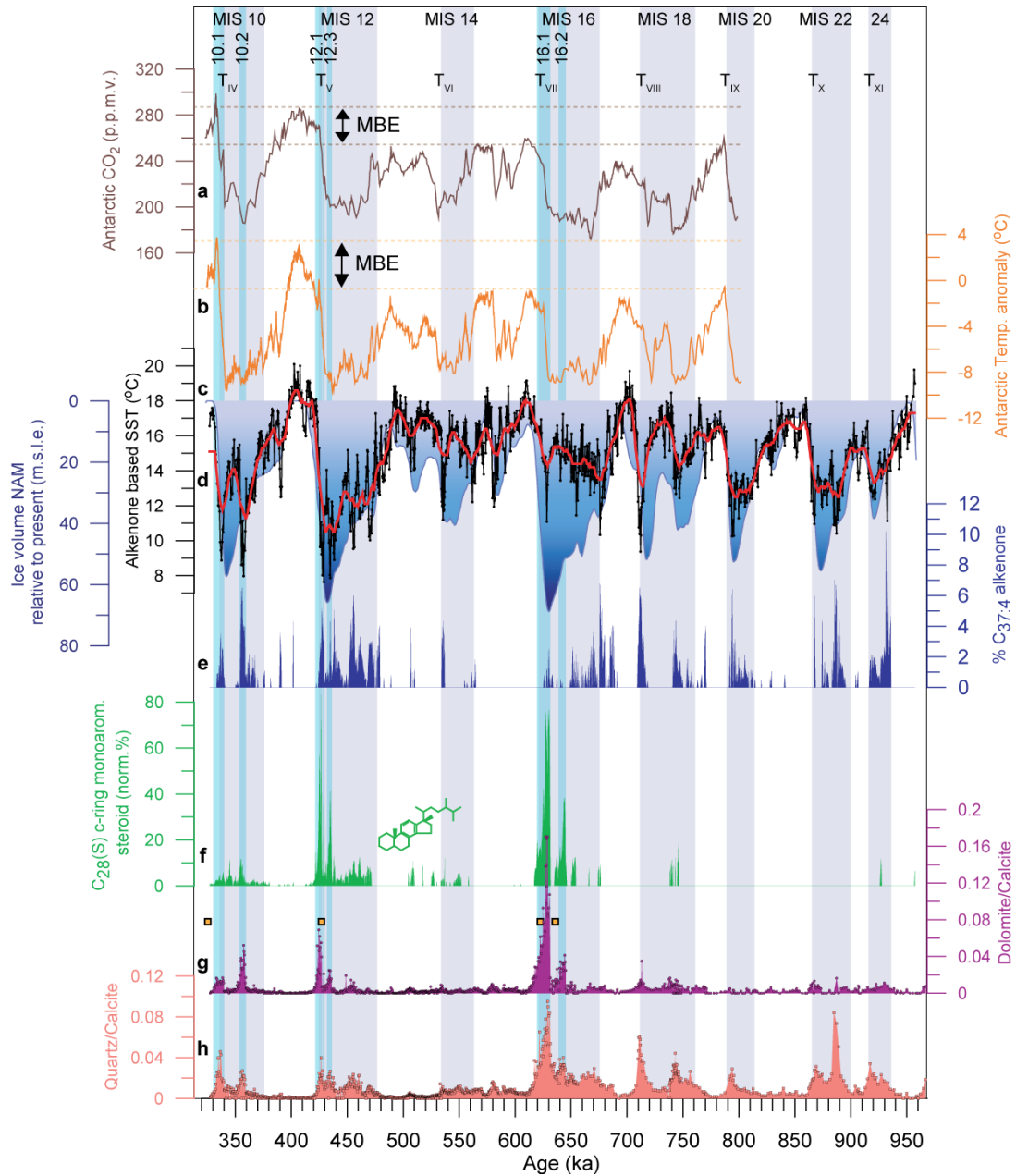
Figure 27; Multi-proxy records of IODP Site U1313 between 960 and 320 ka

a) Atmospheric CO_2-levels, reconstructed from Antarctic ice cores [Lüthi *et al.*, 2008], **b**) Antarctic air temperature anomaly [Jouzel *et al.*, 2007], **c**) Modelled size of the North American ice sheets, based on benthic foraminiferal $\delta^{18}O$ [Bintanja and van de Wal, 2008], **d**) High-resolution alkenone-based SST (black) and 10-ka moving average (thick red line), **e**) Abundance of $C_{37:4}$ alkenones, indicative of high-latitude waters, **f**) Relative abundance of the $C_{28}(S)$ c-ring monoaromatic steroid, indicative for the input of ancient and organic rich material, **g**) Abundance of dolomite, indicative for the input of IRD from the Hudson Bay area, **h**) Abundance of quartz, indicative for the input of IRD from circum-Atlantic ice sheets. Light blue bars indicate the occurrence of HS Heinrich(-like) Events at Site U1313. Grey bars highlight glacials. Orange cubes indicate the timing of HS Heinrich(-like) Events at IODP Site U1308 [Hodell *et al.*, 2008]. The occurrence of the Mid-Brunhes Event (MBE) is indicated by black arrows in **a** and **b**.

The high-resolution (0.4 ka resolution) alkenone-based SST record shows that for most of our record, SSTs follow the typical glacial/interglacial pattern with SSTs of around 19 °C during interglacials and as low as 8 °C during IRD-events. Lowest SSTs are found during MIS 12 and 10. However, MIS 16 stands out as a glacial with SSTs steadily increasing to values as high as 16 °C, opposite to the increasing trend in ice volume (Fig. 27c-d). Only during TVII did SSTs drop again to lower values. High-latitude waters were also absent at Site U1313 during MIS 16 as almost no $C_{37:4}$ alkenones were found in the sediment during this glacial (Fig. 27e).

7.7 Discussion

7.7.1 Occurrence HS Heinrich(-like) Events

The lack of dolomite prior to MIS 16 indicates that no IRD from the Hudson area was deposited at Site U1313 and hence suggests the absence of HS Heinrich(-like) Events prior to MIS 16. At 643 ka (MIS 16) the increased abundance of dolomite indicates the first HS Heinrich(-like) Events at Site U1313. The first HS Heinrich(-like) Event in the sedimentary record was shortly followed by a second HS Heinrich(-like) Event that coincides with termination VII. Following MIS 16, HS Heinrich(-like) Events occurred during the later stages of MIS 12 and 10 [Stein *et al.*, 2009]. All these HS Heinrich Events were also characterized by the input of ancient and organic rich material, possibly originating from the Hudson area, as indicated by the increased abundance of the $C_{28}(S)$ C-ring monoaromatic steroid. In addition, despite the uncertainties in age models all these HS Heinrich(-like) Events coincide with periods of rising CO_2 (Fig. 27), suggesting that the feedback mechanisms in the Southern Hemisphere associated with the HS Heinrich Events of the last glacial cycle [e.g., Sigman *et al.*, 2007] were also present during older glacials.

The timing of the HS Heinrich(-like) Events at U1313 agrees with results from Site U1308 where HS Heinrich(-like) Events were also detected during MIS 16, 12, and 10, but were absent in older glacials [Hodell *et al.*, 2008]. The synchrony between these two sites across the IRD-belt indicates that the onset of HS Heinrich(-like) Events was simultaneous within the (eastern) North Atlantic. More over the synchrony suggests that these events can be traced throughout the (eastern) North Atlantic and we therefore propose to uniformly name the HS Heinrich(-like) Events according to the glacial and order they occur. In this way the HS Heinrich(-like) Events that occurred during the glacial terminations, also referred to as terminal ice rafting events [Venz *et al.*, 1999], are labeled HS Heinrich(-like) Event 16.1, 12.1, and 10.1 (Fig 4).

7.7.2   Sea surface temperatures

The alkenone-based SST record shows that SSTs did not cause the first occurrence of HS Heinrich(-like) Events. Alkenone-based SSTs at Site U1313 were higher during the onset of HS Heinrich(-like) Events (MIS 16) than during other glacials. This is surprising as during all other glacials, a part from the weak glacial of MIS 14, SSTs at Site U1313 indicate significant cooling of surface waters, especially during ice-rafting events as melting icebergs filled the North Atlantic. Although during the HS Heinrich(-like) Event of termination VII (16.1) SSTs at Site U1313 also depict the influence of the melting of icebergs, SSTs remain higher than during other glacials. A lower resolution record of summer and winter SSTs based on census counts of planktonic foraminifera from Site 607 [Ruddiman *et al.*, 1989], of which U1313 is a re-drill, shows the same warming trend during MIS 16. These SSTs thus confirm the higher resolution alkenone-based SSTs during MIS 16 (Fig. 29a). The small temporal offset between the SST records from Site U1313 and Site 607 is probably related to the difference in resolution and age models.
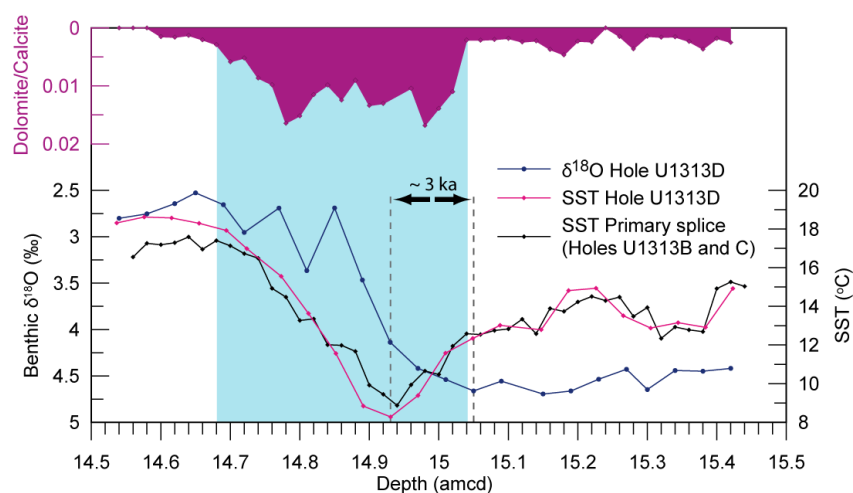
Figure 28; Termination IV
Benthic foraminiferal $\delta^{18}O$ (blue) and alkenone-based SSTs (pink) from samples from Hole U1313D together with alkenone-based SSTs from the primary splice (black), formed from Holes U1313B and U1313C, versus depth. Minima in SSTs lag maxima in benthic foraminiferal $\delta^{18}O$ by 12 cm, which corresponds to ~3 ka using our age model. Dolomite/calcite (purple) is shown to indicate the occurrence of HS Heinrich(-like) Event 10.1 (blue bar).

The occasional lag between minima in SSTs and maxima in benthic foraminiferal $\delta^{18}O$ during glacial terminations demonstrates the impact of ice-rafting events on surface water characteristics in the North Atlantic during the Pleistocene as the melt water pulse for a

short period suppressed the warming of surface waters to interglacial values. This is especially evident during termination IV (Fig. 28). It is important to note that the timing of these ice-rafting events and associated cooling of surface waters at Site U1313 is different compared to those at the Iberian Margin were maximum IRD input preceded minima in SSTs [Rodrigues *et al.*, 2011] and minima in SSTs coincide with maxima in benthic foraminiferal δ^{18}O during termination IV [Martrat *et al.*, 2007; Rodrigues *et al.*, 2011]. As IRD at the Iberian Margin is thought to have various sources, including the European ice sheets [de Abreu *et al.*, 2003; Bigg *et al.*, 2010], the difference between Site U1313 and Iberian Margin could indicate an offset in the timing of the collapse of the European and Laurentide ice sheets. In addition, this apparent difference between the mid-latitude North Atlantic and Iberian Margin urges for care in correlating IRD-events across the North Atlantic.

7.7.3 Stratification water column

To investigate whether the warming of surface waters during MIS 16 was restricted to the upper part of the water column, Mg/Ca in the planktonic foraminifera *Globigerina bulloides* was measured. *G. bulloides* is a mixed-layer-dwelling planktonic foraminifera, which in the North Atlantic can be found throughout the upper 60 meters of the water column [Schiebel et al., 1997]. The Mg/Ca record thus represents a shallow subsurface temperature signal, while alkenone-based SSTs are thought to represent temperatures of the upper 10 meters of the water column [Müller et al., 1998].

The results show that Mg/Ca based temperatures were decreasing during MIS 16, opposite to the trends in the alkenone-based and census counts of planktonic foraminifera based SSTs (Fig 6b). The difference between the alkenone- and Mg/Ca-based SSTs reaches up to 6 °C during MIS 16, while the two temperature records show similar values during the interglacials MIS 17 and 15. This indicates a large temperature gradient between the upper-part of the water column (alkenone-based SSTs) and underlying waters (Mg/Ca-based SSTs) during MIS 16. We interpret this increased temperature gradient to reflect a strong stratification of the water column. This is also supported by the increased offset in δ^{18}O between *G. bulloides* and the surface-dwelling planktonic foraminifera *Globigerinoides ruber* that doubled during MIS 16 (Fig. 29c-d).

The possibility that the difference between alkenone- and planktonic foraminiferal δ^{18}O-based SSTs reflects amplification of seasonal differences as was proposed for the North Pacific [Haug et al., 2005] is unlikely to play a major role at our study site. In the North Atlantic *G. ruber*, *G. bulloides* and coccolithophores, of which a small group produces alkenones, all bloom in (late) spring [Weeks et al., 1993; Elderfield and Ganssen, 2000;

Ganssen and Kroon, 2000; Chapman, 2010]. In addition, alkenone-based SSTs during MIS 16 remain between the seasonal extremes as determined by summer and winter SSTs based on census counts of foraminifera from Site 607 [Ruddiman et al., 1989] and thus do not indicate a shift towards summer temperatures. At the same time, Mg/Ca-based temperatures during MIS 16 are lower than the reconstructed winter SSTs, again suggesting that the Mg/Ca record represents shallow subsurface temperatures.
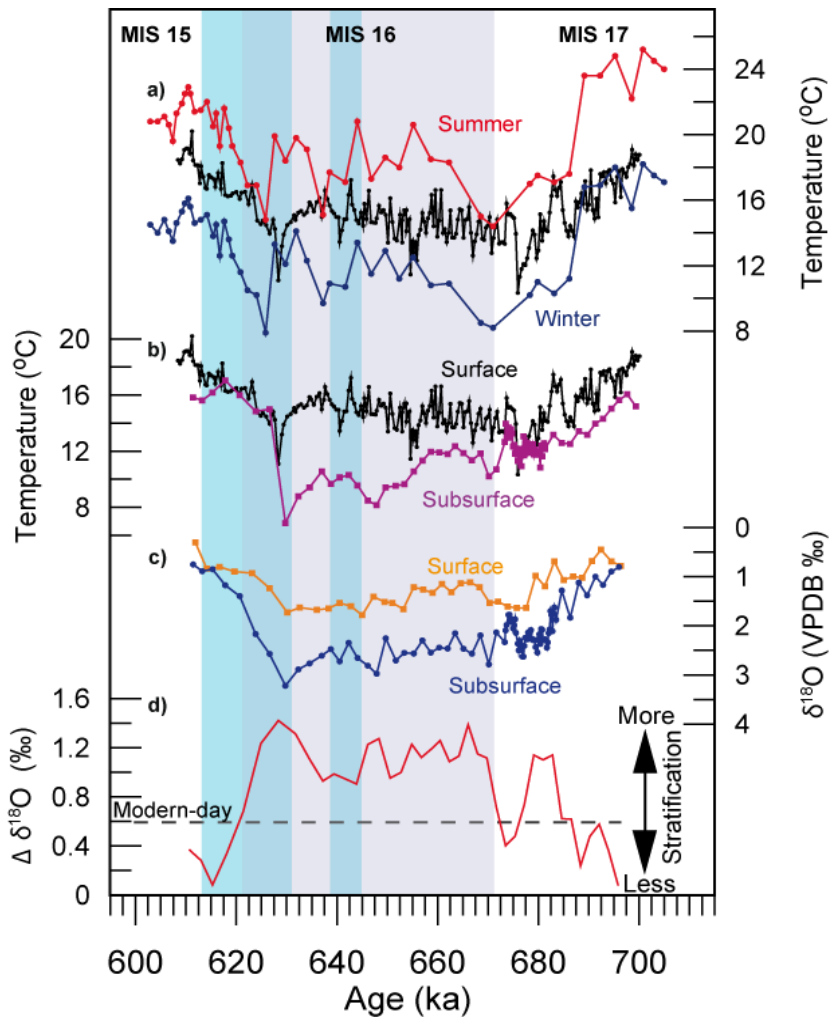
Figure 29;   **MIS 16**

Alkenone-based annual mean SSTs from U1313 (black) and foraminiferal assemblage-based summer (red) and winter (dark blue) SST from DSDP Site 607 [Ruddiman *et al.*, 1989], of which U1313 is a re-drill, **b**) Alkenone-based annual mean SSTs from U1313 (black) together with shallow subsurface temperature estimates at U1313, based on Mg/Ca from the mixed-layer-dwelling planktonic foraminifera *G. bulloides* (purple), **c**) Planktonic foraminiferal δ^{18}O of the surface-dwelling *G. ruber* (orange) and mixed-layer-dwelling *G. bulloides* (blue), **d**) Difference in δ^{18}O between *G. bulloides* and *G. ruber*. Dashed line indicates the present-day offset [Ganssen and Kroon, 2000]. Color bars are like in Figure 27.

7.7.4   Cause for warm SSTs during MIS 16

We interpret the warm and stratified surface waters at Site U1313 to reflect a more northern position of the Arctic Front (AF) during MIS 16, more comparable to interglacial than to glacial conditions. A more northern position of the AF is also supported by foraminiferal data from Ocean Drilling Project (ODP) Sites 984 and 980 that indicate a northward movement of the AF during MIS 16 [Wright and Flower, 2002]. Within the North Atlantic, the AF is characterized by a steep SST gradient and forms the boundary between warm Atlantic waters and cold arctic waters [Swift, 1986]. During the last glacial maximum the southern location of the AF between 45 and 37 ºN led to a strong SST gradient in the mid-latitude North Atlantic with warm surface waters accumulating directly south of the AF [Pflaumann *et al.*, 2003]. Previous results suggested that a slightly more northern position of the AF during MIS 6 led to higher SSTs in the mid-latitude North Atlantic [Calvo *et al.*, 2001]. A more northerly position of the AF during MIS 16 compared to other glacials could thus explain the higher SSTs at Site U1313.

Today, North Atlantic deep water formation establishes the upper ocean and atmospheric circulation that ameliorates the climate of the eastern circum-North Atlantic [Rahmstorf, 2002]. The moderate North Atlantic SSTs of MIS 16 due to a more northerly position of the AF thus suggest greater North Atlantic overturning at that time as compared to other glacials. The ultimate cause for this different ocean circulation in the North Atlantic remains unknown. Possibly the increased input of warm and salty waters by means of Agulhas Leakage during MIS 16, compared to MIS 12 and 10, promoted the greater overturning in the North Atlantic [Bard and Rickaby, 2009]. However, this does not explain why glacials prior to MIS 16 were characterized by low SSTs in the North Atlantic as the Agulhas Leakage during these glacials was comparable to MIS 16 [Bard and Rickaby, 2009]. Future research should therefore focus on the ultimate mechanisms behind the different ocean circulation in the North Atlantic during MIS 16.

7.7.5   Implications

The results presented here confirm the previous suggestion that MIS 16 marks a change in LIS dynamics, possibly due to an increases in LIS ice volume (thickness), as HS Heinrich Events appeared in the sedimentary record of the eastern North Atlantic [Hodell *et al.*, 2008]. This agrees with recent results of ice sheet modeling [Bintanja and van de Wal, 2008] and dating of glacial stratigraphic sections in North America [Roy *et al.*, 2004; Balco and Rovey, 2010] which suggested that the size and volume of the North American ice sheets increased at

the end of the early Pleistocene and highlighted the role of ice sheets, in particular the North American ice sheets, in the MPT [Bintanja and van de Wal, 2008].

In addition, in the context of the feedback mechanisms associated with HS Heinrich Events by which the North Atlantic initiates dramatic deglaciations [Marchitto *et al.*, 2007; Sigman *et al.*, 2007; Anderson *et al.*, 2009], our results add to the data suggesting a correlation between the occurrence of HS Heinrich(-like) Events and the stronger interglacials that characterize the Pleistocene after the Mid-Brunhes Event (MBE) at ~450 ka. The MBE is the most obvious in the Antarctic ice core records of CO_2 and temperature (Fig. 27a-b), but can also be found in other climate records from around the world as a shift towards more intense interglacial conditions [Lang and Wolff, 2010]. Specifically the first strong interglacial defining the MBE is preceded by the HS Heinrich(-like) Events of MIS 12 while, with the exception of MIS 15, the earlier "luke-warm" interglacials (MIS 19-13) with weaker deglacial increases in Antarctic temperature [Jouzel *et al.*, 2007] and CO_2-levels [Lüthi *et al.*, 2008], did not have preceding HS Heinrich(-like) Events.

The major exception to the rule is thus MIS 16, which did have HS Heinrich(-like) Events but even so was followed by the luke-warm interglacial MIS 15 (Fig. 27a-b). This suggests an additional requirement for the dramatic deglaciations that characterize the latest Pleistocene. Our alkenone temperature reconstructions may provide an additional insight into this. Despite the intensity of the MIS 16, unusually moderate North Atlantic SSTs characterized this period possible due to substantial North Atlantic overturning. The hypothesized North-to-South trigger for deglaciations revolves around the shutdown of North Atlantic overturning [Sigman *et al.*, 2007; Anderson *et al.*, 2009]. In a glacial with strong North Atlantic overturning (e.g., MIS 16), even a HS Heinrich(-like) Event may not have been adequate to cause this shut-down. That is, the data from stage 16 may be indicating that the HS Heinrich Event trigger can only work in glacial states with already weak and/or shallow North Atlantic overturning.

7.8   Conclusion

Our high-resolution records depict the detailed relation between surface water characteristics and IRD-events in the mid-latitude North Atlantic for the period between 960 and 320 ka. The IRD-characteristics demonstrate that although regular IRD-events occurred throughout this interval, predominantly during glacial terminations, IRD originating from the Laurentide Ice sheet and thus HS Heinrich(-like) Events was absent prior to MIS 16. During IRD-events SSTs indicate severe cooling of surface waters and increased influence of high-latitude waters. At 643 ka, dolomite for the first time became abundant and indicates the first

occurrence of HS Heinrich(-like) Events. Following MIS 16, HS Heinrich(-like) Events occurred during MIS 12 and 10. All these events are characterized by the input of ancient and organic rich material. The timing of these events is similar as at Site U1308, located further to the North, and indicates a simultaneous onset within the (eastern) North Atlantic.

The alkenone-based SST record shows the first occurrence was not simply related to increased survivability, as SSTs were significantly higher during MIS 16 than during other glacials, probably due to a more northern location of the AF. Lower subsurface temperature estimates based on Mg/Ca from mixed-layer dwelling planktonic foraminifera suggest that the warming was restricted to the upper part of the water column. These results indicate that MIS 16 marks a change in LIS dynamics, in-line with previous studies. This has large implications for the role of HS Heinrich(-like) Events within the broader climate system as the results of HS Heinrich(-like) Events occurring prior to the MBE suggest that the occurrence of HS Heinrich events alone is not enough to initiate dramatic deglaciations, and other mechanisms might be needed to reach the full interglacial conditions that characterize the last 450 ka.

The next step will now be to determine the onset of HS Heinrich(-like) Events in the sedimentary record close to the source area (e,g, Labrador Sea), where even small ice-rafting events can be detected that would not influence the eastern North Atlantic.

7.9   Acknowledgements

8   Conclusions and future perspectives

In this thesis a combination of different organic geochemical and mineralogical proxies were used to reconstruct climate in the mid-latitude North Atlantic over the past 4 million years. This includes, among others, a reconstruction of sea surface temperatures, surface water productivity, aeolian input, and ice-rafting events and characteristics. The main aim was to reconstruct the long-term evolution of (millennial-scale) climate variability in the North Atlantic in order to gain more understanding in the mechanisms that drove Quaternary climate change. This chapter gives a chronological summary of the main results of this thesis and provides some remaining open questions and future research perspectives.

The records of alkenone-based surface water temperatures and productivity from Site U1313 show that the intensification of the Northern Hemisphere glaciation (NHG) in the late Pliocene was characterized by a drastic change in surface water characteristics (*Chapter 5*). Before 3.1 Ma the surface water characteristics indicate an intense North Atlantic current (NAC) that transported warm, nutrient-poor surface waters northwards. Starting at 3.1 Ma during glacials SSTs decreased and surface water productivity increased at Site U1313, indicating a shift in the position of the NAC that ceased to reach into the higher latitudes. The diminished northward heat transport associated with the change in position of the NAC would have caused a cooling of the higher latitudes, which may have encouraged the growth of large continental ice sheets in the Northern Hemisphere. This is supported by recent modeling results [e.g., Hill *et al.*, 2010]. These results provide additional constrains for the mechanisms behind the intensification of the NHG as they argue against an increase in northward heat transport in the North Atlantic during the intensification of the NHG, as previously proposed [Bartoli *et al.*, 2005]. In the future it would be interesting to produce similar biomarker records at more northern sites in order to more accurately determine the variations in ocean circulation in the northern North Atlantic during the intensification of the NHG. As the NAC is mainly a wind-driven current, the observed changes in the NAC could indicate an important role of atmospheric circulation on Quaternary climate change. Future work should therefore focus on reconstructing palaeorecords of variations in wind strength from the mid-latitude North Atlantic, e.g. grain sizes of detrital sediments. In addition, it still remains unknown when the overall cooling trend in the North Atlantic that cumulated in the intensification of the NHG began. Results from the tropical Pacific indicate that SSTs were highest during the early Pliocene [Lawrence *et al.*, 2006]. Continuous orbitally-resolved SSTs records from the North Atlantic extending back to the early Pliocene are needed to address this question, which might shed more light onto the ultimate cause of the intensification of the NHG.

At the same time as the change in ocean circulation, the reconstruction of aeolian input at Site U1313 demonstrates a drastic increase (*Chapter 6*). This record is based on the accumulation of lipids derived from terrestrial higher plant material (long-chain *n*-alkanes and *n*-alkan-1-ols). These lipids are a major component of dust as can easily be removed from the leaf surface by wind or rain, especially by sandblasting during dust storms, or entrained as part of soil and transported over large distances. The different organic characteristics of the terrestrial higher plant material (e.g., carbon preference index and compound specific $\delta^{13}C$) verify that they have an aeolian origin and indicate that they are derived from the North American continent. As the increase in aeolian input coincides with the appearance of continental ice sheets, the results are interpret to reflect the development of glacial outwash plains in North America. This is in line with results of spectral analysis between benthic foraminiferal $\delta^{18}O$ and *n*-alkane records from Site U1313, which indicate that variations in aeolian input are in phase or slightly lag changes in ice volume at the obliquity band. Glacial outwash plains are effective dust sources and the ones in Patagonia are shown to be the main source of the dust accumulating in Antarctica [Sugden *et al.*, 2009]. The onset of increased aeolian input from the North American continent coincides with a global increase in aeolian input as climate changed during the intensification of the NHG [e.g., Dersch and Stein, 1991; Dersch and Stein, 1994; Yang and Ding, 2010]. Together with the close correspondence between aeolian input to the North Atlantic and dust fluxes in Antarctica over the last 800 thousand years (ka) [Lambert *et al.*, 2008] this indicates a globally uniform response of dust sources to Quaternary climate variability.

Since the record of aeolian input at Site U1313 is predominantly related to the dust production at active terrestrial glacial margins in North America, it provides a unique record to test the pacing of the advance and retreat of the North American ice-sheet through the Plio-Pleistocene. Evolutional spectral analysis of the *n*-alkane records demonstrates that throughout the early Pleistocene, variance in the obliquity period (41-ka) dominates aeolian input and hence North American ice sheet dynamics. This argues against suggestions of precession-related variations in Northern Hemisphere ice volume during the early Pleistocene and urges for other mechanisms to explain the dominance of the 41-ka period during the early Pleistocene. So far the role of dust on long-term climate change has been largely neglected. Our results show that the increased dustiness that characterized the most recent glacial cycles has been a persistent feature of Quaternary climate. The close correspondence between aeolian input to the North Atlantic and other dust records indicates a globally uniform response of dust sources to Quaternary climate variability. As we propose the increased aeolian input to the North Atlantic could have had a significant effect on global climate,

future work should focus on more precisely determine the role of dust and associated feedback mechanisms in the development of Quaternary climate.

In addition, preliminary results show that periods of increased accumulation of terrestrial higher plant material coincide with periods of higher accumulation of branched glycerol dialkyl glycerol tetraether lipids (GDGTs) at Site U1313 (see Fig. 30). These lipids are produced by Anaerobic bacteria living in soils [Weijers *et al.*, 2006]. Lately, several indices based on the distribution of these lipids have been used to calculate mean annual air temperature (MAT) in the source area [Weijers *et al.*, 2007]. The presence of these lipids at Site U1313 thus provides future possibilities to determine the MAT in the North American continent over the last 3.5 Ma.
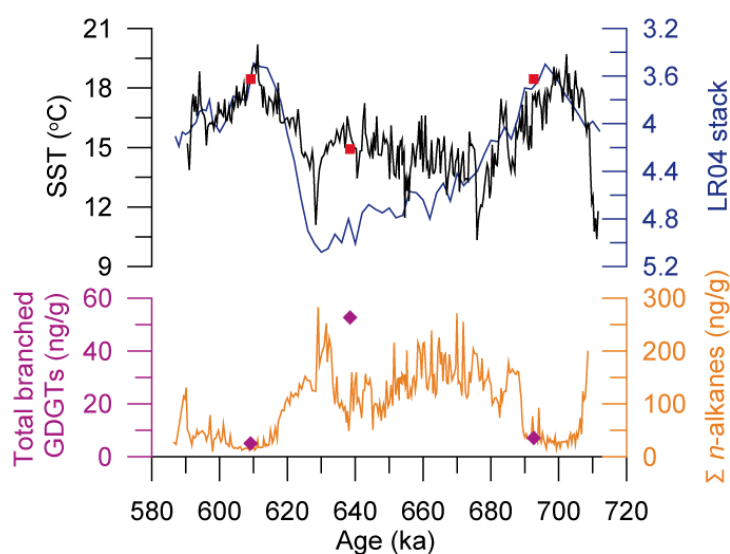

Figure 30; **Marine Isotope stage 16**

Concentration of the long-chain odd *n*-alkanes (orange) together with the abundance of GDGTs (purple) at Site U1313. Also shown are the SST estimates based on two organic proxies $U^{k'}_{37}$ (black) and TEX$_{86}$ (red). GDGT-data from A. Martìnez-Garcia.

The early Pleistocene is characterized by regular 41-paced glacial/interglacial variability in the North Atlantic with increased aeolian input and decreased SSTs during glacials. Interglacial SSTs reach present-day levels around 1 Ma, but glacial SSTs continue to decrease during the entire early Pleistocene with minimum values during MIS 12 and 10 (see Fig. 31). This difference in cooling between glacial and interglacials over the last 1.5 Ma is similar as observed in benthic foraminiferal δ^{18}O and SSTs in the tropical oceans [Herbert *et al.*, 2010] and points to an increased sensitivity of global climate to glacial forcing. At Site U1313 the lowest SSTs of the middle and late Pleistocene are associated with melt water pulses from the

continental ice sheets circum the North Atlantic (*Chapter 7*). In this context, the continuous decrease of glacial SSTs starting around 1.5 Ma and abrupt shift in glacial SSTs during MIS 40 (~ 1.3 Ma) could indicate an increased influence of melt waters reaching Site U1313. Future work should focus on determining the presence of ice-rafting events at Site U1313 before 1 Ma.
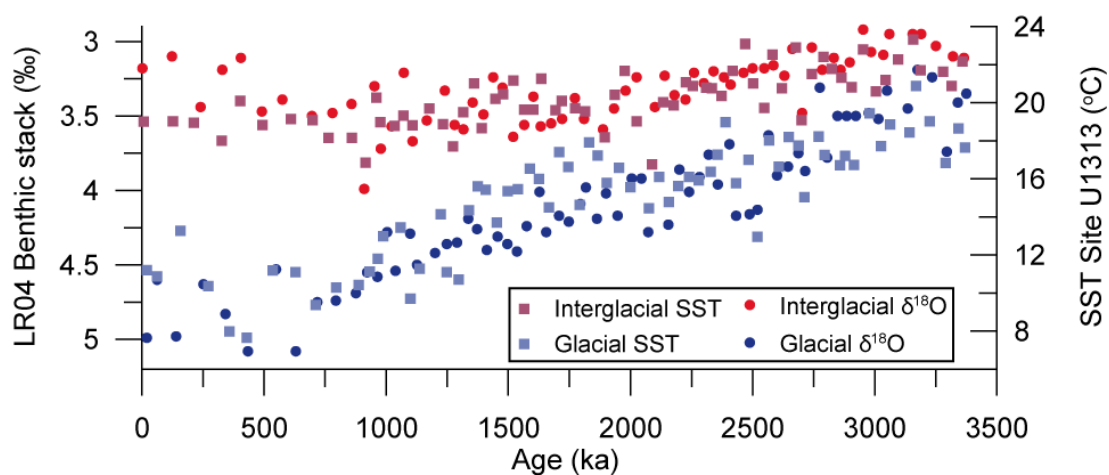
Figure 31; Difference between glacial and interglacial climate
The evolution of glacial and interglacial SSTs at Site U1313 and benthic foraminiferal $\delta^{18}O$. Both proxies demonstrate a similar trend towards more intense glacial conditions, especially during the last 1.5 Ma, while interglacial conditions remained relatively constant.

The combined high-resolution measurements of organic geochemistry and mineralogy for the period between 960 and 320 ka provides new insights in the mechanisms behind millennial-scale climate variability (*Chapter 7*). In general the period between 960 and 320 is characterized by a shift towards more intense glacial conditions during the end of the middle Pleistocene transition. Using newly developed indicators of organic matter originating from the Hudson area, we show that at the same time (643 ka) Hudson Strait (HS) Heinrich(-like) Events, massive ice-rafting events in the North Atlantic originating from the Laurentide ice sheet (LIS), appear in the sedimentary record at Site U1313. The timing is similar as observed at the more northern located IODP Site U1308 [Hodell *et al.*, 2008]. As SSTs where higher during MIS 16 compared to previous glacials the occurrence of HS Heinrich(-like) Events is related to enhanced ice discharge at this time and not simply related to the survivability of icebergs due to cold conditions in the North Atlantic. This has large implications for the role of HS Heinrich(-like) Events within the broader climate system.

Future work should extend these high-resolution records to include the upper 320 ka in order to create a unique record of the last 1 Ma that will serve as a reference site for long-term

millennial-scale climate variability in the North Atlantic. This record will provide valuable insights into the occurrence of millennial-scale climate variability during periods with different boundary conditions and the origin and mechanisms of millennial-scale climate variability in the North Atlantic. Especially the investigation on the timing and phasing of IRD-events relative to orbital parameters over the last 1 Ma will be interesting to gain more knowledge about the mechanisms driving abrupt climate change.

9 Data Handling

All data presented in this thesis will be publicly available online in the Pangaea database (https://www.pangaea.de).

Data from the first manuscript: http://doi.pangaea.de/10.1594/PANGAEA.744483

Data from the second manuscript: http://doi.pangaea.de/10.1594/PANGAEA.757951

Data from the third manuscript: http://doi.pangaea.de/10.1594/PANGAEA.758056

10 References

Acton, G. D., C. J. Borton, and Leg 178 Shipboard Scientific Party (2001), Palmer Deep composite depth scales for Leg 178 Sites 1098 and 1099, in *Procedings of ODP, Scientific Drilling Results*, edited by P. F. Barker, et al., 178, pp. 1-35, College Station, TX.

Anderson, R. F., S. Ali, L. I. Bradtmiller, S. H. H. Nielsen, M. Q. Fleisher, B. E. Anderson, and L. H. Burckle (2009), Wind-Driven Upwelling in the Southern Ocean and the Deglacial Rise in Atmospheric CO_2, *Science*, *323*(5920), 1443-1448, doi: 10.1126/science.1167441

Andrews, J. T., and K. Tedesco (1992), Detrital carbonate-rich sediments, northwestern Labrador Sea: Implications for ice-sheet dynamics and iceberg rafting (Heinrich) events in the North Atlantic, *Geology*, *20*(12), 1087-1090, doi: 10.1130/0091-7613

Andrews, J. T., H. Erlenkeuser, K. Tedesco, A. E. Aksu, and A. J. T. Jull (1994), Late Quaternary (Stage 2 and 3) Meltwater and Heinrich Events, Northwest Labrador Sea, *Quaternary Research*, *41*(1), 26-34, doi: 10.1006/qres.1994.1003

Andrews, J. T. (1998), Abrupt changes (Heinrich events) in late Quaternary North Atlantic marine environments: a history and review of data and concepts, *Journal of Quaternary Science*, *13*(1), 3-16, doi: 10.1002/(SICI)1099-1417

Arz, H. W., J. Pätzold, and G. Wefer (1998), Correlated Millennial-Scale Changes in Surface Hydrography and Terrigenous Sediment Yield Inferred from Last-Glacial Marine Deposits off Northeastern Brazil, *Quaternary Research*, *50*(2), 157-166, doi: 10.1006/qres.1998.1992

Asmerom, Y., V. J. Polyak, and S. J. Burns (2010), Variable winter moisture in the southwestern United States linked to rapid glacial climate shifts, *Nature Geosciences*, *3*(2), 114-117

Balco, G., and C. W. Rovey (2010), Absolute chronology for major Pleistocene advances of the Laurentide Ice Sheet, *Geology*, *38*(9), 795-798, doi: 10.1130/G30946.1

Bard, E., F. Rostek, J.-L. Turon, and S. Gendreau (2000), Hydrological Impact of Heinrich Events in the Subtropical Northeast Atlantic, *Science*, *289*(5483), 1321-1324, doi: 10.1126/science.289.5483.1321

Bard, E., and R. E. M. Rickaby (2009), Migration of the subtropical front as a modulator of glacial climate, *Nature*, *460*(7253), 380-383, doi: 10.1038/nature08189

Barker, S., P. Diz, M. J. Vautravers, J. Pike, G. Knorr, I. R. Hall, and W. S. Broecker (2009), Interhemispheric Atlantic seesaw response during the last deglaciation, *Nature*, *457*(7233), 1097-1102, doi: 10.1038/nature07770

Bartoli, G., M. Sarnthein, M. Weinelt, H. Erlenkeuser, D. Garbe-Schönberg, and D. W. Lea (2005), Final closure of Panama and the onset of northern hemisphere glaciation, *Earth and Planetary Science Letters*, *237*(1-2), 33-44, doi: 10.1016/j.epsl.2005.06.020

Becker, J., L. J. Lourens, and M. E. Raymo (2006), High-frequency climate linkages between the North Atlantic and the Mediterranean during marine oxygen isotope stage 100 (MIS100), *Paleoceanography*, *21*(3), PA3002, doi: 10.1029/2005pa001168

Bendle, J., A. Rosell-Melé, and P. Ziveri (2005), Variability of unusual distributions of alkenones in the surface waters of the Nordic seas, *Paleoceanography, 20*, PA2001, doi: 10.1029/2004PA001025

Benway, H. M., J. F. McManus, D. W. Oppo, and J. L. Cullen (2010), Hydrographic changes in the eastern subpolar North Atlantic during the last deglaciation, *Quaternary Science Reviews, 29*(23-24), 3336-3345, doi: 10.1016/j.quascirev.2010.08.013

Berger, W. H., and G. Wefer (1996), Expeditions into the Past: Paleoceanographic studies in the South Atlantic, in *The South Atlantic*, edited by G. Wefer, et al. pp. 363-410. Springer, Berlin.

Bettis, A. E., D. R. Muhs, H. M. Roberts, and A. G. Wintle (2003), Last Glacial loess in the conterminous USA, *Quaternary Science Reviews, 22*(18-19), 1907-1946, doi: 10.1016/S0277-3791(03)00169-0

Bi, X., G. Sheng, X. Liu, C. Li, and J. Fu (2005), Molecular and carbon and hydrogen isotopic composition of n-alkanes in plant leaf waxes, *Organic Geochemistry, 36*(10), 1405-1417, doi: 10.1016/j.orggeochem.2005.06.001

Bianchi, G. (1995), Plant waxes, in *Waxes: Chemistry, Molecular Biology and Functions*, edited by R. J. Hamilton pp. 175-222. The oily press, Dundee.

Bigg, G. R., R. C. Levine, C. D. Clark, S. L. Greenwood, H. Haflidason, A. L. C. Hughes, A. Nygård, and H. P. Sejrup (2010), Last glacial ice-rafted debris off southwestern Europe: the role of the British–Irish Ice Sheet, *Journal of Quaternary Science, 25*(5), 689-699, doi: 10.1002/jqs.1345

Bintanja, R., and R. S. W. van de Wal (2008), North American ice-sheet dynamics and the onset of 100,000-year glacial cycles, *Nature, 454*(7206), 869-872, doi: 10.1038/nature07158

Blunier, T., and E. J. Brook (2001), Timing of Millennial-Scale Climate Change in Antarctica and Greenland During the Last Glacial Period, *Science, 291*(5501), 109-112, doi: 10.1126/science.291.5501.109

Bolton, C. T., P. A. Wilson, I. Bailey, O. Friedrich, C. J. Beer, J. Becker, S. Baranwal, and R. Schiebel (2010), Millennial-scale climate variability in the subpolar North Atlantic Ocean during the late Pliocene, *Paleoceanography, 25*, PA4218, doi: 10.1029/2010PA001951

Bond, G., H. Heinrich, W. Broecker, L. Labeyrie, J. McManus, J. Andrews, S. Huon, R. Jantschik, et al. (1992), Evidence for massive discharges of icebergs into the North Atlantic ocean during the last glacial period, *Nature, 360*(6401), 245-249

Bond, G., W. Broecker, S. Johnsen, J. McManus, L. Labeyrie, J. Jouzel, and G. Bonani (1993), Correlations between climate records from North Atlantic sediments and Greenland ice, *Nature, 365*(6442), 143-147, doi: 10.1038/365143a0

Bond, G. C., and R. Lotti (1995), Iceberg Discharges into the North Atlantic on Millennial Time Scales During the Last Glaciation, *Science, 267*(5200), 1005-1010, doi: 10.1126/science.267.5200.1005

Brassell, S. C., G. Eglinton, I. T. Marlowe, U. Pflaumann, and M. Sarnthein (1986), Molecular stratigraphy: a new tool for climatic assessment, *Nature, 320*(6058), 129-133, doi: 10.1038/320129a0

Bray, E. E., and E. D. Evans (1961), Distribution of n-paraffins as a clue to recognition of source beds, *Geochimica et Cosmochimica Acta*, *22*(1), 2-15, doi: 10.1016/0016-7037(61)90069-2

Brierley, C. M., A. V. Fedorov, Z. Liu, T. D. Herbert, K. T. Lawrence, and J. P. LaRiviere (2009), Greatly Expanded Tropical Warm Pool and Weakened Hadley Circulation in the Early Pliocene, *Science*, *323*(5922), 1714-1718, doi: 10.1126/science.1167625

Brierley, C. M., and A. V. Fedorov (2010), The relative importance of meridional and zonal SST gradients for the onset of the ice ages and Pliocene-Pleistocene climate evolution, *Paleoceanography*, *25*, PA2214, doi: 10.1029/2009PA001809

Broecker, W., G. Bond, M. Klas, E. Clark, and J. McManus (1992), Origin of the northern Atlantic's Heinrich events, *Climate Dynamics*, *6*(3), 265-273, doi: 10.1007/BF00193540

Brown, E. T., T. C. Johnson, C. A. Scholz, A. S. Cohen, and J. W. King (2007), Abrupt change in tropical African climate linked to the bipolar seesaw over the past 55,000 years, *Geophys. Res. Lett.*, *34*(20), L20702, doi: 10.1029/2007gl031240

Cacho, I., J. O. Grimalt, F. J. Sierro, N. Shackleton, and M. Canals (2000), Evidence for enhanced Mediterranean thermohaline circulation during rapid climatic coolings, *Earth and Planetary Science Letters*, *183*(3-4), 417-429, doi: 10.1016/S0012-821X(00)00296-X

Calvo, E., J. Villanueva, J. O. Grimalt, A. Boelaert, and L. Labeyrie (2001), New insights into the glacial latitudinal temperature gradients in the North Atlantic. Results from UK'37 sea surface temperatures and terrigenous inputs, *Earth and Planetary Science Letters*, *188*(3-4), 509-519, doi: 10.1016/S0012-821X(01)00316-8

Calvo, E., C. Pelejero, P. De Deckker, and G. A. Logan (2007), Antarctic deglacial pattern in a 30 kyr record of sea surface temperature offshore South Australia, *Geophys. Res. Lett.*, *34*(13), L13707, doi: 10.1029/2007gl029937

Channell, J. E. T., T. Sato, T. Kanamatsu, R. Stein, M. J. Malone, and Expedition 303/306 Project Team (2004), North Atlantic climate, *IODP Scientific Prospectus*, https://iodp.tamu.edu/publications/SP/303306SP.PDF

Channell, J. E. T., T. Kanamatsu, T. Sato, R. Stein, C. A. Alvarez Zarikian, M. J. Malone, and Expedition 303/306 Scientists (2006), Volume 303/306 expedition reports North Atlantic climate, *Proceedings of the Integrated Ocean Drilling Program, 303/306*

Chapman, M. R. (2010), Seasonal production patterns of planktonic foraminifera in the NE Atlantic Ocean: Implications for paleotemperature and hydrographic reconstructions, *Paleoceanography*, *25*(1), PA1101, doi: 10.1029/2008pa001708

Cheng, H., R. L. Edwards, W. S. Broecker, G. H. Denton, X. Kong, Y. Wang, R. Zhang, and X. Wang (2009), Ice Age Terminations, *Science*, *326*(5950), 248-252, doi: 10.1126/science.1177840

Chikaraishi, Y., and H. Naraoka (2003), Compound-specific δD-δ13C analyses of n-alkanes extracted from terrestrial and aquatic plants, *Phytochemistry*, *63*(3), 361-371, doi: 10.1016/S0031-9422(02)00749-5

Chikaraishi, Y., H. Naraoka, and S. R. Poulson (2004), Carbon and hydrogen isotopic fractionation during lipid biosynthesis in a higher plant (Cryptomeria japonica), *Phytochemistry*, *65*(3), 323-330, doi: 10.1016/j.phytochem.2003.12.003

Chikaraishi, Y., and H. Naraoka (2006), Carbon and hydrogen isotope variation of plant biomarkers in a plant-soil system, *Chemical Geology*, *231*(3), 190-202, doi: 10.1016/j.chemgeo.2006.01.026

Clark, P. U., R. B. Alley, and D. Pollard (1999a), Northern Hemisphere Ice-Sheet Influences on Global Climate Change, *Science*, *286*(5442), 1104-1111, doi: 10.1126/science.286.5442.1104

Clark, P. U., R. S. Webb, and L. D. Keigwin (1999b), Preface, in *Mechanisms of global clime change at millennial time scales*, edited by P. U. Clark, et al., 112, pp. vii-viii. Geophysical Monography Washington.

Clark, P. U., D. Archer, D. Pollard, J. D. Blum, J. A. Rial, V. Brovkin, A. C. Mix, N. G. Pisias, et al. (2006), The middle Pleistocene transition: characteristics, mechanisms, and implications for long-term changes in atmospheric pCO2, *Quaternary Science Reviews*, *25*(23-24), 3150-3184, doi: 10.1016/j.quascirev.2006.07.008

Collister, J. W., G. Rieley, B. Stern, G. Eglinton, and B. Fry (1994), Compound-specific [delta] 13C analyses of leaf lipids from plants with differing carbon dioxide metabolisms, *Organic Geochemistry*, *21*(6-7), 619-627, doi: 10.1016/0146-6380(94)90008-6

Conte, M. H., and J. C. Weber (2002), Long-range atmospheric transport of terrestrial biomarkers to the western North Atlantic, *Global Biogeochem. Cycles*, *16*(4), 1142, doi: 10.1029/2002gb001922

Conte, M. H., J. C. Weber, P. J. Carlson, and L. B. Flanagan (2003), Molecular and carbon isotopic composition of leaf wax in vegetation and aerosols in a northern prairie ecosystem, *Oecologia*, *135*(1), 67-77, doi: 10.1007/s00442-002-1157-4

Conte, M. H., M.-A. Sicre, C. Rühlemann, J. C. Weber, S. Schulte, D. Schulz-Bull, and T. Blanz (2006), Global temperature calibration of the alkenone unsaturation index (Uk'37) in surface waters and comparison with surface sediments, *Geochem. Geophys. Geosyst.*, *7*(2), Q02005, doi: 10.1029/2005gc001054

Cortijo, E., L. Labeyrie, L. Vidal, M. Vautravers, M. Chapman, J.-C. Duplessy, M. Elliot, M. Arnold, et al. (1997), Changes in sea surface hydrology associated with Heinrich event 4 in the North Atlantic Ocean between 40∞ and 60∞N, *Earth and Planetary Science Letters*, *146*(1-2), 29-45, doi: 10.1016/S0012-821X(96)00217-8

Croll, J. (1875), *Climate and Time in Their Geological Relations. A theory of secular changes of the earth's climate*, New York.

Cronin, T. M. (1991), Pliocene shallow water paleoceanography of the North Atlantic ocean based on marine ostracodes, *Quaternary Science Reviews*, *10*(2-3), 175-188, doi: 10.1016/0277-3791(91)90017-O

Dahl, K. A., A. J. Broccoli, and R. J. Stouffer (2005), Assessing the role of North Atlantic freshwater forcing in millennial scale climate variability: a tropical Atlantic perspective, *Climate Dynamics*, *24*(4), 325-346, doi: 10.1007/s00382-004-0499-5

Dansgaard, W., S. J. Johnsen, H. B. Clausen, D. Dahl-Jensen, N. S. Gundestrup, C. U. Hammer, C. S. Hvidberg, J. P. Steffensen, et al. (1993), Evidence for general instability of past climate from a 250-kyr ice-core record, *Nature*, *364*(6434), 218-220, doi: 10.1038/364218a0

de Abreu, L., N. J. Shackleton, J. Schönfeld, M. Hall, and M. Chapman (2003), Millennial-scale oceanic climate variability off the Western Iberian margin during the last two glacial periods, *Marine Geology*, *196*(1-2), 1-20, doi: 10.1016/S0025-3227(03)00046-X

De Schepper, S., M. J. Head, and J. Groeneveld (2009), North Atlantic Current variability through marine isotope stage M2 (circa 3.3 Ma) during the mid-Pliocene, *Paleoceanography*, *24*, PA4206, doi: 10.1029/2008pa001725

Dekens, P. S., A. C. Ravelo, and M. D. McCarthy (2007), Warm upwelling regions in the Pliocene warm period, *Paleoceanography*, *22*, PA3211, doi: 10.1029/2006PA001394

deMenocal, P. B. (1995), Plio-Pleistocene African Climate, *Science*, *270*(5233), 53-59, doi: 10.1126/science.270.5233.53

Denton, G. H., R. F. Anderson, J. R. Toggweiler, R. L. Edwards, J. M. Schaefer, and A. E. Putnam (2010), The Last Glacial Termination, *Science*, *328*(5986), 1652-1656, doi: 10.1126/science.1184119

Dersch, M., and R. Stein (1991), Paläoklima und paläoozeanische Verhältnisse im SW-Pazifik während der letzten 6 Millionen Jahre (DSDP-Site 594, Chatham Rücken, östlich Neuseeland), *Geologische Rundschau*, *80*(3), 535-556

Dersch, M., and R. Stein (1994), Late Cenozoic records of eolian quartz flux in the Sea of Japan (ODP Leg 128, Sites 798 and 799) and paleoclimate in Asia, *Palaeogeography, Palaeoclimatology, Palaeoecology*, *108*(3-4), 523-535, doi: 10.1016/0031-0182(94)90250-X

Dowsett, H. J., T. M. Cronin, R. Z. Poore, R. S. Thompson, R. C. Whatley, and A. M. Wood (1992), Micropaleontological Evidence for Increased Meridional Heat Transport in the North Atlantic Ocean During the Pliocene, *Science*, *258*(5085), 1133-1135, doi: 10.1126/science.258.5085.1133

Dowsett, H. J., M. M. Robinson, and K. M. Foley (2009), Pliocene three-dimensional global ocean temperature reconstruction, *Climate of the Past*, *5*(4), 769-783, doi: 10.5194/cp-5-769-2009

Driscoll, N. W., and G. H. Haug (1998), A Short Circuit in Thermohaline Circulation: A Cause for Northern Hemisphere Glaciation?, *Science*, *282*(5388), 436-438, doi: 10.1126/science.282.5388.436

Eglinton, G., and R. J. Hamilton (1967), Leaf Epicuticular Waxes, *Science*, *156*(3780), 1322-1335, doi: 10.1126/science.156.3780.1322

Elderfield, H., and G. Ganssen (2000), Past temperature and δ18O of surface ocean waters inferred from foraminiferal Mg/Ca ratios, *Nature*, *405*(6785), 442-445, doi: 10.1038/35013033

Eltgroth, M. L., R. L. Watwood, and G. V. Wolfe (2005), Production and cellular localization of neutral long-chain lipids in the Haptophyte algae *Isochrysis Galbana* and *Emiliania Huxleyi*, *Journal of Phycology*, *41*(5), 1000-1009, doi: 10.1111/j.1529-8817.2005.00128.x

EPICA Community Members (2006), One-to-one coupling of glacial climate variability in Greenland and Antarctica, *Nature, 444*(7116), 195-198, doi: 10.1038/nature05301

Expedition 303 Scientists (2006), Sites U1302 and U1303, in *Proceedings of Integrated Ocean Drilling Program* edited by J. E. T. Channell, et al., 303/306. Integrated Ocean Drilling Program Management International, Inc., College Station TX.

Expedition 306 Scientists (2006), Site U1313, in *Proceedings of Integrated Ocean Drilling Program* edited by J. E. T. Channell, et al., 303/306. Integrated Ocean Drilling Program Management International, Inc., College Station TX.

Ferretti, P., S. J. Crowhurst, M. A. Hall, and I. Cacho (2010), North Atlantic millennial-scale climate variability 910 to 790 ka and the role of the equatorial insolation forcing, *Earth and Planetary Science Letters, 293*, 24-41, doi: 10.1016/j.epsl.2010.02.016

Flatau, M. K., L. Talley, and P. P. Niiler (2003), The North Atlantic Oscillation, Surface Current Velocities, and SST Changes in the Subpolar North Atlantic, *Journal of Climate, 16*(14), 2355-2369

Fung, I. Y., S. K. Meyn, I. Tegen, S. C. Doney, J. G. John, and J. K. B. Bishop (2000), Iron supply and demand in the upper ocean, *Global Biogeochemical Cycles, 14*(1), 281-295, doi: 10.1029/1999gb900059

Gagosian, R. B., E. T. Peltzer, and O. C. Zafiriou (1981), Atmospheric transport of continentally derived lipids to the tropical North Pacific, *Nature, 291*(5813), 312-314, doi: 10.1038/291312a0

Ganopolski, A., R. Calov, and M. Claussen (2010), Simulation of the last glacial cycle with a coupled climate ice-sheet model of intermediate complexity, *Climate of the Past, 6*(2), 229-244, doi: 10.5194/cp-6-229-2010

Ganssen, G. M., and D. Kroon (2000), The isotopic signature of planktonic foraminifera from NE Atlantic surface sediments: implications for the reconstruction of past oceanic conditions, *Journal of the Geological society, 157*(3), 693-699, doi: 10.1144/jgs.157.3.693

Giraudeau, J., M. Grelaud, S. Solignac, J. T. Andrews, M. Moros, and E. Jansen (2010), Millennial-scale variability in Atlantic water advection to the Nordic Seas derived from Holocene coccolith concentration records, *Quaternary Science Reviews, 29*(9-10), 1276-1287, doi: 10.1016/j.quascirev.2010.02.014

Gregg, W. W., and N. W. Casey (2007), Modeling coccolithophores in the global oceans, *Deep Sea Research Part II: Topical Studies in Oceanography, 54*(5-7), 447-477, doi: 10.1016/j.dsr2.2006.12.007

Grimm, E. C., W. A. Watts, G. L. Jacobson Jr, B. C. S. Hansen, H. R. Almquist, and A. C. Dieffenbacher-Krall (2006), Evidence for warm wet Heinrich events in Florida, *Quaternary Science Reviews, 25*(17-18), 2197-2211, doi: 10.1016/j.quascirev.2006.04.008

Grootes, P. M., E. J. Steig, M. Stuiver, E. D. Waddington, D. L. Morse, and M.-J. Nadeau (2001), The Taylor Dome Antarctic 18O Record and Globally Synchronous Changes in Climate, *Quaternary Research, 56*(3), 289-298, doi: 10.1006/qres.2001.2276

Grousset, F. E., L. Labeyrie, J. A. Sinko, M. Cremer, G. Bond, J. Duprat, E. Cortijo, and S. Huon (1993), Patterns of Ice-Rafted Detritus in the Glacial North Atlantic (40-55 oN), *Paleoceanography*, *8*(2), 175-192, doi: 10.1029/92pa02923

Grousset, F. E., E. Cortijo, S. Huon, L. Hervè, T. Richter, D. Burdloff, J. Duprat, and O. Weber (2001), Zooming in on Heinrich Layers, *Paleoceanography*, *16*(3), 240-259, doi: 10.1029/2000pa000559

Gwiazda, R. H., S. R. Hemming, and W. S. Broecker (1996), Provenance of Icebergs During Heinrich Event 3 and the Contrast to their Sources During Other Heinrich Episodes, *Paleoceanography*, *11*(4), 371-378, doi: 10.1029/96pa01022

Handley, L., P. N. Pearson, I. K. McMillan, and R. D. Pancost (2008), Large terrestrial and marine carbon and hydrogen isotope excursions in a new Paleocene/Eocene boundary section from Tanzania, *Earth and Planetary Science Letters*, *275*(1-2), 17-25, doi: 10.1016/j.epsl.2008.07.030

Harada, N., N. Ahagon, T. Sakamoto, M. Uchida, M. Ikehara, and Y. Shibata (2006), Rapid fluctuation of alkenone temperature in the southwestern Okhotsk Sea during the past 120 ky, *Global and Planetary Change*, *53*(1-2), 29-46, doi: 10.1016/j.gloplacha.2006.01.010

Haug, G. H., and R. Tiedemann (1998), Effect of the formation of the Isthmus of Panama on Atlantic Ocean thermohaline circulation, *Nature*, *393*(6686), 673-676, doi: 10.1038/31447

Haug, G. H., D. M. Sigman, R. Tiedemann, T. F. Pedersen, and M. Sarnthein (1999), Onset of permanent stratification in the subarctic Pacific Ocean, *Nature*, *401*(6755), 779-782, doi: 10.1038/44550

Haug, G. H., A. Ganopolski, D. M. Sigman, A. Rosell-Melé, G. E. A. Swann, R. Tiedemann, S. L. Jaccard, J. Bollmann, et al. (2005), North Pacific seasonality and the glaciation of North America 2.7 million years ago, *Nature*, *433*(7028), 821-825, doi: 10.1038/nature03332

Hays, J. D., J. Imbrie, and N. J. Shackleton (1976), Variations in the Earth's Orbit: Pacemaker of the Ice Ages, *Science*, *194*(4270), 1121-1132, doi: 10.1126/science.194.4270.1121

Haywood, A. M., B. W. Sellwood, and P. J. Valdes (2000), Regional warming: Pliocene (3 Ma) paleoclimate of Europe and the Mediterranean, *Geology*, *28*(12), 1063-1066, doi: 10.1130/0091-7613

Haywood, A. M., and P. J. Valdes (2004), Modelling Pliocene warmth: contribution of atmosphere, oceans and cryosphere, *Earth and Planetary Science Letters*, *218*(3-4), 363-377, doi: 10.1016/S0012-821X(03)00685-X

Haywood, A. M., P. Dekens, A. C. Ravelo, and M. Williams (2005), Warmer tropics during the mid-Pliocene? Evidence from alkenone paleothermometry and a fully coupled ocean-atmosphere GCM, *Geochem. Geophys. Geosyst.*, *6*(3), Q03010, doi: 10.1029/2004GC000799

Haywood, A. M., M. A. Chandler, P. J. Valdes, U. Salzmann, D. J. Lunt, and H. J. Dowsett (2009), Comparison of mid-Pliocene climate predictions produced by the HadAM3 and GCMAM3 General Circulation Models, *Global and Planetary Change*, *66*(3-4), 208-224, doi: 10.1016/j.gloplacha.2008.12.014

Hefter, J. (2008), Analysis of Alkenone Unsaturation Indices with Fast Gas Chromatography/Time-of-Flight Mass Spectrometry, *Analytical Chemistry*, *80*(6), 2161-2170, doi: 10.1021/ac702194m

Heinrich, H. (1988), Origin and consequences of cyclic ice rafting in the Northeast Atlantic Ocean during the past 130,000 years, *Quaternary Research*, *29*(2), 142-152, doi: 10.1016/0033-5894(88)90057-9

Hemming, S. R. (2004), Heinrich events: Massive late Pleistocene detritus layers of the North Atlantic and their global climate imprint, *Review of Geophysics*, *42*(1), RG1005, doi: 10.1029/2003rg000128

Herbert, T. D., L. C. Peterson, K. T. Lawrence, and Z. Liu (2010), Tropical Ocean Temperatures Over the Past 3.5 Million Years, *Science*, *328*(5985), 1530-1534, doi: 10.1126/science.1185435

Hessler, I., L. Dupont, R. Bonnefille, H. Behling, C. Gonz·lez, K. F. Helmens, H. Hooghiemstra, J. Lebamba, et al. (2010), Millennial-scale changes in vegetation records from tropical Africa and South America during the last glacial, *Quaternary Science Reviews*, *29*(21-22), 2882-2899, doi: 10.1016/j.quascirev.2009.11.029

Hill, D. J., A. M. Dolan, A. M. Haywood, S. J. Hunter, and D. K. Stoll (2010), Sensitivity of the Greenland Ice Sheet to Pliocene sea surface temperatures, *Stratigraphy*, *7*(2-3), 111-122

Hodell, D. A., J. E. T. Channell, J. H. Curtis, O. E. Romero, and U. Röhl (2008), Onset of "Hudson Strait" Heinrich events in the eastern North Atlantic at the end of the middle Pleistocene transition (~640 ka)?, *Paleoceanography*, *23*, PA4218, doi: 10.1029/2008PA001591

Hodell, D. A., H. F. Evans, J. E. T. Channell, and J. H. Curtis (2010), Phase relationships of North Atlantic ice-rafted debris and surface-deep climate proxies during the last glacial period, *Quaternary Science Reviews*, *29*(27-28), 3875-3886, doi: 10.1016/j.quascirev.2010.09.006

Huang, Y., L. Dupont, M. Sarnthein, J. M. Hayes, and G. Eglinton (2000), Mapping of C4 plant input from North West Africa into North East Atlantic sediments, *Geochimica et Cosmochimica Acta*, *64*(20), 3505-3513, doi: 10.1016/S0016-7037(00)00445-2

Huybers, P., and C. Wunsch (2005), Obliquity pacing of the late Pleistocene glacial terminations, *Nature*, *434*(7032), 491-494, doi: 10.1038/nature03401

Huybers, P. (2006), Early Pleistocene Glacial Cycles and the Integrated Summer Insolation Forcing, *Science*, *313*(5786), 508-511, doi: 10.1126/science.1125249

Imbrie, J., E. A. Boyle, S. C. Clemens, A. Duffy, W. R. Howard, G. Kukla, J. Kutzbach, D. G. Martinson, et al. (1992), On the Structure and Origin of Major Glaciation Cycles 1. Linear Responses to Milankovitch Forcing, *Paleoceanography*, *7*(6), 701-738, doi: 10.1029/92pa02253

Imbrie, J., A. Berger, E. A. Boyle, S. C. Clemens, A. Duffy, W. R. Howard, G. Kukla, J. Kutzbach, et al. (1993), On the Structure and Origin of Major Glaciation Cycles 2. The 100,000-Year Cycle, *Paleoceanography*, *8*, 699-735, doi: 10.1029/93PA02751

Incarbona, A., B. Martrat, E. Di Stefano, J. O. Grimalt, N. Pelosi, B. Patti, and G. Tranchida (2010), Primary productivity variability on the Atlantic Iberian Margin over the last 70,000 years: Evidence from coccolithophores and fossil organic compounds, *Paleoceanography*, *25*(2), PA2218, doi: 10.1029/2008pa001709

Ivy-Ochs, S., H. Kerschner, P. W. Kubik, and C. Schlüchter (2006), Glacier response in the European Alps to Heinrich Event 1 cooling: the Gschnitz stadial, *Journal of Quaternary Science*, *21*(2), 115-130, doi: 10.1002/jqs.955

Ji, J., Y. Ge, W. Balsam, J. E. Damuth, and J. Chen (2009), Rapid identification of dolomite using a Fourier Transform Infrared Spectrophotometer (FTIR): A fast method for identifying Heinrich events in IODP Site U1308, *Marine Geology*, *258*(1-4), 60-68, doi: 10.1016/j.margeo.2008.11.007

Jouzel, J., C. Lorius, J. R. Petit, C. Genthon, N. I. Barkov, V. M. Kotlyakov, and V. M. Petrov (1987), Vostok ice core: a continuous isotope temperature record over the last climatic cycle (160,000 years), *Nature*, *329*(6138), 403-408, doi: 10.1038/329403a0

Jouzel, J., V. Masson-Delmotte, O. Cattani, G. Dreyfus, S. Falourd, G. Hoffmann, B. Minster, J. Nouet, et al. (2007), Orbital and Millennial Antarctic Climate Variability over the Past 800,000 Years, *Science*, *317*(5839), 793-796, doi: 10.1126/science.1141038

Jullien, E., F. Grousset, B. MalaizÈ, J. Duprat, M. F. Sanchez-Goni, F. Eynaud, K. Charlier, R. Schneider, et al. (2007), Low-latitude "dusty events" vs. high-latitude "icy Heinrich events", *Quaternary Research*, *68*(3), 379-386, doi: 10.1016/j.yqres.2007.07.007

Keigwin, L. D., W. B. Curry, S. J. Lehman, and S. Johnsen (1994), The role of the deep ocean in North Atlantic climate change between 70 and 130 kyr ago, *Nature*, *371*(6495), 323-326, doi: 10.1038/371323a0

Khélifi, N. (2010), Variations in Mediterranean Outflow Water and its salt discharge versus Pliocene changes in North Atlantic thermohaline circulation over the onset of Northern Hemisphere Glaciation, 3.7 – 2.6 Ma ago, *PhD Thesis, Kiel University*, 150 pp.

Khélifi, N., and M. Sarnthein (2010), Major shifts in age control at ODP S. 982 near the Pliocene onset of Northern Hemisphere Glaciation - Composite depths and d18O stratigraphy revisited, *Geophysical Research Abstracts*, *12*, EGU2010-12762-12761

Kiefer, T., and M. Kienast (2005), Patterns of deglacial warming in the Pacific Ocean: a review with emphasis on the time interval of Heinrich event 1, *Quaternary Science Reviews*, *24*(7-9), 1063-1081, doi: 10.1016/j.quascirev.2004.02.021

Kleiven, H. F., E. Jansen, T. Fronval, and T. M. Smith (2002), Intensification of Northern Hemisphere glaciations in the circum Atlantic region (3.5-2.4 Ma) - ice-rafted detritus evidence, *Palaeogeography, Palaeoclimatology, Palaeoecology*, *184*(3-4), 213-223, doi: 10.1016/S0031-0182(01)00407-2

Kotilainen, A. T., and N. J. Shackleton (1995), Rapid climate variability in the North Pacific Ocean during the past 95,000 years, *Nature*, *377*(6547), 323-326, doi: 10.1038/377323a0

Lambert, F., B. Delmonte, J. R. Petit, M. Bigler, P. R. Kaufmann, M. A. Hutterli, T. F. Stocker, U. Ruth, et al. (2008), Dust-climate couplings over the past 800,000 years from the EPICA Dome C ice core, *Nature*, *452*(7187), 616-619, doi: 10.1038/nature06763

Lamy, F., J. Kaiser, H. W. Arz, D. Hebbeln, U. Ninnemann, O. Timm, A. Timmermann, and J. R. Toggweiler (2007), Modulation of the bipolar seesaw in the Southeast Pacific during Termination 1, *Earth and Planetary Science Letters*, *259*(3-4), 400-413, doi: 10.1016/j.epsl.2007.04.040

Lang, N., and E. W. Wolff (2010), Interglacial and glacial variability from the last 800 ka in marine, ice and terrestrial archives, *Clim. Past Discuss.*, *6*(5), 2223-2266, doi: 10.5194/cpd-6-2223-2010

Laskar, J., P. Robutel, F. Joutel, M. Gastineau, A. C. M. Correia, and B. Levrard (2004), A long-term numerical solution for the insolation quantities of the Earth, *Astronomy and Astrophysics*, *428*, 261-285, doi: 10.1051/0004-6361:20041335

Lawrence, K. T., Z. Liu, and T. D. Herbert (2006), Evolution of the Eastern Tropical Pacific Through Plio-Pleistocene Glaciation, *Science*, *312*(5770), 79-83, doi: 10.1126/science.1120395

Lawrence, K. T., T. D. Herbert, P. S. Dekens, and A. C. Ravelo (2007), The application of the alkenone organic proxy to the study of Plio-Pleistocene climate, in *Deep-time perspectives on climate change: Marrying the signal from computer models and biological proxies*, edited by M. Williams, et al. pp. 539-565. The Geological Society, London.

Lawrence, K. T., T. D. Herbert, C. M. Brown, M. E. Raymo, and A. M. Haywood (2009), High-amplitude variations in North Atlantic sea surface temperature during the early Pliocene warm period, *Paleoceanography*, *24*, PA2218, doi: 10.1029/2008pa001669

Lawrence, K. T., S. Sosdian, H. E. White, and Y. Rosenthal (2010), North Atlantic climate evolution through the Plio-Pleistocene climate transitions, *Earth and Planetary Science Letters*, *300*(3-4), 329-342 doi: 10.1016/j.epsl.2010.10.013

Leduc, G., R. Schneider, J. H. Kim, and G. Lohmann (2010), Holocene and Eemian sea surface temperature trends as revealed by alkenone and Mg/Ca paleothermometry, *Quaternary Science Reviews*, *29*(7-8), 989-1004, doi: 10.1016/j.quascirev.2010.01.004

Leuschner, D. C., and F. Sirocko (2000), The low-latitude monsoon climate during Dansgaard-Oeschger cycles and Heinrich Events, *Quaternary Science Reviews*, *19*(1-5), 243-254, doi: 10.1016/S0277-3791(99)00064-5

Li, T., Z. Liu, M. A. Hall, S. Berne, Y. Saito, S. Cang, and Z. Cheng (2001), Heinrich event imprints in the Okinawa Trough: evidence from oxygen isotope and planktonic foraminifera, *Palaeogeography, Palaeoclimatology, Palaeoecology*, *176*(1-4), 133-146, doi: 10.1016/S0031-0182(01)00332-7

Lisiecki, L. E., and P. A. Lisiecki (2002), Application of dynamic programming to the correlation of paleoclimate records, *Paleoceanography*, *17*, PA1049, doi: 10.1029/2001pa000733

Lisiecki, L. E., and M. E. Raymo (2005), A Pliocene-Pleistocene stack of 57 globally distributed benthic δ18O records, *Paleoceanography*, *20*, PA1003, doi: 10.1029/2004PA001071

Locarnini, R. A., A. V. Mishonov, J. I. Antonov, T. P. Boyer, and H. E. Garcia (2006), Volume 1: Temperature, in *World Ocean Atlas 2005*, edited by S. Levitus pp. 182. U.S. Government Printing Office, Washington, D.C.

Lockheart, M. J., P. F. Van Bergen, and R. P. Evershed (1997), Variations in the stable carbon isotope compositions of individual lipids from the leaves of modern angiosperms: implications for the study of higher land plant-derived sedimentary organic matter, *Organic Geochemistry*, *26*(1-2), 137-153, doi: 10.1016/S0146-6380(96)00135-0

López-Martínez, C., J. O. Grimalt, B. Hoogakker, J. Gruetzner, M. J. Vautravers, and I. N. McCave (2006), Abrupt wind regime changes in the North Atlantic Ocean during the past 30,000 - 60,000 years, *Paleoceanography*, *21*, PA4215, doi: 10.1029/2006PA001275

Lowell, T. V., C. J. Heusser, B. G. Andersen, P. I. Moreno, A. Hauser, L. E. Heusser, C. Schlüchter, D. R. Marchant, et al. (1995), Interhemispheric Correlation of Late Pleistocene Glacial Events, *Science*, *269*(5230), 1541-1549, doi: 10.1126/science.269.5230.1541

Lunt, D. J., G. L. Foster, A. M. Haywood, and E. J. Stone (2008), Late Pliocene Greenland glaciation controlled by a decline in atmospheric CO_2 levels, *Nature*, *454*(7208), 1102-1105, doi: 10.1038/nature07223

Lüthi, D., M. Le Floch, B. Bereiter, T. Blunier, J.-M. Barnola, U. Siegenthaler, D. Raynaud, J. Jouzel, et al. (2008), High-resolution carbon dioxide concentration record 650,000-800,000 years before present, *Nature*, *453*(7193), 379-382, doi: 10.1038/nature06949

Madureira, L. A. S., S. A. van Kreveld, G. Eglinton, M. H. Conte, G. Ganssen, J. E. van Hinte, and J. J. Ottens (1997), Late Quaternary High-Resolution Biomarker and Other Sedimentary Climate Proxies in a Northeast Atlantic Core, *Paleoceanography*, *12*, 255-269, doi: 10.1029/96pa03120

Maher, B. A., J. M. Prospero, D. Mackie, D. Gaiero, P. P. Hesse, and Y. Balkanski (2010), Global connections between aeolian dust, climate and ocean biogeochemistry at the present day and at the last glacial maximum, *Earth-Science Reviews*, *99*(1-2), 61-97, doi: 10.1016/j.earscirev.2009.12.001

Mahowald, N., S. Albani, S. Engelstaedter, G. Winckler, and M. Goman (2011), Model insight into glacial-interglacial paleodust records, *Quaternary Science Reviews*, *30*(7-8), 832-854, doi: 10.1016/j.quascirev.2010.09.007

Mahowald, N. M., and L. M. Kiehl (2003), Mineral aerosol and cloud interactions, *Geophys. Res. Lett.*, *30*(9), 1475, doi: 10.1029/2002gl016762

Mahowald, N. M., D. R. Muhs, S. Levis, P. J. Rasch, M. Yoshioka, C. S. Zender, and C. Luo (2006a), Change in atmospheric mineral aerosols in response to climate: Last glacial period, preindustrial, modern, and doubled carbon dioxide climates, *Journal of Geophysical Research*, *111*(D10), D10202, doi: 10.1029/2005jd006653

Mahowald, N. M., M. Yoshioka, W. D. Collins, A. J. Conley, D. W. Fillmore, and D. B. Coleman (2006b), Climate response and radiative forcing from mineral aerosols during the last glacial maximum, pre-industrial, current and doubled-carbon dioxide climates, *Geophysical Research Letters*, *33*(20), L20705, doi: 10.1029/2006gl026126

Marchitto, T. M., S. J. Lehman, J. D. Ortiz, J. Flückiger, and A. van Geen (2007), Marine Radiocarbon Evidence for the Mechanism of Deglacial Atmospheric CO_2 Rise, *Science*, *316*(5830), 1456-1459, doi: 10.1126/science.1138679

Martin, J. H. (1990), Glacial interglacial CO2 change: The Iron Hypothesis, *Paleoceanography*, *5*(1), 1-13, doi: 10.1029/PA005i001p00001

Martìnez-Garcia, A., A. Rosell-Melé, W. Geibert, R. Gersonde, P. Masquè, V. Gaspari, and C. Barbante (2009), Links between iron supply, marine productivity, sea surface temperature, and CO_2 over the last 1.1 Ma, *Paleoceanography*, *24*(1), PA1207, doi: 10.1029/2008pa001657

Martrat, B., J. O. Grimalt, N. J. Shackleton, L. de Abreu, M. A. Hutterli, and T. F. Stocker (2007), Four Climate Cycles of Recurring Deep and Surface Water Destabilizations on the Iberian Margin, *Science*, *317*(5837), 502-507, doi: 10.1126/science.1139994

Maslin, M. A., X. S. Li, M. F. Loutre, and A. Berger (1998), The contribution of orbital forcing to the progressive intensification of northern hemisphere glaciation, *Quaternary Science Reviews*, *17*(4-5), 411-426, doi: 10.1016/S0277-3791(97)00047-4

Maslin, M. A., and A. J. Ridgwell (2005), Mid-Pleistocene revolution and the 'eccentricity myth', in *Early-Middle Pleistocene transitions: The land-ocean evidence*, edited by M. J. Head and P. L. Gibbard, Special Publications, 247, pp. 19-34. Geological Society, London.

Mayewski, P. A., L. D. Meeker, S. Whitlow, M. S. Twickler, M. C. Morrison, P. Bloomfield, G. C. Bond, R. B. Alley, et al. (1994), Changes in Atmospheric Circulation and Ocean Ice Cover over the North Atlantic During the Last 41,000 Years, *Science*, *263*(5154), 1747-1751, doi: 10.1126/science.263.5154.1747

McClymont, E. L., A. Rosell-MelÈ, J. Giraudeau, C. Pierre, and J. M. Lloyd (2005), Alkenone and coccolith records of the mid-Pleistocene in the south-east Atlantic: Implications for the index and South African climate, *Quaternary Science Reviews*, *24*(14-15), 1559-1572, doi: 10.1016/j.quascirev.2004.06.024

McGee, D., W. S. Broecker, and G. Winckler (2010), Gustiness: The driver of glacial dustiness?, *Quaternary Science Reviews*, *29*(17-18), 2340-2350, doi: 10.1016/j.quascirev.2010.06.009

McIntyre, A., W. F. Ruddiman, and R. Jantzen (1972), Southward penetrations of the North Atlantic Polar Front: faunal and floral evidence of large-scale surface water mass movements over the last 225,000 years, *Deep-Sea Research*, *19*, 61-77

McManus, J. F., R. F. Anderson, W. S. Broecker, M. Q. Fleisher, and S. M. Higgins (1998), Radiometrically determined sedimentary fluxes in the sub-polar North Atlantic during the last 140,000 years, *Earth and Planetary Science Letters*, *155*(1-2), 29-43, doi: 10.1016/S0012-821X(97)00201-X

McManus, J. F., D. W. Oppo, and J. L. Cullen (1999), A 0.5-Million-Year Record of Millennial-Scale Climate Variability in the North Atlantic, *Science*, *283*(5404), 971-975, doi: 10.1126/science.283.5404.971

McManus, J. F., R. Francois, J. M. Gherardi, L. D. Keigwin, and S. Brown-Leger (2004), Collapse and rapid resumption of Atlantic meridional circulation linked to deglacial climate changes, *Nature*, *428*(6985), 834-837, doi: 10.1038/nature02494

Meyers, S. R., and L. A. Hinnov (2010), Northern Hemisphere glaciation and the evolution of Plio-Pleistocene climate noise, *Paleoceanography*, *25*(3), PA3207, doi: 10.1029/2009pa001834

Milankovitch, M. (1941), *Kanon der Erdbestrahlungen und seine Anwendung auf das Eiszeitenproblem* Royal Serbian Academy, Belgrade.

Mills, M. M., C. Ridame, M. Davey, J. La Roche, and R. J. Geider (2004), Iron and phosphorus co-limit nitrogen fixation in the eastern tropical North Atlantic, *Nature*, *429*(6989), 292-294, doi: 10.1038/nature02550

Mollenhauer, G., M. Kienast, F. Lamy, H. Meggers, R. R. Schneider, J. M. Hayes, and T. I. Eglinton (2005), An evaluation of 14C age relationships between co-occurring foraminifera, alkenones, and total organic carbon in continental margin sediments, *Paleoceanography*, *20*(1), PA1016, doi: 10.1029/2004pa001103

Mudelsee, M., and M. E. Raymo (2005), Slow dynamics of the Northern Hemisphere glaciation, *Paleoceanography*, *20*, PA4022, doi: 10.1029/2005PA001153

Muhs, D. R., and E. A. Bettis (2000), Geochemical Variations in Peoria Loess of Western Iowa Indicate Paleowinds of Midcontinental North America during Last Glaciation, *Quaternary Research*, *53*(1), 49-61, doi: 10.1006/qres.1999.2090

Mulitza, S., M. Prange, J.-B. Stuut, M. Zabel, T. von Dobeneck, A. C. Itambi, J. Nizou, M. Schulz, et al. (2008), Sahel megadroughts triggered by glacial slowdowns of Atlantic meridional overturning, *Paleoceanography*, *23*(4), PA4206, doi: 10.1029/2008pa001637

Muller, J., M. Kylander, R. A. J. Wüst, D. Weiss, A. Martinez-Cortizas, A. N. LeGrande, T. Jennerjahn, H. Behling, et al. (2008), Possible evidence for wet Heinrich phases in tropical NE Australia: the Lynch's Crater deposit, *Quaternary Science Reviews*, *27*(5-6), 468-475, doi: 10.1016/j.quascirev.2007.11.006

Müller, P. J., G. Kirst, G. Ruhland, I. von Storch, and A. Rosell-Melé (1998), Calibration of the alkenone paleotemperature index Uk'37 based on core-tops from the eastern South Atlantic and the global ocean (60 oN-60 oS), *Geochimica et Cosmochimica Acta*, *62*(10), 1757-1772, doi: 10.1016/S0016-7037(98)00097-0

Naafs, B. D. A., R. Stein, J. Hefter, N. Khèlifi, S. De Schepper, and G. H. Haug (2010), Late Pliocene changes in the North Atlantic Current, *Earth and Planetary Science Letters*, *298*(3-4), 434-442, doi: 10.1016/j.epsl.2010.08.023

Naafs, B. D. A., J. Hefter, P. Ferretti, R. Stein, and G. H. Haug (accepted), Sea surface temperatures did not control the first occurrence of Hudson Strait Heinrich Events during MIS 16, *Paleoceanography*

Naafs, B. D. A., J. Hefter, P. Ferretti, R. Stein, and G. H. Haug (submitted), Sea surface temperatures did not control the first occurrence of Hudson Strait Heinrich Events during MIS 16

NGRIP members (2004), High-resolution record of Northern Hemisphere climate extending into the last interglacial period, *Nature*, *431*(7005), 147-151, doi: 10.1038/nature02805

Nielsdóttir, M. C., C. M. Moore, R. Sanders, D. J. Hinz, and E. P. Achterberg (2009), Iron limitation of the postbloom phytoplankton communities in the Iceland Basin, *Global Biogeochem. Cycles*, *23*(3), GB3001, doi: 10.1029/2008gb003410

O'Leary, M. H. (1981), Carbon isotope fractionation in plants, *Phytochemistry*, *20*(4), 553-567, doi: 10.1016/0031-9422(81)85134-5

Pagani, M., Z. Liu, J. LaRiviere, and A. C. Ravelo (2010), High Earth-system climate sensitivity determined from Pliocene carbon dioxide concentrations, *Nature Geosciences*, *3*(1), 27-30, doi: 10.1038/ngeo724

Paillard, D., L. Labeyrie, and P. Yiou (1996), Macintosh program performs time-series analysis, *Eos Trans. AGU*, *77*(39), 379, doi: 10.1029/96EO00259

Peck, V. L., I. R. Hall, R. Zahn, F. Grousset, S. R. Hemming, and J. D. Scourse (2007), The relationship of Heinrich events and their European precursors over the past 60 ka BP: a multi-proxy ice-rafted debris provenance study in the North East Atlantic, *Quaternary Science Reviews*, *26*(7-8), 862-875, doi: 10.1016/j.quascirev.2006.12.002

Pedentchouk, N., W. Sumner, B. Tipple, and M. Pagani (2008), δ^{13}C and δD compositions of n-alkanes from modern angiosperms and conifers: An experimental set up in central Washington State, USA, *Organic Geochemistry*, *39*(8), 1066-1071, doi: 10.1016/j.orggeochem.2008.02.005

Pena, L. D., E. Calvo, I. Cacho, S. Eggins, and C. Pelejero (2005), Identification and removal of Mn-Mg-rich contaminant phases on foraminiferal tests: Implications for Mg/Ca past temperature reconstructions, *Geochem. Geophys. Geosyst.*, *6*(9), Q09P02, doi: 10.1029/2005gc000930

Penaud, A., F. Eynaud, J. L. Turon, D. Blamart, L. Rossignol, F. Marret, C. Lopez-Martinez, J. O. Grimalt, et al. (2010), Contrasting paleoceanographic conditions off Morocco during Heinrich events (1 and 2) and the Last Glacial Maximum, *Quaternary Science Reviews*, *29*(15-16), 1923-1939, doi: 10.1016/j.quascirev.2010.04.011

Peterson, L. C., G. H. Haug, K. A. Hughen, and U. Röhl (2000), Rapid Changes in the Hydrologic Cycle of the Tropical Atlantic During the Last Glacial, *Science*, *290*(5498), 1947-1951, doi: 10.1126/science.290.5498.1947

Pflaumann, U., M. Sarnthein, M. Chapman, L. de Abreu, B. Funnell, M. Huels, T. Kiefer, M. Maslin, et al. (2003), Glacial North Atlantic: Sea-surface conditions reconstructed by GLAMAP 2000, *Paleoceanography*, *18*, 1065, doi: 10.1029/2002PA000774

Phillips, F. M., M. G. Zreda, L. V. Benson, M. A. Plummer, D. Elmore, and P. Sharma (1996), Chronology for Fluctuations in Late Pleistocene Sierra Nevada Glaciers and Lakes, *Science*, *274*(5288), 749-751, doi: 10.1126/science.274.5288.749

Pisias, N. G., P. U. Clark, and E. J. Brook (2010), Modes of Global Climate Variability during Marine Isotope Stage 3 (60-26 ka), *Journal of Climate*, *23*(6), 1581-1588, doi: 10.1175/2009JCLI3416.1

Pollard, D., and S. L. Thompson (1997), Climate and ice-sheet mass balance at the last glacial maximum from the GENESIS version 2 global climate model, *Quaternary Science Reviews*, *16*(8), 841-863, doi: 10.1016/S0277-3791(96)00115-1

Prahl, F. G., and S. G. Wakeham (1987), Calibration of unsaturation patterns in long-chain ketone compositions for palaeotemperature assessment, *Nature*, *330*(6146), 367-369, doi: 10.1038/330367a0

Rahmstorf, S. (2002), Ocean circulation and climate during the past 120,000 years, *Nature*, *419*(6903), 207-214, doi: 10.1038/nature01090

Rahmstorf, S. (2007), Glacial climates - Thermohaline Circulation, in *Encyclopedia of Quaternary Science*, edited by S. A. Elias pp. 739-750. Elsevier, Oxford.

Rashid, H., and E. Grosjean (2006), Detecting the source of Heinrich layers: An organic geochemical study, *Paleoceanography*, *21*(3), PA3014, doi: 10.1029/2005pa001240

Rashid, H., and E. A. Boyle (2007), Mixed-Layer Deepening During Heinrich Events: A Multi-Planktonic Foraminiferal δ18O Approach, *Science*, *318*(5849), 439-441, doi: 10.1126/science.1146138

Ravelo, A. C., D. H. Andreasen, M. Lyle, A. Olivarez Lyle, and M. W. Wara (2004), Regional climate shifts caused by gradual global cooling in the Pliocene epoch, *Nature*, *429*(6989), 263-267, doi: 10.1038/nature02567

Raymo, M. E., W. F. Ruddiman, J. Backman, B. M. Clement, and D. G. Martinson (1989), Late Pliocene Variation in Northern Hemisphere Ice Sheets and North Atlantic Deep Water Circulation, *Paleoceanography*, *4*(4), 413-446, doi: 10.1029/PA004i004p00413

Raymo, M. E., W. F. Ruddiman, N. J. Shackleton, and D. W. Oppo (1990), Evolution of Atlantic-Pacific [delta]13C gradients over the last 2.5 m.y, *Earth and Planetary Science Letters*, *97*(3-4), 353-368, doi: 10.1016/0012-821X(90)90051-X

Raymo, M. E., D. Hodell, and E. Jansen (1992), Response of Deep Ocean Circulation to Initiation of Northern Hemisphere Glaciation (3-2 MA), *Paleoceanography*, *7*, 645-672, doi: 10.1029/92pa01609

Raymo, M. E., and K. Nisancioglu (2003), The 41 kyr world: Milankovitch's other unsolved mystery, *Paleoceanography*, *18*(1), 1011, doi: 10.1029/2002pa000791

Raymo, M. E., L. E. Lisiecki, and K. H. Nisancioglu (2006), Plio-Pleistocene Ice Volume, Antarctic Climate, and the Global δ18O Record, *Science*, *313*(5786), 492-495, doi: 10.1126/science.1123296

Reichart, G. J., L. J. Lourens, and W. J. Zachariasse (1998), Temporal Variability in the Northern Arabian Sea Oxygen Minimum Zone (OMZ) during the Last 225,000 Years, *Paleoceanography*, *13*(6), 607-621, doi: 10.1029/98pa02203

Ridgwell, A. J. (2002), Dust in the Earth system: the biogeochemical linking of land, air and sea, *Philosophical Transactions of the Royal Society of London. Series A: Mathematical, Physical and Engineering Sciences*, *360*(1801), 2905-2924, doi: 10.1098/rsta.2002.1096

Ridgwell, A. J., and A. J. Watson (2002), Feedback between aeolian dust, climate, and atmospheric CO_2 in glacial time, *Paleoceanography*, *17*(4), 1059, doi: 10.1029/2001pa000729

Rieley, G., R. J. Collier, D. M. Jones, G. Eglinton, P. A. Eakin, and A. E. Fallick (1991), Sources of sedimentary lipids deduced from stable carbon-isotope analyses of individual compounds, *Nature*, *352*(6334), 425-427, doi: 10.1038/352425a0

Rieley, G. (1994), Derivatization of organic compounds prior to gas chromatographic-combustion-isotope ratio mass spectrometric analysis: identification of isotope fractionation processes, *Analyst*, *119*(5), 915-919, doi: 10.1039/AN9941900915

Robinson, M. M., H. J. Dowsett, G. S. Dwyer, and K. T. Lawrence (2008), Reevaluation of mid-Pliocene North Atlantic sea surface temperatures, *Paleoceanography*, *23*, PA3213, doi: 10.1029/2008pa001608

Robinson, M. M. (2009), New quantitative evidence of extreme warmth in the Pliocene Arctic, *Stratigraphy*, *6*(4), 265-275

Robinson, S. G., M. A. Maslin, and I. N. McCave (1995), Magnetic Susceptibility Variations in Upper Pleistocene Deep-Sea Sediments of the NE Atlantic: Implications for Ice Rafting and Paleocirculation at the Last Glacial Maximum, *Paleoceanography*, *10*(2), 221-250, doi: 10.1029/94pa02683

Rodrigues, T., A. H. L. Voelker, J. O. Grimalt, F. Abrantes, and F. Naughton (2011), Iberian Margin Sea Surface Temperature during MIS 15 to 9 (580-300 ka): Glacial suborbital variability vs interglacial stability, *Paleoceanography*, *26*, PA1204, doi: 10.1029/2010PA001927

Rommerskirchen, F., A. Plader, G. Eglinton, Y. Chikaraishi, and J. Rullkötter (2006), Chemotaxonomic significance of distribution and stable carbon isotopic composition of long-chain alkanes and alkan-1-ols in C4 grass waxes, *Organic Geochemistry*, *37*(10), 1303-1332, doi: 10.1016/j.orggeochem.2005.12.013

Rosell-Melé, A., M. A. Maslin, J. R. Maxwell, and P. Schaeffer (1997), Biomarker evidence for "Heinrich" events, *Geochimica et Cosmochimica Acta*, *61*(8), 1671-1678, doi: 10.1016/S0016-7037(97)00046-X

Rosell-Melé, A., P. Comes, P. J. Müller, and P. Ziveri (2000), Alkenone fluxes and anomalous Uk'37 values during 1989-1990 in the Northeast Atlantic (48 oN 21 oW), *Marine Chemistry*, *71*(3-4), 251-264, doi: 10.1016/S0304-4203(00)00052-9

Rosell-Melé, A., E. Bard, F. Rostek, C. Sonzogni, K. C. Emeis, J. O. Grimalt, C. Pelejero, P. Müller, et al. (2001), Precision of the current methods to measure the alkenone proxy U37k' and absolute alkenone abundance in sediments: Results of an interlaboratory comparison study, *Geochem. Geophys. Geosyst.*, *2*(7), doi: 10.1029/2000gc000141

Rosell-Melé, A., E. Jansen, and M. Weinelt (2002), Appraisal of a molecular approach to infer variations in surface ocean freshwater inputs into the North Atlantic during the last glacial, *Global and Planetary Change*, *34*(3-4), 143-152, doi: 10.1016/S0921-8181(02)00111-X

Roy, M., P. Clark, R. Barendregt, J. Glasmann, and R. Enkin (2004), Glacial stratigraphy and paleomagnetism of late Cenozoic deposits of the north-central United States, *Geological Society of America Bulletin*, *116*, 30-41, doi: 10.1130/B25325.1

Ruddiman, W. F. (1977), Late Quaternary deposition of ice-rafted sand in the subpolar North Atlantic (lat 40° to 65°N), *Geological Society of America Bulletin*, *88*(12), 1813-1827

Ruddiman, W. F., R. B. Kidd, J. G. Baldauf, B. M. Clement, J. F. Dolan, M. R. Eggers, P. R. Hill, L. D. Keigwin, Jr., et al. (1987a), Site 607, in *Initial reports of the Deep Sea Drilling Project covering Leg 94 of the cruises of the drilling vessel Glomar Challenger, Norfolk,*

Virginia, to St. John's, Newfoundland, June-August 1983, edited by S. Orlofsky pp. 75-147. Texas A & M University, Ocean Drilling Program, College Station, TX.

Ruddiman, W. F., A. McIntyre, and M. Raymo (1987b), Paleoenvironmental results from North Atlantic Sites 607 and 609, in *Initial Reports, DSDP 94*, edited by W. F. Ruddiman, et al. pp. 855-878. U.S. Govt. Printing Office, Washington.

Ruddiman, W. F., M. E. Raymo, D. G. Martinson, B. M. Clement, and J. Backman (1989), Pleistocene Evolution: Northern Hemisphere Ice Sheets and North Atlantic Ocean, *Paleoceanography*, *4*, 353-412, doi: 10.1029/PA004i004p00353

Ruggieri, E., T. Herbert, K. T. Lawrence, and C. E. Lawrence (2009), Change point method for detecting regime shifts in paleoclimatic time series: Application to d18O time series of the Plio-Pleistocene, *Paleoceanography*, *24*, PA1204, doi: 10.1029/2007pa001568

Sachs, J. P., and R. F. Anderson (2005), Increased productivity in the subantarctic ocean during Heinrich events, *Nature*, *434*(7037), 1118-1121, doi: 10.1038/nature03544

Sakamoto, T., M. Ikehara, K. Aoki, K. Iijima, N. Kimura, T. Nakatsuka, and M. Wakatsuchi (2005), Ice-rafted debris (IRD)-based sea-ice expansion events during the past 100 kyrs in the Okhotsk Sea, *Deep Sea Research Part II: Topical Studies in Oceanography*, *52*(16-18), 2275-2301, doi: 10.1016/j.dsr2.2005.08.007

Sarnthein, M., G. Bartoli, M. Prange, A. Schmittner, B. Schneider, M. Weinelt, N. Andersen, and D. Garbe-Schönberg (2009), Mid-Pliocene shifts in ocean overturning circulation and the onset of Quaternary-style climates, *Climate of the Past*, *5*(2), 269-283, doi: 10.5194/cp-5-269-2009

Schefuss, E., V. Ratmeyer, J.-B. W. Stuut, J. H. F. Jansen, and J. S. Sinninghe Damsté (2003a), Carbon isotope analyses of n-alkanes in dust from the lower atmosphere over the central eastern Atlantic, *Geochimica et Cosmochimica Acta*, *67*(10), 1757-1767, doi: 10.1016/S0016-7037(02)01414-X

Schefuss, E., S. Schouten, J. H. F. Jansen, and J. S. Sinninghe Damsté (2003b), African vegetation controlled by tropical sea surface temperatures in the mid-Pleistocene period, *Nature*, *422*(6930), 418-421, doi: 10.1038/nature01500

Schiebel, R., J. Bijma, and C. Hemleben (1997), Population dynamics of the planktic foraminifer Globigerina bulloides from the eastern North Atlantic, *Deep Sea Research Part I: Oceanographic Research Papers*, *44*(9-10), 1701-1713, doi: 10.1016/S0967-0637(97)00036-8

Schmidt, M. W., M. J. Vautravers, and H. J. Spero (2006), Rapid subtropical North Atlantic salinity oscillations across Dansgaard-Oeschger cycles, *Nature*, *443*(7111), 561-564, doi: 10.1038/nature05121

Schulz, H., U. von Rad, and H. Erlenkeuser (1998), Correlation between Arabian Sea and Greenland climate oscillations of the past 110,000 years, *Nature*, *393*(6680), 54-57, doi: 10.1038/31750

Seki, O., G. L. Foster, D. N. Schmidt, A. Mackensen, K. Kawamura, and R. D. Pancost (2010), Alkenone and boron-based Pliocene pCO$_2$ records, *Earth and Planetary Science Letters*, *292*(1-2), 201-211, doi: 10.1016/j.epsl.2010.01.037

Shackleton, N. J., J. Backman, H. Zimmerman, D. V. Kent, M. A. Hall, D. G. Roberts, D. Schnitker, J. G. Baldauf, et al. (1984), Oxygen isotope calibration of the onset of ice-rafting and history of glaciation in the North Atlantic region, *Nature*, *307*(5952), 620-623, doi: 10.1038/307620a0

Sigman, D., A. M. de Boer, and G. H. Haug (2007), Antarctic Stratification, Atmospheric Water Vapor, and Heinrich Events: A Hypothesis for Late Pleistocene Deglaciations (Geophysical Monograph), in *Ocean Circulation: Mechanisms and Impacts Past and future Changes of Meridional Overturning*, edited by A. Schmittner, et al., Geophysical Monograph Series 173, pp. 335-349. American Geophysical Union.

Sigman, D. M., M. P. Hain, and G. H. Haug (2010), The polar ocean and glacial cycles in atmospheric CO_2 concentration, *Nature*, *466*(7302), 47-55, doi: 10.1038/nature09149

Simoneit, B. R. T., R. Chester, and G. Eglinton (1977), Biogenic lipids in particulates from the lower atmosphere over the eastern Atlantic, *Nature*, *267*(5613), 682-685

Sosdian, S., and Y. Rosenthal (2009), Deep-Sea Temperature and Ice Volume Changes Across the Pliocene-Pleistocene Climate Transitions, *Science*, *325*(5938), 306-310, doi: 10.1126/science.1169938

Stager, J. C., P. A. Mayewski, and L. D. Meeker (2002), Cooling cycles, Heinrich event 1, and the desiccation of Lake Victoria, *Palaeogeography, Palaeoclimatology, Palaeoecology*, *183*(1-2), 169-178, doi: 10.1016/S0031-0182(01)00468-0

Stager, J. C., D. B. Ryves, B. M. Chase, and F. S. R. Pausata (2011), Catastrophic Drought in the Afro-Asian Monsoon Region During Heinrich Event 1, *Science*, *331*(6022), 1299-1302, doi: 10.1126/science.1198322

Stein, R., and M. Sarnthein (1984), Late Neogene events of atmospheric and oceanic circulation offshore Northwest Africa: High-resolution record from deep-sea sediments, *Paleoecology of Africa*, *16*, 9-36

Stein, R. (1985), Late neogene changes of paleoclimate and paleoproductivity off northwest africa (D.S.D.P. Site 397), *Palaeogeography, Palaeoclimatology, Palaeoecology*, *49*(1-2), 47-59, doi: 10.1016/0031-0182(85)90004-5

Stein, R., T. Kanamatsu, C. Alvarez-Zarikian, S. M. Higgins, J. E. T. Channell, and Expedition 306 Scientists (2006), Ocean Drilling Expedition Explores North Atlantic Paleoceanography, *EOS*, *87*(13), 129-133, doi: 10.1029/2006EO130002.

Stein, R., J. Hefter, J. Grützner, A. Voelker, and B. D. A. Naafs (2009), Variability of surface-water characteristics and Heinrich-like Events in the Pleistocene mid-latitude North Atlantic Ocean: Biomarker and XRD records from IODP Site U1313 (MIS 16-9), *Paleoceanography*, *24*, PA2203, doi: 10.1029/2008PA001639

Sugden, D. E., R. D. McCulloch, A. J. M. Bory, and A. S. Hein (2009), Influence of Patagonian glaciers on Antarctic dust deposition during the last glacial period, *Nature Geosciences*, *2*(4), 281-285, doi: 10.1038/ngeo474

Swift, J. (1986), The Arctic waters, in *The Nordic Seas*, edited by B. G. Hurdle pp. 129-151. Springer, New York.

Thouveny, N., J.-L. de Beaulieu, E. Bonifay, K. M. Creer, J. Guiot, M. Icole, S. Johnsen, J. Jouzel, et al. (1994), Climate variations in Europe over the past 140 kyr deduced from rock magnetism, *Nature*, *371*(6497), 503-506, doi: 10.1038/371503a0

Tiedemann, R., M. Sarnthein, and N. J. Shackleton (1994), Astronomic Timescale for the Pliocene Atlantic d18O and Dust Flux Records of Ocean Drilling Program Site 659, *Paleoceanography*, *9*, 619-638, doi: 10.1029/94pa00208

Tierney, J. E., and J. M. Russell (2007), Abrupt climate change in southeast tropical Africa influenced by Indian monsoon variability and ITCZ migration, *Geophys. Res. Lett.*, *34*(15), L15709, doi: 10.1029/2007gl029508

Tipple, B. J., and M. Pagani (2010), A 35 Myr North American leaf-wax compound-specific carbon and hydrogen isotope record: Implications for C4 grasslands and hydrologic cycle dynamics, *Earth and Planetary Science Letters*, *299*(1-2), 250-262, doi: 10.1016/j.epsl.2010.09.006

Venz, K. A., D. A. Hodell, C. Stanton, and D. A. Warnke (1999), A 1.0 Myr Record of Glacial North Atlantic Intermediate Water Variability from ODP Site 982 in the Northeast Atlantic, *Paleoceanography*, *14*(1), 42-52, doi: 10.1029/1998pa900013

Versteegh, G. J. M., H. Brinkhuis, H. Visscher, and K. A. F. Zonneveld (1996), The relation between productivity and temperature in the Pliocene North Atlantic at the onset of northern hemisphere glaciation: a palynological study, *Global and Planetary Change*, *11*(4), 155-165, doi: 10.1016/0921-8181(95)00054-2

Versteegh, G. J. M., and K. A. F. Zonneveld (2002), Use of selective degradation to separate preservation from productivity, *Geology*, *30*(7), 615-618, 10.1130/0091-7613(2002)030<0615:uosdts>2.0.co;2

Vidal, L., L. Labeyrie, E. Cortijo, M. Arnold, J. C. Duplessy, E. Michel, S. Becquè, and T. C. E. van Weering (1997), Evidence for changes in the North Atlantic Deep Water linked to meltwater surges during the Heinrich events, *Earth and Planetary Science Letters*, *146*(1-2), 13-27, doi: 10.1016/S0012-821X(96)00192-6

Villanueva, J., J. O. Grimalt, E. Cortijo, L. Vidal, and L. Labeyriez (1997), A biomarker approach to the organic matter deposited in the North Atlantic during the last climatic cycle, *Geochimica et Cosmochimica Acta*, *61*(21), 4633-4646, doi: 10.1016/S0016-7037(97)83123-7

Villanueva, J., E. Calvo, C. Pelejero, J. O. Grimalt, A. Boelaert, and L. Labeyrie (2001), A Latitudinal Productivity Band in the Central North Atlantic Over the Last 270 kyr: An Alkenone Perspective, *Paleoceanography*, *16*, 617-626, doi: 10.1029/2000PA000543

Villanueva, J., J. A. Flores, and J. O. Grimalt (2002), A detailed comparison of the Uk'37 and coccolith records over the past 290 kyears: implications to the alkenone paleotemperature method, *Organic Geochemistry*, *33*(8), 897-905, doi: 10.1016/S0146-6380(02)00067-0

Voelker, A. H. L. (2002), Global distribution of centennial-scale records for Marine Isotope Stage (MIS) 3: a database, *Quaternary Science Reviews*, *21*(10), 1185-1212, doi: 10.1016/S0277-3791(01)00139-1

Voelker, A. H. L., and L. de Abrue (2010), A Review of Abrupt Climate Change Events in the Northeastern Atlantic Ocean (Iberian Margin): Latitudinal, Longitudinal and Vertical

Gradients, in *Understanding the causes, mechanisms and extent of the Abrupt Climate Change*, edited by H. Rashid, et al., Geophysical Monograph Series in press. American Geophysical Union.

Voelker, A. H. L., T. Rodrigues, K. Billups, D. Oppo, J. McManus, R. Stein, J. Hefter, and J. O. Grimalt (2010), Variations in mid-latitude North Atlantic surface water properties during the mid-Brunhes (MIS 9–14) and their implications for the thermohaline circulation, *Climate of the Past*, *6*, 531-552, doi: 10.5194/cpd-6-531-2010

Vogts, A., H. Moossen, F. Rommerskirchen, and J. Rullkötter (2009), Distribution patterns and stable carbon isotopic composition of alkanes and alkan-1-ols from plant waxes of African rain forest and savanna C3 species, *Organic Geochemistry*, *40*(10), 1037-1054, doi: 10.1016/j.orggeochem.2009.07.011

Volkman, J. K., G. Eglinton, E. D. S. Corner, and T. E. V. Forsberg (1980), Long-chain alkenes and alkenones in the marine coccolithophorid Emiliania huxleyi, *Phytochemistry*, *19*(12), 2619-2622, doi: 10.1016/S0031-9422(00)83930-8

Volkman, J. K., S. M. Barrett, S. I. Blackburn, and E. L. Sikes (1995), Alkenones in Gephyrocapsa oceanica: Implications for studies of paleoclimate, *Geochimica et Cosmochimica Acta*, *59*(3), 513-520, doi: 10.1016/0016-7037(95)00325-T

Wang, X., A. S. Auler, R. L. Edwards, H. Cheng, P. S. Cristalli, P. L. Smart, D. A. Richards, and C.-C. Shen (2004), Wet periods in northeastern Brazil over the past 210 kyr linked to distant climate anomalies, *Nature*, *432*(7018), 740-743, doi: 10.1038/nature03067

Wang, Y. J., H. Cheng, R. L. Edwards, Z. S. An, J. Y. Wu, C. C. Shen, and J. A. Dorale (2001), A High-Resolution Absolute-Dated Late Pleistocene Monsoon Record from Hulu Cave, China, *Science*, *294*(5550), 2345-2348, doi: 10.1126/science.1064618

Watson, A. J., D. C. E. Bakker, A. J. Ridgwell, P. W. Boyd, and C. S. Law (2000), Effect of iron supply on Southern Ocean CO_2 uptake and implications for glacial atmospheric CO_2, *Nature*, *407*(6805), 730-733, doi: 10.1038/35037561

Weeks, A. R., M. J. R. Fasham, J. Aiken, D. S. Harbour, J. F. Read, and I. Bellan (1993), The spatial and temporal development of the spring bloom during the JGOFS North Atlantic Bloom Experiment, 1989, *Journal of the Marine Biological Association of the UK*, *73*(02), 253-282, doi: 10.1017/S0025315400032847

Weijers, J. W. H., S. Schouten, E. C. Hopmans, J. A. J. Geenevasen, O. R. P. David, J. M. Coleman, R. D. Pancost, and J. S. Sinninghe Damsté (2006), Membrane lipids of mesophilic anaerobic bacteria thriving in peats have typical archaeal traits, *Environmental Microbiology*, *8*(4), 648-657, doi: 10.1111/j.1462-2920.2005.00941.x

Weijers, J. W. H., S. Schouten, J. C. van den Donker, E. C. Hopmans, and J. S. Sinninghe Damsté (2007), Environmental controls on bacterial tetraether membrane lipid distribution in soils, *Geochimica et Cosmochimica Acta*, *71*(3), 703-713, doi: 10.1016/j.gca.2006.10.003

Whittaker, T. E., C. H. Hendy, and J. C. Hellstrom (2011), Abrupt millennial-scale changes in intensity of Southern Hemisphere westerly winds during marine isotope stages 2–4, *Geology*, *39*(5), 455-458, doi: 10.1130/G31827.1

Williams, R. G., and M. J. Follows (1998), Oceanography: Eddies make ocean deserts bloom, *Nature*, *394*(6690), 228-229, doi: 10.1038/28285

Winckler, G., R. F. Anderson, M. Q. Fleisher, D. McGee, and N. Mahowald (2008), Covariant Glacial-Interglacial Dust Fluxes in the Equatorial Pacific and Antarctica, *Science*, *320*(5872), 93-96, doi: 10.1126/science.1150595

Wright, A. K., and B. P. Flower (2002), Surface and deep ocean circulation in the subpolar North Atlantic during the mid-Pleistocene revolution, *Paleoceanography*, *17*(4), 1068, doi: 10.1029/2002pa000782

Yang, S., and Z. Ding (2010), Drastic climatic shift at ~2.8 Ma as recorded in eolian deposits of China and its implications for redefining the Pliocene-Pleistocene boundary, *Quaternary International*, *219*(1-2), 37-44, doi: 10.1016/j.quaint.2009.10.029

Yao, Z., G. Xiao, H. Wu, W. Liu, and Y. Chen (2010), Plio-Pleistocene vegetation changes in the North China Plain: Magnetostratigraphy, oxygen and carbon isotopic composition of pedogenic carbonates, *Palaeogeography, Palaeoclimatology, Palaeoecology*, *297*(2), 502-510, doi: 10.1016/j.palaeo.2010.09.003

Yung, Y. L., T. Lee, C.-H. Wang, and Y.-T. Shieh (1996), Dust: A Diagnostic of the Hydrologic Cycle During the Last Glacial Maximum, *Science*, *271*(5251), 962-963, doi: 10.1126/science.271.5251.962

Zhao, M., N. A. S. Beveridge, N. J. Shackleton, M. Sarnthein, and G. Eglinton (1995), Molecular stratigraphy of cores off northwest Africa: Sea surface temperature history over the last 80 ka, *Paleoceanography*, *10*(3), 661-675, doi: 10.1029/94pa03354

Zhisheng, A., H. Yongsong, L. Weiguo, G. Zhengtang, S. Clemens, L. Li, W. Prell, N. Youfeng, et al. (2005), Multiple expansions of C4 plant biomass in East Asia since 7 Ma coupled with strengthened monsoon circulation, *Geology*, *33*(9), 705-708, doi: 10.1130/g21423.1

Zonneveld, K. A. F., G. J. M. Versteegh, S. Kasten, T. I. Eglinton, K. C. Emeis, C. Huguet, B. P. Koch, G. J. de Lange, et al. (2010), Selective preservation of organic matter in marine environments; processes and impact on the sedimentary record, *Biogeosciences*, *7*(2), 483-511, doi: 10.5194/bg-7-483-2010

11 Acknowledgements

My short research stay in Bristol would not have been possible without Daniela Schmidt. Dani, thank you for your hospitality and patience. Prof. Richard Pancost introduced me into the world of compound specific isotope measurements. Rich, thank you for your help and allowing me to come to Bristol. Special thanks also go to James Williams, who helped with the laboratory work in Bristol.

Of course I also want to thank my family. First of all my parents, who supported me throughout the years, were always willing to come to Bremerhaven when needed, and made me feel at home when I came back to Holland during the various holidays. In addition my siblings and their families are thanked. Dennis, where it not for you, I would probably never have become an earth scientist. Thank you for making me enthusiastic for the topic and your support of the years. Thank you also to Monique, Dave, and Marc. Marinka, Maraïcha, Malik, and Salma are thanked for always making me feel at home during those sparse moments I was actually at home in Papendrecht. Martine is thanked for her down-to-earth comments that, I know, are needed sometimes. In addition I would like to thank my grandmother, Oma Verhoek, who was always happy to see me whenever I came home and provide a listening ear and a cup of tea during these visits.

Last, but certainly not least, Evgenia is thanked for all her help and support during the last 2.5 years. Мышь, спасибо. I will never forget this.

Die **"Berichte zur Polar- und Meeresforschung"** (ISSN 1866-3192) werden beginnend mit dem Heft Nr. 569 (2008) als Open-Access-Publikation herausgegeben. Ein Verzeichnis aller Hefte einschließlich der Druckausgaben (Heft 377-568) sowie der früheren **"Berichte zur Polarforschung** (Heft 1-376, von 1982 bis 2000) befindet sich im Internet in der Ablage des electronic Information Center des AWI (**ePIC**) unter der URL http://epic.awi.de. Durch Auswahl "Reports on Polar- and Marine Research" auf der rechten Seite des Fensters wird eine Liste der Publikationen in alphabetischer Reihenfolge (nach Autoren) innerhalb der absteigenden chronologischen Reihenfolge der Jahrgänge erzeugt.

To generate a list of all Reports past issues, use the following URL: http://epic.awi.de and select the right frame to browse "Reports on Polar and Marine Research". A chronological list in declining order, author names alphabetical, will be produced, and pdf-icons shown for open access download.

Verzeichnis der zuletzt erschienenen Hefte:

Heft-Nr. 626/2011 — "Towards data assimilation in ice-dynamic models: the (geo)physical basis", by Olaf Eisen

Heft-Nr. 627/2011 — "The Expedition of the Research Vessel 'Polarstern' to the Arctic in 2007 (ARK-XXII/1a-c)", edited by Michael Klages and Jörn Thiede

Heft-Nr. 628/2011 — "The Expedition of the Research Vessel 'Polarstern' to the Antarctic in 2010 (ANT-XXVII/1)", edited by Karl Bumke

Heft-Nr. 629/2011 — "Russian-German Cooperation SYSTEM LAPTEV SEA: The expedition Eastern Laptev Sea - Buor Khaya Peninsula 2010" edited by Sebastian Wetterich, Pier Paul Overduin and Mikhail Grigoriev

Heft-Nr. 630/2011 — "Comparative aerosol studies based on multi-wavelength Raman LIDAR at Ny-Ålesund, Spitsbergen", by Anne Hoffmann

Heft-Nr. 631/2011 — "The Expedition of the Research Vessel 'Polarstern' to the Antarctic in 2010 (ANT-XXVI/4), edited by Arne Körtzinger

Heft-Nr. 632/2011 — "The Expedition of the Research Vessel 'Polarstern' to the polar South Pacific in 2009/2010 (ANT-XXVI/2 - BIPOMAC), edited by Rainer Gersonde

Heft-Nr. 633/2011 — "Investigation of Katabatic winds and Polynyas during Summer – IKAPOS Field Phase Report", by Günther Heinemann, Thomas Ernsdorf and Clemens Drüe"

Heft-Nr. 634/2011 — "The Expedition of the Research Vessel 'Polarstern' to the Antarctic in 2010/11 (ANT-XXVII/2)", edited by Eberhard Fahrbach

Heft-Nr. 635/2011 — "Direkte numerische Simulation von Salzfingern", by Thomas Zweigle

Heft-Nr. 636/2011 — "The joint Russian-German Expedition BERINGIA/KOLYMA 2008 during the International Polar Year (IPY) 2007/2008", edited by Sebastian Wetterich, Lutz Schirrmeister and Aleksander L. Kholodov

Heft-Nr. 637/2011 — "The European Research Icebreaker AURORA BOREALIS Conceptual Design Study — Summary Report", edited by Lester Lembke-Jene, Nicole Biebow and Jörn Thiede

Heft-Nr. 638/2011 — "Long-term evolution of (millennial-scale) climate variability in the North Atlantic over the last four million years - Results from Integrated Ocean Drilling Project Site U1313", by Bernhard David Adriaan Naafs